

**UCLA
School
of
Engineering
and
Applied
Science**

UCLA ENG 90-11
October 1989

**RISK-BASED FIRE SAFETY EXPERIMENT
DEFINITION FOR MANNED SPACECRAFT**

G.E. Apostolakis, V.S. Ho, E. Marcus, A.T. Perry, S.L. Thompson



(NASA-CR-183835) RISK-BASED FIRE SAFETY
EXPERIMENT DEFINITION FOR MANNED SPACECRAFT
Final Report (California Univ.) 121 p

N90-14262

CSLL 220

Unclass

G3/18

0233935

UCLA ENG 90-11
October 1989

RISK-BASED FIRE SAFETY EXPERIMENT DEFINITION FOR MANNED SPACECRAFT

by

G.E. Apostolakis, V.S. Ho, E. Marcus*, A.T. Perry*, S.L. Thompson

*Mechanical, Aerospace and
Nuclear Engineering Department
University of California
Los Angeles, CA 90024-1597*

* *American Space Technology, Inc., 2800 28th Street, Suite 351, Santa Monica, CA 90405-2934*

Contract No: NAS8-³7750
Principal Investigator: G.E. Apostolakis

Prepared for:

George C. Marshall Space Flight Center
National Aeronautics and Space Administration
Marshall Space Flight Center, AL 35812

Sponsored by:

Office of Aeronautics and Space Technology
In-Space Technology Experiments Program
National Aeronautics and Space Administration
Washington, DC 20546-0001

TABLE OF CONTENTS

	Page
LIST OF FIGURES	viii
LIST OF TABLES	xi
ABSTRACT	xii
ACKNOWLEDGMENT	xiii
1.0 INTRODUCTION AND SUMMARY	1.1
References	1.6
2.0 PROBABILISTIC RISK ASSESSMENT	2.1
2.1 Introduction	2.1
2.2 Ground-Based Fire Risk Methodology	2.3
2.2.1 Overview and Critical Locations	2.3
2.2.2 Fire Growth	2.4
2.2.3 Detection and Suppression	2.7
2.2.4 Risk Calculations	2.8
2.3. Uncertainties	2.9
2.4. Risk Management	2.10
References	2.11
3.0 SCIENCE REQUIREMENTS	3.1
3.1 Introduction	3.1
3.1.1 Purpose	3.1
3.1.2 Scope	3.1
3.1.3 Sensitivity Studies	3.2

3.2	Heat and Smoke Release Model	3.2
3.2.1	Model Description	3.2
3.2.1.1	Heat release	3.3
3.2.1.2	Mass burning rate	3.6
3.2.1.3	Smoke Release	3.11
3.2.2	Objectives	3.22
3.2.3	Justification	3.23
3.2.4	Science Requirements	3.23
3.2.4.1	Mass Burning Rate	3.23
3.2.4.2	Rate of Heat Release	3.24
3.2.4.3	External Heat Flux	3.24
3.2.4.4	Surface Temperature	3.24
3.2.4.5	Light Attenuation	3.24
3.2.4.6	Radiant Heat Flux	3.24
3.2.4.7	Smoke Particle Size	3.24
3.3	Heat Transfer Model	3.25
3.3.1	Model Description	3.25
3.3.1.1	Flame Spread	3.25
3.3.1.2	Heat Transfer to Secondary Sources	3.29
3.3.1.3	Scaling Methods	3.30
3.3.2	Objectives	3.36
3.3.3	Justification	3.38
3.3.4	Science Requirements	3.38
3.3.4.1	Flame Spread Rate	3.38
3.3.4.2	Temperature	3.39
3.3.4.3	Gas Flow Rate	3.39
3.3.4.4	Species Concentration	3.39
3.3.4.5	Smoke Concentration	3.39
3.3.4.6	Visual Record	3.39
3.4	Damage Model	3.39
3.4.1	Model Description	3.39
3.4.2	Objectives	3.42
3.4.3	Justification	3.43
3.4.4	Science Requirements	3.43

3.4.4.1	Smoke Particle Deposit Rate	3.43
3.4.4.2	Temperature	3.43
3.4.4.3	Smoke Particle Size	3.43
3.4.4.4	Heat Flux	3.43
3.5	Fire Protection in Microgravity	3.43
3.5.1	Purpose	3.46
3.5.2	Scope	3.46
3.5.3	Time Characteristics of Fire Detection and Suppression Processes	3.47
3.5.4	Hazard Time Model	3.47
3.6	Fire Detection Experiment	3.48
3.6.1	Thermal Detector Response Model	3.49
3.6.2	Smoke Detector Response Model	3.53
3.6.2.1	Photoelectric Smoke Detector Response Model	3.53
3.6.2.2	Ionization Smoke Detector Response Model	3.58
3.6.3	Gas Detector Response Model	3.58
3.6.4	Flame Detectors	3.59
3.6.5	Objectives	3.59
3.6.6	Justification	3.60
3.6.7	Science Requirements	3.61
3.6.7.1	Hot Gas Flow Rate	3.61
3.6.7.2	Local Hot Gas Temperature	3.61
3.6.7.3	Hot Gas Temperature	3.61
3.6.7.4	Pressure	3.61
3.6.7.5	Detector Temperature	3.61
3.6.7.6	Detector Response Time	3.62
3.6.7.7	Gas Concentration	3.62
3.6.7.8	Optical Density	3.62
3.7	Fire Suppression Experiment	3.62
3.7.1	Suppressant Selection	3.63
3.7.1.1	Oxidant Restriction	3.64
3.7.1.2	Temperature Reduction	3.65
3.7.1.3	Free Radicals Reduction	3.65
3.7.2	Fire-Suppressant Interaction Modeling	3.65
3.7.3	Objectives	3.66
3.7.4	Justification	3.68
3.7.5	Science Requirements	3.68

3.7.5.1	Drop Size	
3.7.5.2	Suppression Time	3.68
3.7.5.3	Suppressant Discharge Pressure	3.68
3.7.5.4	Suppressant Discharge Rate	3.68
3.7.5.5	Suppressant Flow Rate	3.69
3.7.5.6	Suppressant Temperature	3.69
3.7.5.7	Flame Temperature	3.69
References		
		3.69
4.0	EXPERIMENT SYSTEM DESCRIPTION AND MISSION PLAN	4.1
4.1	Introduction	4.1
4.1.1	Purpose	4.1
4.1.2	Scope	4.1
4.1.3	Applicable Documents	4.2
4.2	Science Requirements on Fire Safety Experiment System	4.2
4.3	Engineering Approach	4.5
4.3.1	Mass Loss Rate and Heat Release Rate	4.5
4.3.1.1	Changes in Oxygen Concentration	4.6
4.3.1.1.1	Ohio State University Set-up	4.9
4.3.1.1.2	Swedish Forest Products Research Laboratory Set-up	4.9
4.3.1.1.3	NBS Cone Calorimeter Set-up	4.10
4.3.1.1.4	Equipment Approach	4.10
4.3.1.2	Video Image Analysis	4.12
4.3.1.3	Change in Frequency Response	4.12
4.3.2	Heat Flux	4.14
4.3.2.1	External Heat Flux	4.14
4.3.2.2	Radiant Heat Flux	4.14
4.3.3	Temperature	4.15
4.3.3.1	Sample and Target Surface Temperature	4.15
4.3.3.2	Chamber Wall, Atmosphere, and Inlet/Outlet Gas Temperature	4.16
4.3.3.3	Fire Detector Local Hot Gas Temperature	4.16
4.3.3.4	Fire Detector Temperature	4.17
4.3.3.5	Suppressant Temperature	4.17
4.3.3.6	Flame Temperature	4.17

4.3.4	Light Attenuation	4.17
4.3.5	Particle and Droplet Size	4.18
4.3.5.1	Smoke Particle Size	4.18
4.3.5.2	Droplet Size	4.19
4.3.6	Flame Spread Rate	4.19
4.3.7	Species Concentration	4.19
4.3.8	Visual Record	4.20
4.3.9	Smoke Particle Deposit Rate	4.20
4.3.10	Flow Rates	4.20
4.3.10.1	Chamber Gas Flow Rates	4.20
4.3.10.2	Hot Gas Flow Rate	4.21
4.3.10.3	Suppressant Discharge Rate	4.21
4.3.10.4	Suppressant Flow Rate	4.21
4.3.11	Pressure	4.23
4.3.11.1	Chamber Pressure	4.23
4.3.11.2	Suppression Discharge Pressure	4.23
4.3.12	Time	4.23
4.3.12.1	Fire Detector Response Time	4.23
4.3.12.2	Suppression Time	4.23
4.3.13	Other Parameters to be Measured and Controlled (Sensitivity Studies)	4.24
4.3.13.1	Atmospheric Pressure	4.24
4.3.13.2	Fuel Orientation	4.24
4.3.13.3	Fuel Geometry	4.26
4.3.13.4	Ambient Temperature	4.26
4.3.13.5	Relative Humidity	4.27
4.4	Experiment System and Subsystem Description	4.27
4.4.1	Introduction	4.27
4.4.2	System Description	4.28
4.4.2.1	Combustion Module	4.33
4.4.2.2	Fluids Module	4.34
4.4.2.3	Command and Power Module	4.35
4.4.2.4	Subsystem Summary	4.35

4.4.2.4.1	Instrumentation Subsystem	4.37
4.4.2.4.2	Electrical Power Subsystem	4.37
4.4.2.4.3	Fluids Control Subsystem	4.38
4.4.2.4.4	Thermal Control Subsystem	4.39
4.4.2.4.5	Structures Subsystem	4.40
4.4.2.4.6	Command and Data Subsystem	4.41
4.4.2.4.7	Software Subsystem	4.42
4.4.3	Instrumentation Subsystem Detailed Description and Requirements	4.47
4.4.3.1	Residual Gas Analyzer	4.47
4.4.3.1.1	Introduction	4.47
4.4.3.1.2	Quadrupole and RF Unit	4.48
4.4.3.1.3	Residual Gas Analyzer Computer and Software Functions	4.48
4.4.3.1.4	Other Equipment	4.50
4.4.3.1.5	Functional Requirements	4.52
4.4.3.2	Radiometer	4.55
4.4.3.2.1	Introduction	4.55
4.4.3.2.2	Radiometer	4.55
4.4.3.2.3	Radiometer Functional Requirements [4.12]	4.58
4.4.3.3	Particle Dynamics Analyzer [4.13]	4.59
4.4.3.3.1	Introduction	4.59
4.4.3.3.2	Optics	4.60
4.4.3.3.3	Signal Processor	4.60
4.4.3.3.4	Computer/Software	4.60
4.4.3.3.5	Operations	4.61
4.4.3.3.6	Requirements	4.62
4.4.3.4	Thermal Imager	4.63
4.4.3.4.1	Introduction	4.63
4.4.3.4.2	Operation and Data Acquisition	4.63
4.4.3.5	Pressure Transducers	4.65
4.4.3.5.1	Introduction	4.65
4.4.3.5.2	Operation and Data Retrieval	4.65

4.4.3.6	Flowmeters	4.66
4.4.3.6.1	Introduction	4.66
4.4.3.6.2	Operation and Data Acquisition	4.67
4.4.3.6.3	Functional Requirements	4.67
4.4.3.7	Humidity Control	4.68
4.5	Fire Safety Experiment System Interfaces	4.69
4.5.1	Shuttle and/or Spacelab and/or Space Station Interfaces	4.69
4.5.2	Experiment System and Subsystem Interfaces	4.69
4.6	Fire Safety Experiment System Support Equipment Functional Philosophy	4.69
4.7	Fire Safety Experiment System Safety Requirements	4.70
4.8	Fire Safety Experiment System Design Verification	4.70
4.9	Mission Plan	4.71
4.9.1	Flight Sequence Implementation	4.71
4.9.1.1	Pre-Launch	4.71
4.9.1.2	In-orbit	4.71
4.9.1.2.1	Experiment Set-up	4.71
4.9.1.2.2	Performing the Experiments	4.72
4.9.1.2.3	Between Experiment Runs	4.73
4.9.1.2.4	Experiment Shut-down and Stowage	4.73
	References	4.73
5.0	PRELIMINARY DEVELOPMENT PHASE PLAN	5.1
5.1	Implementation Plan	5.1
5.2	Project Management	5.2
5.3	Cost Estimate	5.5

LIST OF FIGURES

		Page
Figure 1.1.	Examples of Common Fire Causes in Spacecraft [1.4].	1.2
Figure 1.2.	System Configuration with Spacelab or Space Station as Host Spacecraft.	1.5
Figure 2.1	Sample Critical Location.	2.4
Figure 2.2.	Hot-Gas-Layer Model [2.8].	2.5
Figure 2.3.	Flowchart of Computational Process in COMPBRN [2.6].	2.6
Figure 3.1.	Comparison of Sample Weight Loss Rate with Particulate Concentration for PVC [3.28].	3.13
Figure 3.2.	Particle Weight distribution for Urethane Smoke in Air [3.28].	3.13
Figure 3.3.	Rate of Smoke Generation During the Whole Combustion Process [3.36].	3.17
Figure 3.4.	Overall Smoke Generation Coefficient for Various Materials [3.36].	3.18
Figure 3.5.	Effect of Temperature on Smoke Generation.	3.18
Figure 3.6.	Increase in the Fire Propagation Rate Due to Increase in Oxygen Concentration for a Vertical, 1.29 m (4 ft) Long Cable. m_{O_2} Represents Mass Fraction of Oxygen [3.30].	3.27
Figure 3.7.	Representation of Steady Smoldering Along a Horizontal Cellulose Rod [3.50].	3.28
Figure 3.8.	Data Showing the Correlation Between Rate of Spread and the Maximum Temperature in Zone 2 for Smoldering Along Horizontal Cellulose Rods. The Various Symbols Refer to Different Proportions of Oxygen in Nitrogen, Except for the Symbol O which Refers to Oxygen/Helium Mixtures [3.50].	3.29
Figure 3.9.	Temperatures; Average of Readings at Sampling Point and Image Near Opposite Vent [3.62].	3.34
Figure 3.10.	Burning Rate versus Grashof Number Correlation. (a) for Plexiglass Cylinder Burning; (b) for Plexiglass Tube Burning Inside; (c) for Pine Wood Cylinder Burning [3.63].	3.35

Figure 3.11.	Behavior of the Net Radiant Flux Back to the PMMA Wall Surface with Grashof Number Based on Distance from the Bottom of the Wall. Symbols Correspond to $d = h/10$ [3.64].	3.36
Figure 3.12.	Variation of Nondimensional Pool Burning Rate with Grashof Number Based on PMMA Width [3.64].	3.37
Figure 3.13.	Typical Ignition Curves for an Range of Upholstered Furniture Fabric/Padding Combinations [3.65].	3.41
Figure 3.14.	Fire Protection System for the Spacelab [3.68].	3.44
Figure 3.15.	Arrangement of Fire Protection System for the Space Shuttle [3.68].	3.45
Figure 3.16.	Illustration of Typical Thermal Detectors [3.73].	3.51
Figure 3.17.	Illustration of Photoelectric Smoke Detectors [3.8].	3.54
Figure 3.18.	Illustration of Ionization Smoke Detector [3.8].	3.55
Figure 3.19.	Illustration of a Typical Ionization Detector Used in Space Applications [3.68].	3.56
Figure 3.20.	Illustration of a Flame Detector [3.8].	3.60
Figure 3.21.	Feedback Mechanism in Fire [3.80].	3.63
Figure 3.22.	The Critical Fire Rate Curve for Fire Suppressant [3.80].	3.67
Figure 3.23.	Quantity Curve for Fire Suppressant [3.80].	3.67
Figure 4.1.	Combustion Chamber with Sample Holder.	4.6
Figure 4.2.	Top View of Combustion Chamber Configuration.	4.7
Figure 4.3.	OSU Apparatus with Instrumentation for O_2 [4.6].	4.9
Figure 4.4.	Swedish Open Arrangement [4.6].	4.10
Figure 4.5.	Optical Mass Loss Rate and Heat Flux Detection.	4.13
Figure 4.6.	Sample Support Assembly.	4.15
Figure 4.7.	Air Flow Rates and Patterns.	4.22

Figure 4.8.	Sheet Sample in Sample Holder.	4.25
Figure 4.9.	Redundant Cable Sample in Holder.	4.25
Figure 4.10.	Redundant Sheet Sample in Holder.	4.25
Figure 4.11.	Redundant Sheets with Non-parallel Geometry.	4.26
Figure 4.12.	System Configuration with Spacelab or Space Station as Host Spacecraft.	4.31
Figure 4.13.	Shuttle Middeck Installation of Experiment System.	4.32
Figure 4.14.	System Functional Block Diagram.	4.36
Figure 4.15.	Instrumentation Subsystem Functional Block Diagram.	4.38
Figure 4.16.	Command and Data Subsystem Functional Block Diagram.	4.42
Figure 5.1.	Preliminary Project Schedule.	5.3
Figure 5.2.	Development Phase Organizational Responsibilities.	5.4

LIST OF TABLES

	Page
Table 3.1. Dimensionless Groups.	3.32
Table 4.1. Preliminary Experiment Combustible Materials and Suppressants.	4.3
Table 4.2. Science Requirements and Associated Models.	4.4
Table 4.3. Future Detailed Design Documentation.	4.27
Table 4.4. Experiment System Mass Estimate.	4.29
Table 4.5. Experiment System Peak Power Estimate.	4.30

ABSTRACT

Risk methodology is used in this work to define fire safety experiments to be conducted in space which will help to construct and test the models relevant to manned spacecraft required for accident sequence identification. The development of accident scenarios is based on the realization that whether damage occurs depends on the time competition of two processes: the ignition and creation of an adverse environment and the detection and suppression activities. If the fire grows and causes damage faster than it is detected and suppressed then an accident has occurred. The proposed integrated experiments will provide information on individual models that apply to each of the above processes, as well as previously unidentified interactions and processes, if any. Initially, models that are used in terrestrial fire risk assessments are considered. These include heat and smoke release models, detection and suppression models, as well as damage models. In cases where the absence of gravity substantially invalidates a model, alternate models will be developed. Models that depend on buoyancy effects, such as the multizone compartment fire models, are included in these cases. The experiments will be performed in a variety of geometries simulating habitable areas, racks, and other spaces. These simulations will necessitate theoretical studies of scaling effects. Sensitivity studies will also be carried out including the effects of varying oxygen concentrations, pressures, fuel orientation and geometry, and air flow rates. The experimental apparatus described herein includes three major modules: the Combustion, the Fluids, and the Command and Power modules.

ACKNOWLEDGMENT

We thank Professor Ivan Catton of UCLA for his comments and useful advice throughout the course of this work. The following individuals have provided valuable information and insights: M.D. Brandyberry of UCLA, R. Friedman and W. Meyer of LeRC; E. Thomas of Brunswick; R. Crumbley of MSFC; H. Kimzey, Consultant; M. Buderer and E. Jung of JSC; K.L. Vivian, B. Krishnan, and D. Fox-Briggs of McDonnell Douglas; and D.M. Karydas and M. Delihatsios of Factory Mutual Research Corporation. Foster E. Anthony, Jr., the MSFC contract manager was very supportive. Finally, we express our appreciation to Cindy Gilbert of UCLA for lending us her word processing expertise during the preparation of this report.

1.0 INTRODUCTION AND SUMMARY

As manned spacecraft have evolved into larger and more complex configurations, the mandate for preventing, detecting, and extinguishing on-board fires has grown proportionately to ensure the success of progressively ambitious missions. The closed environment and high value of manned spacecraft offer the systems designer significant challenges. He must provide a habitable facility for conducting useful business in space using an earth-like atmosphere which possesses sufficient oxygen partial pressure to comfortably sustain human life, while still considering limiting oxygen concentration to inhibit combustion of the on-board materials. Additional challenges are created by the need to accommodate a variety of users in missions of long duration, such as those planned for the Space Station Freedom.

The state of the art in spacecraft fire safety was reviewed extensively at a National Aeronautics and Space Administration (NASA) workshop in 1986 [1.1,1.2]. A more recent review is given in [1.3]. These reviews have naturally been focused on the fire-related basic science concerns that a low-gravity environment creates and on the identification of possible preventive and mitigative strategies. A general conclusion is that it is not possible to determine a priori whether the fire risk is greater or smaller in microgravity. There are research needs in all areas of the problem, i.e., ignition, fire propagation, detection, suppression, and damage assessment.

The preventive and mitigative strategies thus far have been based on the traditional triangle of the three essential elements for the existence of a fire, i.e., the presence of fuel, sufficient amounts of oxygen, and of an ignition source. Figure 1.1, taken from [1.4], shows some of the hazards that are associated with each side of the triangle, as well as their controls. It is recognized that the complete elimination of all the hazards associated with any side of the fire triangle is impossible, particularly for the kinds of missions that are of concern to us. Reference 1.4 also provides a fairly high level discussion of possible fire-safety strategies and groups them into three classes: 1. control, e.g., the exclusion of fire-causing elements; 2. response, e.g. the timely detection of a fire; and, 3. recovery, e.g. extinguishment, cleaning, and repairs.

The above approach to the formulation of safety strategies does not explicitly consider the various scenarios (sequences of events) that may occur given a fire. These scenarios would include the initial ignition and growth of the fire, the competing processes of detection and suppression, the potential human intervention, the release of hot gases and their distribution in a

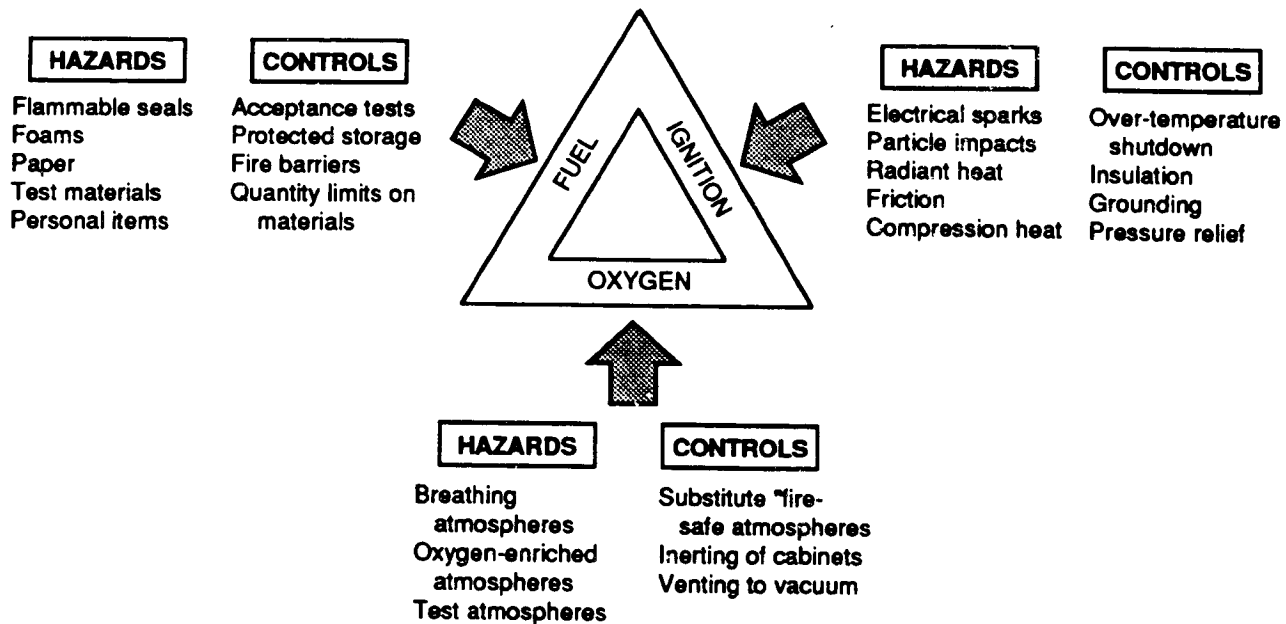


Figure 1.1. Examples of Common Fire Causes in Spacecraft [1.4].

compartment, as well as the potential damage that may be inflicted on critical components or systems. The availability of the important fire-initiated scenarios would greatly enhance our ability to manage the risk from fires, because the preventive and mitigative strategies would be formulated so as to significantly reduce the probability or the severity of these scenarios. The systematic generation of scenarios and their ranking according to their likelihood of occurrence (so that the important scenarios can be identified) is the subject of Probabilistic Risk Assessment (PRA), which has been applied to nuclear power plants [1.5,1.6], chemical plants [1.7,1.8], hazardous waste repositories [1.9,1.10], office buildings and residences [1.11,1.12], as well as other systems and processes.

While the identification of fire-related accident scenarios on earth is now possible [1.13-1.14], it is clear that the development of a methodology applicable to low-gravity environments will require the construction of new models for the individual elements of the risk methodology that are affected by the absence of gravity. These models will have to be tested and verified by experiments. We, thus, recognize that developing a PRA methodology for space applications at this time means to focus our attention on the development of models that will help us identify accident scenarios and that a probabilistic evaluation of these scenarios will have to be postponed until these models are validated.

The purpose of this work is to use risk methodology to define experiments to be conducted in space which will help us construct and test the models required for accident sequence identification. Furthermore, by simulating complete scenarios, we may discover interactions and processes previously unidentified. Previous work on the fundamental laws governing flames in low gravity environments has resulted from ground-based studies (drop-tower, airplane parabolic trajectory flights) with short term low gravity exposures of 2 to 30 seconds, augmented by a few simple, space-based experiments, such as the flaming characteristics of various small samples [1.15-1.18]. The drop tower studies involve the combustion of premixed gases in relatively small, closed vessels and examine the flammability limits, burning velocities, and minimum ignition energies for laminar premixed flame propagation via spark ignition. The present effort defines experiments which will permit shuttle, Spacelab, or space station experimentation on the ignition, combustion, detection, and extinguishment characteristics of a variety of relevant samples and geometries at longer periods of time. The proposed experiments build on the microgravity work previously accomplished, and significantly expand the space technology database in the understanding of fire risk assessment.

To implement the scenario approach, the proposed experiments are integrated so that the evolution in time of accidents can be simulated. The main elements that comprise such scenarios are the following:

1. The ignition of a fuel element and the subsequent release of heat and smoke.
2. The characterization of the environment that the fire creates, e.g. heat fluxes, flow rates, and species concentrations.
3. The assessment of the damage that the above environment can cause to various targets; the time from the ignition of the fuel element until a certain amount of damage to components or systems occurs is denoted by T_G .
4. The evaluation of the detection and suppression times; the sum of these times is denoted by T_H .

5. The development of accident scenarios is based on the realization that whether or not damage occurs depends on the competition in time of two processes: the ignition and creation of an adverse environment, represented by the time T_G , and the detection and suppression activities, represented by T_H . If T_G is smaller than T_H , i.e., if the fire grows and causes damage faster than it is detected and suppressed, then an accident has occurred.

The proposed integrated experiments will provide information on individual models that apply to each of the above elements. Initially, models that are used in terrestrial fire risk assessments are considered. These include heat and smoke release models, detection and suppression models, as well as damage models. In cases where the absence of gravity substantially invalidates a model, alternate models will be developed. Models that depend on buoyancy effects, such as the multizone compartment fire models, are included in these cases. The experiments will be performed in a variety of geometries simulating habitable areas, racks, and other spaces. These simulations will necessitate theoretical studies of scaling effects. Sensitivity studies will also be carried out including the effects of varying oxygen concentrations, pressures, fuel orientation and geometry, and air flow rates.

As seen in Figure 1.2, the current experimental apparatus concept includes three major modules: the Combustion Module, the Fluids Module, and the Command and Power Module. The Combustion Module is the chamber within which combustion, detection, and suppression experiments will be run. The Fluids Module will provide the various atmospheric gases to the Combustion Module. Operation of the equipment will be controlled by the Command and Power Module which provides control, data handling and storage, and electrical power conditioning of the host spacecraft's power. Crew interaction with the experimental apparatus is envisioned.

Chapter 2 of this report contains the general formulation of PRA and a general discussion of uncertainties; it also elaborates on the available ground-based fire risk methodology and the various models on which it is based. Chapter 3 provides justification for the proposed experiments and identifies the science requirements. Chapter 4 contains an experimental apparatus description, the functional requirements, and the mission plan. Finally, Chapter 5 contains the costs and associated plan for accomplishing the development phase.

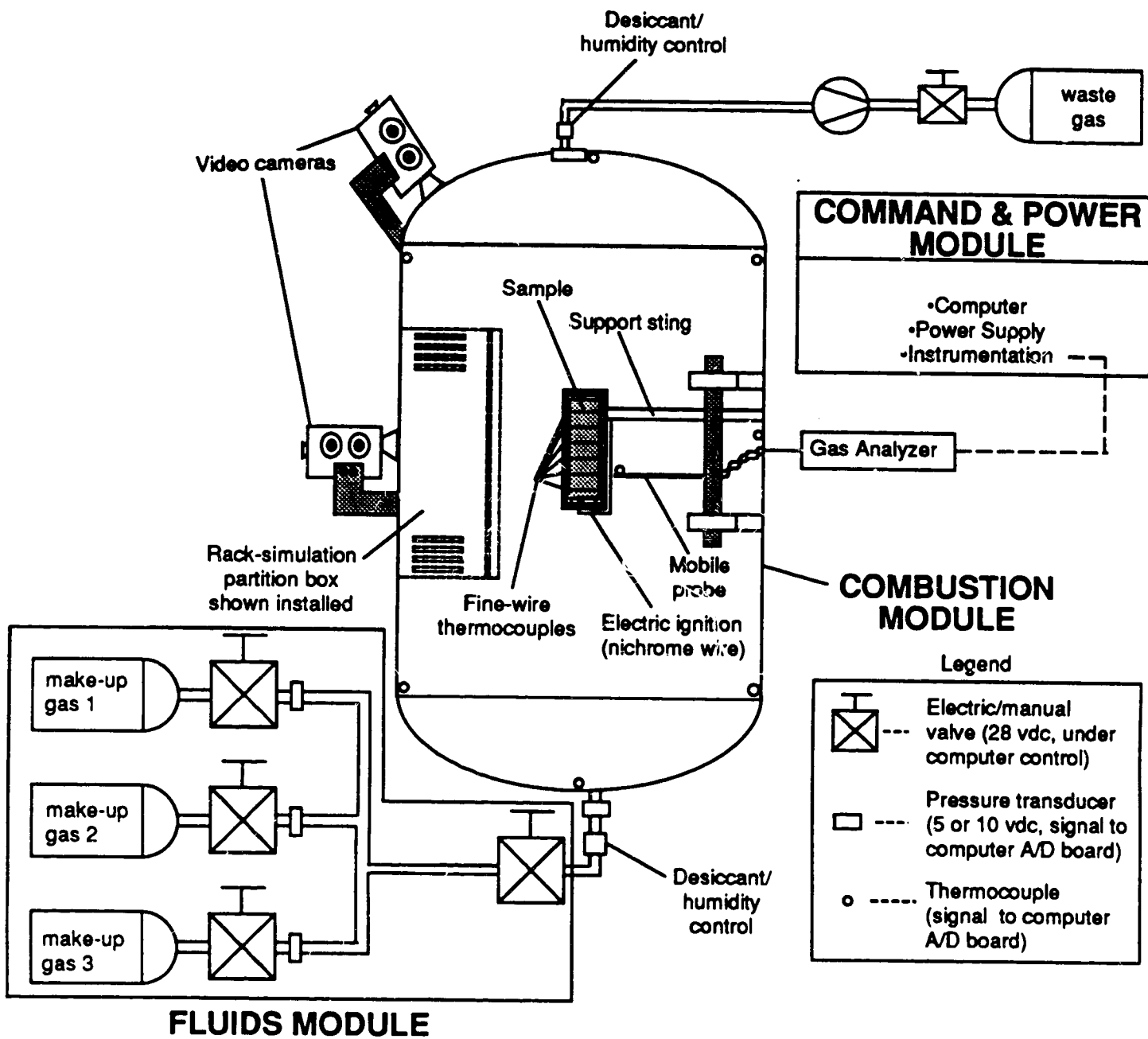


Figure 1.2. Experiment System Configuration Schematic.

References

- 1.1 *Spacecraft Fire Safety*, Proceedings of a Workshop held at NASA Lewis Research Center, Cleveland, Ohio, August 20-21, 1986, NASA Conference Publication 2476, Scientific and Technical Information Branch, 1987.
- 1.2 R. Friedman and K.R. Sacksteder, "Science and Technology Issues in Spacecraft Fire Safety," AIAA 25th Aerospace Sciences Meeting, Reno, Nevada, January 12-15, 1987.
- 1.3 R. Friedman and S.L. Olson, "Fire Safety Applications for Spacecraft," presented at the Symposium on Aircraft Fire Safety sponsored by the AGARD/NATO Propulsion Energetics Panel, Sintra, Portugal, May 22-26, 1989.
- 1.4 R. Friedman and K.R. Sacksteder, "Fire Behavior and Risk Analysis in Spacecraft," presented at the Winter Annual ASME Meeting, Chicago, Illinois, November 28 - December 3, 1988.
- 1.5 American Nuclear Society and Institute of Electrical and Electronics Engineers, *PRA Procedures Guide: A Guide to the Performance of Probabilistic Risk Assessments for Nuclear Power Plants*, U.S. Nuclear Regulatory Commission Report NUREG/CR-2300, 1982.
- 1.6 M. Kazarians, N.O. Siu, and G. Apostolakis, "Risk Management Application of Fire Risk Analysis," *Proceedings of the First International Symposium on Fire Safety Science*, National Bureau of Standards, Gaithersburg, Maryland, October 7-11 1985, pp. 1029-1038, C.E. Grant and P.J. Pagni, eds., Hemisphere Publishing Corporation, NY.
- 1.7 United Kingdom Health and Safety Executive, *Canvey: An Investigation of Potential Hazards from Operations in the Canvey Island/Thurrock Area*, London: Her Majesty's Stationary Office, 1978.
- 1.8 The American Institute of Chemical Engineers, *Guidelines for Hazard Evaluation Procedures*, New York, 1985.
- 1.9 R.M. Cranwell, et al., *Risk Methodology for Geologic Disposal of Radioactive Waste: Final Report*, NUREG/CR-2452, U.S. Nuclear Regulatory Commission, 1987.

- 1.10 J. Massmann and R. A. Freeze, "Ground-water Contamination from Waste Management Sites: The Interaction between Risk-based Engineering Design and Regulatory Policy Methodology," *Water Resources Research*, 23, 351-367, 1987.
- 1.11 J.R. Hall, R.W. Bukowski, S.W. Stiefel, and A. Sekizawa, *Fire Risk Assessment: Description of Methodology*, National Bureau of Standards Draft Report, May 1987.
- 1.12 M.D. Brandyberry and G.E. Apostolakis, *Fire Risk Analysis Methodology: Initiating Events*, National Institute of Standards and Technology, Report NIST-GCR- 89-562, March 1989.
- 1.13 M. Kazarians, N.O. Siu, and G. Apostolakis, "Fire Risk Analysis for Nuclear Power Plants: Methodological Developments and Applications," *Risk Analysis*, 5, 33-51, 1985.
- 1.14 V. Ho, N. Siu, and G. Apostolakis, "COMPBRN III - A Fire Hazard Model for Risk Analysis," *Fire Safety Journal*, 13, 137-154, 1988.
- 1.15 P.D. Ronney and H.Y. Wachman, "Effect of Gravity on Laminar Premixed Combustion I: Flammability Limits and Burning Velocities," *Combustion and Flame*, 62, 107-119, 1985.
- 1.16 P.D. Ronney, "Effect of Gravity on Laminar Premixed Combustion II: Ignition and Extinction Phenomena," *Combustion and Flame*, 62, 121-133, 1985.
- 1.17 R. A. Strenlow and D.L. Reuss, in: *Combustion Experiments in a Zero Gravity Laboratory*, T.H. Cochran, ed., *Progress in Aeronautics and Astronautics*, 73, AIAA, 1981.
- 1.18 J.H. Kimzey, *Skylab Experiment NM-479, Zero Gravity Flammability*, Final Report, NASA, JSC 22293, 1986.

2.0 PROBABILISTIC RISK ASSESSMENT

2.1 Introduction

The complexity of engineering systems and the requirements for reliable and safe operations have created the need for the development of models that accurately represent these systems. The occurrence of major accidents (e.g., Bhopal, Chernobyl, Challenger) has focused the attention of the public on the safety of these facilities and has accelerated the development and use of these models. It has also made it clear that the events of interest are rare and any decision-making process that involves them must include the large uncertainties that are associated with their occurrence.

The methodology that consists of these models is known as Probabilistic Risk Assessment (PRA), although the same methodology can be employed for reliability assessment. It essentially consists of two steps:

1. The identification of scenarios (event sequences) that lead to the consequence of interest, e.g., the release of hazardous materials, crew injuries; and
2. The quantification of the uncertainty associated with the occurrence of these scenarios.

There are many methods that have been developed for the identification of scenarios. They include Failure Modes and Effects of Analysis (FMEA), Hazard and Operability Analysis (HAZOP), Fault Tree Analysis (FTA), and Event Tree Analysis (ETA). These analyses include failures of the hardware, operator actions during maintenance as well as during accidents, fires, and other relevant events. Of particular interest to the present work is the development of scenarios from physical models that describe the evolution of the accident in terms of physical variables like heat release rates, temperature rise, and so forth.

After the scenarios have been identified there remains the issue of quantifying our uncertainty regarding their occurrence. While various methods are employed to varying degrees of sophistication, the rigorous and formal methods of Bayesian Probability Theory [2.1-2.3] are gaining increasing acceptance. This is due to the fact that the events of interest are rare and

statistical evidence is either weak or nonexistent (which, of course, is the case for low-gravity environments). Furthermore, it is important to identify and classify the various kinds of uncertainties that are encountered early, so that misunderstandings of these uncertainties will be prevented.

It is convenient to consider the following categories of uncertainties [2.4]:

1. Statistical or stochastic uncertainties arise when one or more quantities are treated as random variables. An example is the occurrence time of a fire. We usually construct a stochastic model for such phenomena by making a number of assumptions. In our example, if we assume that fires occur at a constant average rate (events per unit time), then the model for the number of fires in a given time interval is the Poisson model. We note that the stochastic model (the "model of the world" in the terminology of Decision Theory) introduces a set of parameters as well as a set of modeling assumptions.
2. State-of-knowledge uncertainties arise when the parameters of the stochastic model are not known precisely and its assumptions are not universally accepted as being true. Thus, we can distinguish between two subcategories of state-of-knowledge uncertainties, namely, parameter uncertainties and model uncertainties. While most of the statistical literature deals with the assessment of parameter uncertainties in the light of some evidence (usually in the form of a random sample, e.g., the number of fires over a period of time), it is becoming increasingly evident in PRA that a major source of uncertainty could be the model itself.

After the probabilities of occurrence of the scenarios have been evaluated, they are used to rank these scenarios, so that the most likely ones can be identified. These major (dominant) scenarios contribute the most to risk and can serve as the basis for decision making. If the expected consequences (risk) are judged to be unacceptably high, then the design or operation of the system can be modified to reduce the contribution from one or more of the dominant scenarios. Furthermore, the sensitivity of the total risk to various parameters, such as the

system's pressure and oxygen concentration, can be investigated and appropriate decisions can be made. These issues are discussed in the following sections.

2.2 Ground-Based Fire Risk Methodology

2.2.1 Overview and Critical Locations

The methodology for the assessment of the risks associated with fires in a system consists of the following three major tasks [2.5-2.6]:

1. The identification of the "critical" locations and the assessment of the frequency of fires.
2. The estimation of fire growth times and the competing detection and suppression times.
3. The response of the process.

A location is declared "critical" when the occurrence of a fire there has the potential of creating an abnormal condition, and at the same time, damaging the safety systems. Thus, the response of the process (Task 3) is crucial in the identification of the critical locations (Task 1).

In order to identify the critical areas, the analyst may use a number of methods. The first and simplest method employs only engineering judgment; the analyst surveys the entire system and identifies areas in which a fire may have safety significance. Although this method usually identifies the critical areas, the possibility of missing some areas is real.

A more systematic method structures the use of engineering judgment with an explicit system logical model. The analyst first constructs a representation of the system behavior using either event tree or fault tree logic. An event tree depicts possible accident scenarios following an initial perturbation (an "initiating event") and a fault tree indicates what failure events are required to cause a specified off-normal condition. Using either form with knowledge of the locations of important equipment within the plant, the analyst may then directly observe how a fire in a given area can initiate or contribute to important accident scenarios.

An example of a hypothetical critical area involving control and power cables is shown in Fig. 2.1. The logic model has already determined that trays A, B, and C carry cables, which, if failed, would lead to undesirable consequences. The occurrence of a large fire on the floor, as shown, could fail these cables, therefore, this location merits a detailed analysis, and is declared to be "critical". In other situations the cable trays are closer to the floor and one worries about a fire starting on one tray and propagating to the others.

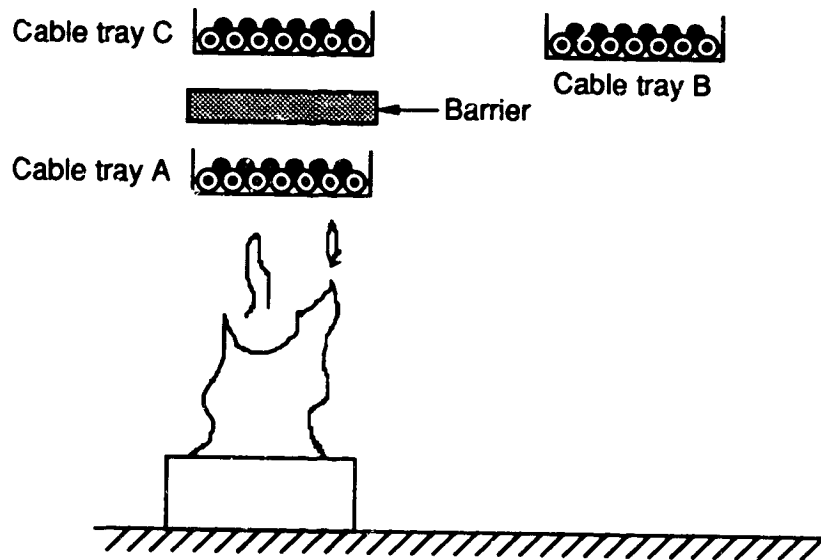


Figure 2.1. Sample Critical Location.

2.2.2 Fire Growth

In the second step, the time, T_G that it takes for the fire to propagate and damage redundant components is estimated. This requires the characterization of the environment (e.g., temperatures, velocities, concentrations of species) that is created by the fire in the compartment. The complexity of solving the three-dimensional time-dependent conservation equations has led to the development of approximate models. A model that is fairly representative of the kinds of approximations that have been made is COMPBRN, which has been developed at UCLA and is in its third generation at this time [2.7,2.8].

The basic approximation of the code is the division of the compartment into three regions, i.e., the layer of the hot gases that accumulate near the ceiling, the rest of the room, which is assumed to be in ambient conditions, and the fire plume. Figure 2.2 shows the essential elements of this approximation, as well as the heat transfer mechanisms that influence the target in the upper right-hand corner of the compartment.

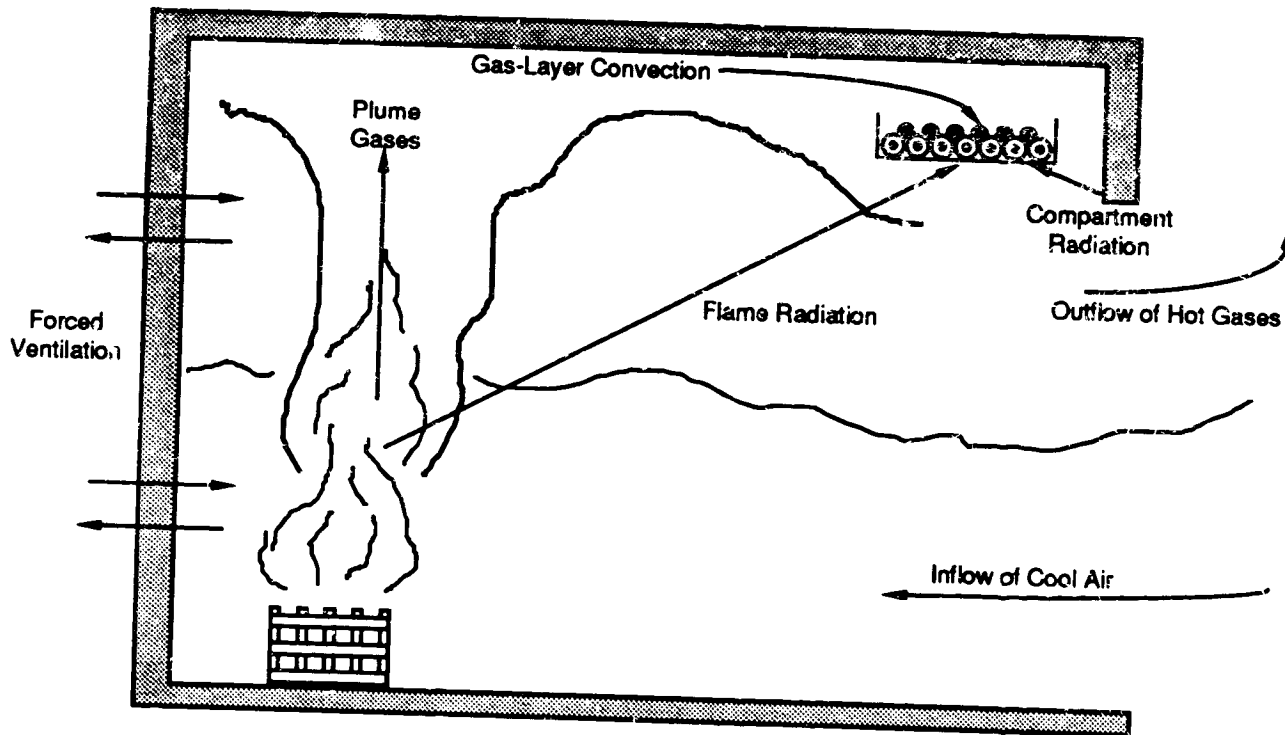


Figure 2.2. Hot-Gas-Layer Model [2.8].

In general, COMPBRN characterizes the environment surrounding selected fuel elements and determines each element's thermal response to its environment. It models the time-dependent development of the fire as well as the behavior of other sources of heat. The latter include the compartment walls and ceiling, and the hot-gas layer that develops and accumulates at the ceiling. A flow diagram for the basic computational scheme is shown in Fig. 2.3.

The fire is modeled using a quasi-static approach which incorporates a large number of steady-state models available in the literature for the different aspects of a fire's behavior. At each point in time, the steady-state mass burning rate of an ignited fuel element is computed with the aid of an appropriate model (the choice of model depends on the nature of the fuel and

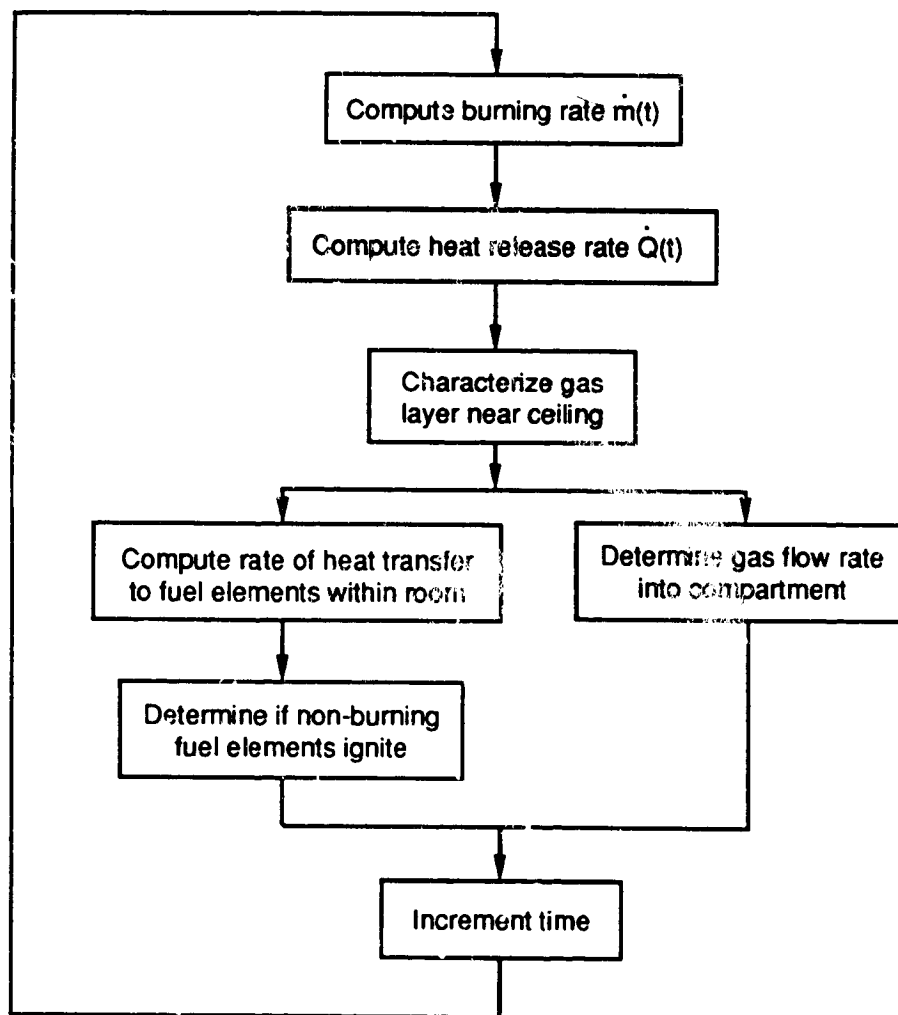


Figure 2.3. Flowchart of Computational Process in COMPBRN [2.6].

whether the fire is ventilation controlled; details on some of these models, as well as their applicability to low-gravity environments, are given in Chapter 3). The heat release rate is computed from the burning rate and the effective heating value of the fuel; this quantity, in turn, is used to compute the heat transferred to the surroundings by radiation and to the accumulating layer of hot gases near the ceiling by convection. Upon determining the average temperature and thickness of the ceiling gas layer, the heat fluxes to any fuel element in the room are calculated, and the element is considered ignited, if specified ignition criteria are met. The size, intensity and overall characteristics of the fire are thereby updated and serve as input for the next time step.

The hot-gas layer (HGL) is quasi-static and is determined by performing a heat balance on the hot-gas layer and mass balances on the hot zone at the ceiling and the cooler zone below. The hot-gas layer gains mass (hot gas and air) via the plume, and loses mass through the door or the forced ventilation system.

Damage is predicted to occur when the surface temperature exceeds its ignition temperature. To calculate the damage time, T_G , the general transient heat conduction equation in one spatial dimension (assuming constant properties), is solved for a semi-infinite medium subjected to a constant external heat flux at its boundary, as well as radiative and convective heat exchange.

2.2.3 Detection and Suppression

The sum of the detection and suppression times is represented by the "hazard" time, T_H . Since both the detection and the fire fighting phases of the suppression process can involve a number of different modes of action, a variety of fire suppression scenarios can be envisioned for a fire in any given location.

Fire detection can be via one of three modes: automatic, local, or indirect. Automatic detectors are installed in many of the rooms; they generally sound an alarm in the control room. Local detection by personnel in the area can either be essentially instantaneous (if the same people actually initiate the fire) or delayed (if the fire is detected by personnel arriving randomly in the involved room). The indirect detection mode involves the indication of some problem via abnormal control board displays; the operators, upon recognition of the problem, may send a person to investigate the source of the problem.

Once a fire is detected, a finite amount of time will pass before it is extinguished or at least controlled to the extent that it can cause no further damage. As in the case of the fire detection phase, different methods may be used to extinguish the fire. Two modes can be readily identified: (1) extinguishment by fixed installed systems (e.g., Halon flooding), and (2) extinguishment via portable equipment (e.g. manual hose stations, portable chemical extinguishers, etc.). Unlike detection, these modes generally are used consecutively rather than simultaneously. Furthermore, a significant delay may result while the plant operators decide which mode to use.

Probability distributions for the hazard time are developed by using the available statistical evidence, which is sparse and imprecise, experimental results, and engineering judgment [2.9,2.10]. The potential occurrence of fire damage to components is modeled as the outcome of a competition between the fire growth and fire suppression processes over time, with the conditional frequency of damage (given that fire occurs) given by

$$Q_{d/j} = \text{Fr}\{T_G < T_H/\text{fire}\} \quad (2.1)$$

2.2.4 Risk Calculations

The last task of the methodology outlined in Section 2.2.1 is highly process specific. It requires an assessment of the damage that the fires of the first two steps can cause in the system. This analysis is carried out for all the critical locations and the total frequency of damage due to fires is

$$\lambda_D = \sum_j \lambda_j Q_{d/j} Q_{D/d,j} \quad (2.2)$$

where

λ_j = frequency of fires of class j , where classes are determined by location and initial severity of the fire (step 1).

$Q_{d/j}$ = fraction of class j fires that lead to damage to specified components (step 2, see also equation (2.1)).

$Q_{D/d,j}$ = fraction of class j fires causing damage to components which lead to process damage (step 3).

Equation (2.2) represents a summation of risk contributions of different fire-initiated accident sequences; each product in that equation contains terms that represent system and component failures due to fire and to other causes such as human errors. Thus, the primary contributors to risk can be identified by ranking the scenarios according to their contribution to the total damage frequency λ_D .

2.3 Uncertainties

As discussed in Section 2.2.2, a major element in the risk methodology is the time to damage T_G for a given component. This time can be estimated by a computer code such as COMPBRN. The question, now, is what kinds of uncertainties are associated with this number.

As discussed in Section 2.1, the uncertainties associated with modeling of physical processes can be thought of as being of two kinds: the statistical uncertainties and the state-of-knowledge uncertainties. It is judged that the variation of the estimated propagation (growth) time is dominated by state-of-knowledge uncertainties. This means that the uncertainties in the models and the parameter values are considered to overwhelm the statistical uncertainty, an assumption which is reasonable in the light of the current state of the art.

Most of the parameters that must be used as input to COMPBRN are either fixed by the problem, e.g., its geometry, or are known to a satisfactory degree. On the other hand, significant uncertainties (at least to the extent that they must be represented by probability distributions) exist regarding the thermal and combustion properties of cable insulation and jacket material. The principal sources of uncertainty are the lack of information regarding the composition of these materials and of experimental evidence.

To propagate the parameter uncertainties to the code's output (the damage time), either Monte Carlo methods or response surface methods can be used [2.11]. The purpose of the response surface is to replace expensive computer run time with a much simpler analytical expression, that is, to represent the output of a computer code by a simple function of its inputs. The form of the specific response surface depends on the specific application. The coefficients in the response surface are estimated by using the data from a few runs of the computer code.

The model uncertainty is due to simplifying assumptions and the fact that the models used may not represent accurately the true physical process. The code is a collection of approximate models which are valid under certain conditions. The model uncertainty is due not only to our uncertainty in the accuracy of each model's predictions under the conditions they were developed for, but also to our uncertainty in the synthesis of these independent models. One of our primary concerns is whether this synthesis contains enough component models (i.e., if all important phenomena have been modeled).

To treat the model uncertainties, Reference 2.12 proposes to use an "error" or "uncertainty" factor E , which is multiplied with the code prediction to yield the actual growth time. Thus the actual growth (damage) time is given by

$$T_G = ET_{\text{DRM}} \quad (2.3)$$

where E is the "error" factor representing the analyst's confidence in the prediction of the code (called the deterministic reference model, or DRM) and T_{DRM} is the code's prediction. Both E and T_{DRM} are uncertain variables and, thus, are characterized by probability distributions. The distribution of T_{DRM} is determined by propagating input parameter uncertainties through the code, as discussed above. The distribution of E is assessed subjectively on the basis of comparisons of the code's predictions with experimental data or from expert opinions.

2.4 Risk Management

From the standpoint of risk management, the results of PRAs are of interest when applied to the following questions [2.13]:

- What possible options are there for reducing risk?
- How effective (and believable) are these options in reducing the risk?
- How desirable are these options?

While PRA can help us address these questions, it does not provide criteria for selection of an optimal alternative; this decision is the province of management, which must weigh the benefits and disadvantages of each alternative with respect to economic, regulatory, operational, and risk considerations.

Four general categories of the fire risk management options can be identified, based on the discussion of Section 2.2 and Eq. (2.2). They are options to:

- Improve the models employed in the original analysis.
- Reduce the frequency of occurrence and the potential severity of fires in the critical location of interest.

- Reduce the likelihood of important component damage, given a fire.
- Reduce the likelihood of subsequent system failures, given the loss of important components.

The first option stems from the recognition that the original PRA was performed under specific time, budget, and state of knowledge constraints. It is conceivable that further investigation of the critical fire scenarios will result in the identification and elimination of conservatisms in the original analysis. On the other hand, it is also conceivable that further study will corroborate the earlier results or may even identify some optimistic assumptions.

The frequency of fire in a particular zone (λ_j of Eq. (2.2)) may be reduced by changing the design of equipment in the zone or by improving administrative procedures. From Equation (2.1), it can be seen that the likelihood of component damage can be reduced by increasing the growth time, T_G , or by reducing the hazard time (the sum of the detection and suppression times), T_H . Improvements to the existing automatic detection and suppression system would reduce T_H . The possibility of spurious suppression system actuation may reduce the desirability of this option from an operations and maintenance point of view.

The last set of potential modifications concentrates on improving the system response to the loss of critical components due to fire, i.e., on reducing $Q_{D/d,j}$ of Eq. (2.2). Since the essential characteristic of the dominant fire scenarios is that a single fire damages a large number of important components and thereby renders many systems unavailable, a natural solution is to ensure that one or more critical systems are entirely independent of the dominant fire zone.

The fire risk methodology presented in this chapter has been developed primarily at UCLA and has been used in several PRA for nuclear power plants, e.g., [2.14, 2.15]. It will also serve as the basis for the definition of the proposed experiments.

References

- 2.1 B. De Finetti, *Theory of Probability*, Vols. 1 and 2, John Wiley and Sons, New York, 1974.
- 2.2 G. Apostolakis, "Probability and Risk Assessment: The Subjectivistic Viewpoint and Some Suggestions," *Nuclear Safety*, 19, 305-315, 1979.

- 2.3 S. Kaplan and B.J. Garrick, "On the Quantitative Definition of Risk," *Risk Analysis*, 1, 11-37, 1981.
- 2.4 G. Apostolakis, "Uncertainty in Probabilistic Safety Assessment," Trans. *9th Int'l. Conf. on Structural Mechanics in Reactor Tech.*, Vol. M, 395-401, Lausanne, Switzerland, Aug. 17-21, 1987, A.A. Balkema Publishers, Boston, MA, 1987.
- 2.5 G. Apostolakis, M. Kazarians, and D.C. Bley, "Methodology for Assessing the Risk from Cable Fires," *Nucl. Safety*, 23, 391-407, 1982.
- 2.6 M. Kazarians, N.O. Siu and G. Apostolakis, "Fire Risk Analysis for Nuclear Power Plants, Methodological Developments and Applications," *Risk Analysis*, 5, 33-51, 1985.
- 2.7 V. Ho, N.O. Siu and G. Apostolakis, *COMPBRN III - A Computer Code for Modeling Compartment Fires*, Univ. of Calif. Tech. Report UCLA-ENG-8524, (NUREG/CR-4566), 1985.
- 2.8 V. Ho, N. Siu and G. Apostolakis, "COMPBRN III - A Fire Hazard Model for Risk Analysis," *Fire Safety Journal*, 13, 137-154, 1988.
- 2.9 N. Siu and G. Apostolakis, "A Methodology for Analyzing the Detection and Suppression of Fires in Nuclear Power Plants," *Nucl. Sci. and Engr.*, 94, 213-226, 1986.
- 2.10 N. Siu and G. Apostolakis, "Uncertain Data and Expert Opinions in the Assessment of the Unavailability of Suppression Systems," *Fire Tech.*, 24, 138-162, 1988.
- 2.11 M. Brandyberry and G. Apostolakis, "Response Surface Approximation of a Fire Risk Analysis Computer Code," accepted for publication in *Reliability Engineering and System Safety*.
- 2.12 N.O. Siu and G. Apostolakis, "Probabilistic Models for Cable Tray Fires," *Reliability Engr.*, 3, 213-227, 1982.
- 2.13 M. Kazarians, N.O. Siu and G. Apostolakis, "Risk Management Application of Fire Risk Analysis," Proc. First Int'l. Symp. on Fire Safety Sci., National Bureau of Standards, Gaithersburg, MD, Oct. 7-11, 1985, pp. 1029-1038, C.E. Grant and P.J. Pagni, eds., Hemisphere Publishing Corporation, New York.

- 2.14 *Indian Point Probabilistic Safety Study*, Consolidated Edison Company of New York, Inc. and Power Authority of the State of New York, May, 1982.
- 2.15 *Seabrook Station Probabilistic Safety Assessment*, Prepared for the Public Service Company of New Hampshire and Yankee Atomic Electric Company by Pickard, Lowe and Garrick, Inc., 1983.

3.0 SCIENCE REQUIREMENTS

3.1 Introduction

3.1.1 Purpose

To determine the risk to manned spacecraft due to fire, the frequency that a given component will fail due to fire is needed. In determining this frequency, a physical model of the fire scenario of interest must be constructed. While terrestrial models of fire exist, as described in Section 2.2, there are no such models that describe the behavior of fire in space. The basis of this set of experiments is to validate certain theoretical models of fire behavior in space that can then, in turn, be used in predicting fire behavior and developing accident scenarios that could be used in risk assessment and management, as discussed in Chapter 2. It is clear that, at this stage of development of fire models for space applications, the principal issue is that of model uncertainty (Section 2.3). The models that will be used to describe fire scenarios are as follows:

Heat and Smoke Release Model

Heat Transfer Model

Damage Model

Detection Model

Suppression Model

Each of the above models possesses its own set of science requirements based on uncertainties in each model, and derived sets of equipment functional requirements.

3.1.2 Scope

In Section 3.2 this document presents requirements based on the Heat and Smoke Release Model, including the model description and the summarized science requirements for the experiments. Section 3.3 deals similarly with the Heat Transfer Model and Section 3.4 lists the requirements for the Damage Model. Section 3.5 introduces concepts related to detection and suppression, and Sections 3.6 and 3.7 deal with the detection and suppression scenarios and present associated science requirements for experiments.

3.1.3 Sensitivity Studies

Sensitivity studies will be performed during the proposed experiments. They will involve varying the oxygen concentration, atmospheric pressure, fuel orientation, fuel geometry, air flow rate, air flow pattern and ambient temperature. Possible atmospheres to be studied in the proposed experiments include recommendations from [3.1], and they are:

1. 12 percent O₂ at 150 kPa total pressure.
2. 16-21 percent O₂ at 100 kPa total pressure.
3. 30 percent O₂ at 70 kPa total pressure (to simulate the atmosphere of an airlock).

Fuel orientation and geometry will simulate, among other configurations, typical spacecraft redundant component arrangements and they will be varied to observe the mechanisms of flame propagation and radiative heat transfer between them. Air flows will simulate typical spacecraft air flow patterns and rates.

3.2 Heat and Smoke Release Model

3.2.1 Model Description

The rate of heat released from a fire is extremely important in modeling and predicting its performance (refer to the top two boxes of the flow chart in Figure 2.3). To determine the heat released from a fire in microgravity, the mass burning rate and its functional dependencies in microgravity must be determined. Several models exist for the mass burning rate for both flaming fires and smoldering fires. Their validity in microgravity must be determined. The rate of smoke released may be extremely important in microgravity as smoke may be a potential source of damage to sensitive components as well as aiding secondary ignition of other fuel sources through heat transfer and the presence of combustible gases (from smoldering fires). The size and amount of smoke particles will be determined from light attenuation measurements using optical densities. Models for the rate of growth of smoke concentration will be examined and tested.

3.2.1.1 Heat release

The heat released by a burning object is an important measure of the severity of the fire. The rate of heat release is a function of the properties of the material (heat of combustion) and the rate of reaction (mass burning rate). Combustion of the material is usually incomplete and, therefore, an efficiency term is often used to represent the extent of the combustion reaction.

The equation for the rate at which heat is released, \dot{Q} (kW), from the burning of a solid fuel (used in terrestrial fire models) is given by an expression of the following form [3.2]:

$$\dot{Q} = \eta \dot{m} H_f \quad (3.1)$$

where

η = the burning efficiency which accounts for incomplete combustion

\dot{m} = the mass burning rate [kg/s]

H_f = total heat of combustion of the volatiles [kJ/kg].

Equation (3.1) should be valid for a burning element in microgravity since it doesn't depend on gravity, however, the numerical value of the mass burning rate, and thus the heat generated, will be different for an object burned in space compared to the value for the same object burned in normal gravity because of the lack of buoyancy-induced flows to aid in pyrolysis. The burning efficiency is scenario dependent and will also be different in microgravity due to the different conditions of combustion. The heat of combustion is a tabulated material constant and although not directly measurable, it is the ratio of the actual heat of combustion to the theoretical heat of combustion.

Two methods of calculating the heat release are described below. Since oxygen is consumed in the combustion process, the first method measures the rate of oxygen consumption to estimate the rate of heat release in fire tests [3.3-3.9]. Based on the observation that the heat of combustion per unit oxygen consumed is approximately the same for most fuels commonly present in terrestrial fires, the basic correlation for the heat released is expressed as follows [3.4]:

$$\dot{Q} = \left(\frac{H_f}{r_o} \right) \left(\dot{m}_{O_2, in} - \dot{m}_{O_2, out} \right) \quad (3.2)$$

where

H_f = the heat of combustion

r_o = the stoichiometric oxygen/fuel mass ratio

$\dot{m}_{O_2, in}$ = mass flow rate of oxygen in inlet air

$\dot{m}_{O_2, out}$ = mass flow rate of oxygen in exhaust gas.

The stoichiometric oxygen/fuel mass ratio, r_o , is the ratio of the atomic weights of the fuel and oxygen required for complete combustion. Tabulated values of r_o for various materials can be found in Reference [3.8]. For example, in the complete combustion of propane:



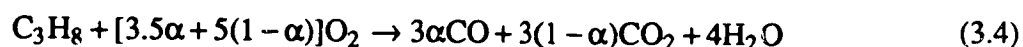
the ratio r_o is:

$$5(2 \times M_{\text{oxygen}}) / M_{\text{propane}} = 160/44 = 3.63$$

where

M_x = atomic weight of the compound x.

Since it is not feasible to measure the mass flow rate of oxygen, techniques have been proposed to measure the change in the volume fraction of oxygen molecules [3.3-3.9]. Correlations are provided to calculate the rate of heat release from the mole fractions of oxygen in the inlet and exhaust flow with or without the inclusion of CO_2 [3.6], assuming that either no other gaseous byproducts from the combustion (e.g., CO, H_2O , etc.) are formed, or all the byproducts can be trapped out. However, the neglect of the byproducts and the assumption of complete combustion can introduce a significant error in the estimation of the heat release rate [3.5]. As a remedy, r_o is treated as a function of a new quantity, α , which allows for the formation of CO. For example, in the combustion of propane, the following reaction scheme is not uncommon [3.9]:



where

$\alpha =$ the CO molar fraction in the CO + CO₂ mixture due to incomplete combustion.

In the case of propane in the above chemical reaction (3.4), α can be estimated in terms of $\Delta\dot{m}_{\text{CO}}$ and $\Delta\dot{m}_{\text{CO}_2}$:

$$\alpha = \Delta\dot{m}_{\text{CO}} / (\Delta\dot{m}_{\text{CO}} + (28/44)\Delta\dot{m}_{\text{CO}_2}) \quad (3.4b)$$

The stoichiometric oxygen/fuel mass ratio, r_o , in this case, will then be $[3.5\alpha + 5(1 - \alpha)](2 \times M_{\text{oxygen}}) / M_{\text{propane}}$.

The second technique that has been proposed measures the rate of production or depletion of several gaseous species, such that the heat release rate is [3.9]:

$$\Delta\dot{Q} = \sum H_i \Delta\dot{m}_i \quad (3.5)$$

where

$\Delta\dot{Q} =$ rate of heat released from the combustion

$H_i =$ the heat of formation of the molecular species i , which can be found in [3.8]

$\Delta\dot{m}_i =$ the rate of production/depletion of a given molecular species i , and

$$\Delta\dot{m}_i = Y_{i,\text{in}} \dot{m}_{\text{in}} + Y_{i,\text{f}} \dot{m}_{\text{f}} - Y_{i,\text{out}} \dot{m}_{\text{out}} \quad (3.6)$$

where

$Y_i =$ mass fraction of species i , (the subscripts f , in , and out refer to conditions in the fuel, inlet flow, and exhaust flow)

$\dot{m}_{\text{out}} =$ mass flow rate of the exhaust gas

$\dot{m}_{\text{f}} =$ mass burning rate of the fuel

$\dot{m}_{\text{in}} =$ mass flow rate of the inlet gas.

The heat release rate may, thus, be determined by the measurement of most of the gaseous products of combustion.

3.2.1.2 Mass burning rate

The burning rate, \dot{m} , is not only a function of temperature, available ventilation, and the nature, shape and size of the fuel, but also depends on the magnitude of the gravitational acceleration. This is due to the fact that the basic process of burning in normal gravity relies mainly on buoyancy forces which are not present in microgravity. Burning processes in microgravity are driven mostly by forced convection when ventilation is present, therefore, accurate representation of the ventilation patterns inside the spacecraft is very important in modeling fires in space (see Section 3.3.1). Several terrestrial models and correlations exist that express the mass burning rate as a function of many parameters, including air velocity, surface area and temperature. These models are either linear or exponential in nature, and may apply to flaming fires or smoldering fires. This section presents a review of some of the existing models and discusses their relevance to microgravity applications.

Flaming fires are usually modeled in risk assessments on earth because they are not uncommon and are a very serious threat to life and property. There are several ways of modeling the mass burning rate of flaming fires in terrestrial risk assessments. Linear models for the mass burning rate include "ventilation controlled" and "surface controlled" models [3.10-3.14]. If the burning rate is limited by the amount of oxygen available, the fire is labeled "ventilation controlled" and \dot{m} is given by

$$\dot{m} = C_v \dot{W}_{in} \quad (3.7)$$

where

C_v = a fuel-dependent proportionality constant

\dot{W}_{in} = the mass flow rate of air into the compartment [kg/s].

If the fire is not ventilation controlled then \dot{m} is limited by the fuel surface area, A , and is given by

$$\dot{m}'' = \dot{m}/A = \dot{m}_O'' + C_s \dot{q}_{ext}'' \quad (3.8)$$

Equation (3.8) is a simplified version of a gross heat balance performed at the surface of the fuel. The rate at which heat must be added to volatilize the fuel bed equals the total rate at which heat is supplied to the fuel bed minus the rate of heat lost from the fuel bed, i.e.,

$$\dot{m}'' H_f = \dot{q}_{fl,r}'' + \dot{q}_{ext}'' - \dot{q}_{loss}''$$

or

$$\dot{m}'' = (\dot{q}_{fl,r}'' - \dot{q}_{loss}'')/H_f + (1/H_f)\dot{q}_{ext}'' \quad (3.8a)$$

where

$\dot{q}_{fl,r}'' =$ the radiant heat flux from the flame to the fuel surface

$\dot{q}_{loss}'' =$ the heat flux emitted from the fuel surface

$\dot{m}_O'' =$ a fuel-dependent burning rate constant

$C_s =$ a fuel-dependent constant which is the inverse of the heat of combustion

$\dot{q}_{ext}'' =$ the heat flux impinging on the fuel from the walls and other sources of heat in the chamber.

Exponential models for the mass loss rate can also be found in terrestrial models. When heat losses from the fire are dominated by convection rather than radiation, the mass loss rate may also be related to the relevant convective heat transfer coefficient by the Spalding relationship [3.15]:

$$\dot{m}'' = (h/c) \ln(1 + B) \quad (3.9)$$

where

$h =$ the heat transfer coefficient for convection in the absence of fire (dependent on geometry and aerodynamic conditions)

$c =$ the specific heat of the gas (air)

$B =$ the Spalding mass transfer number.

B is given by:

$$B = A/H_c \quad (3.9a)$$

and

$$A = m_{og}(H_f/r_o) + c(T_g - T_s) \quad (3.9b)$$

where

H_c = the heat transfer by convection to the burning surface associated with the production of unit mass of fuel vapors [kJ/kg]

A = the change in enthalpy of unit mass of air as it moves from outside the flame to the fuel surface [kJ/kg]

m_{og} = the mass fraction of oxygen in the ambient atmosphere

H_f = the heat of combustion of the fuel [kJ/kg]

r_o = the stoichiometric ratio, oxygen:fuel, by mass

T_g = the temperature of the ambient air [K]

T_s = the temperature of the surface [K]

c = the specific heat of the gas in the region of the surface [kJ/kgK]

This model may not be valid for fires in microgravity if radiative heat transfer dominates in microgravity, as is currently believed. Other correlations for the mass burning rate which have exponential dependence on the fuel surface temperature and express heat transfer by conduction through a semi-infinite solid are given in references 3.16 and 3.17. These models are not favored for flaming combustion in microgravity as they describe large heat losses through in-depth conduction and not by radiation. The linear models are favored over exponential models for fires in microgravity based on results of the Skylab M-479 [3.18] experiments which found

that burning rates are much lower in microgravity than they are on earth. It was found that there was no tendency for the burning rates to increase exponentially in microgravity, as compared to horizontal and upward burning of the same material in one-g. This was also true for materials with thicknesses greater or equal to that of paper, when compared to downward burning on earth.

In conditions of microgravity, the burning rate is believed to depend strongly upon the air flow rate past the fuel source. In the absence of the more energetic, buoyancy-driven mixing, propagating flames can be sustained by the combination of the momentum generated in the vapor phase associated with the pyrolysis/vaporization of the fuel generation process and diffusion [3.19]. With some materials, however, this can only be true in the presence of oxygen concentrations much higher than those required on earth, otherwise the flames quickly become oxygen-starved. Therefore, even the presence of very slight forced flows to enhance the mixing process greatly increases the flammability and burning rate of a material. In this context, flames in microgravity could be considered "ventilation controlled."

In areas of high oxygen concentration, such as airlocks, enough oxygen may be present in the vicinity of the fuel so that it becomes "fuel controlled," as represented in Equation 3.8. Flames in microgravity may also be controlled by a combination of the two mechanisms, or by other mechanisms, such as radiative heat losses. It has been found on earth that a fire in a room may begin as "fuel controlled" with the energy release rate depending on the fuel pyrolysis rate. As the fire grows, it becomes "ventilation controlled" due to oxygen depletion of the air and the buildup of gaseous products around the fuel and the rate of energy release will be governed solely by the air supply rate. This turning point is termed flashover and is typically associated with compartment gas temperatures between 573-923K. It results in a sharp increase in room temperature and rate of energy release [3.20]. Studies in earth-based laboratories have shown that closed hatches in a cylindrical chamber accelerated the burning of insulation on the interior wall and raised the temperature above 473K and as high as 1073K in 60 seconds [3.21]. In the event of a fire on-board a spacecraft, the hatches may be closed to prevent the spread of the fire. In that confined volume, flashover could occur more rapidly than it does on earth. On the other hand, if the fires in space are considerably cooler than those on earth, a flashover phenomenon may not be observed. The controlling mechanisms for the mass burning rate must, thus, be identified as a basis for creating a heat release model in space.

Smoldering fires, rather than flaming ones, may be a greater threat in spacecraft due to the abundant presence of char-forming materials such as cellulose and polyurethane foams. Smoldering is a combustion mode characterized by thermal degradation and charring of the material, evolution of smoke and emission of a visible glow. Only porous materials, which form a solid carbonaceous char when heated, can undergo a self-sustained smoldering combustion. Smolder temperatures as well as spread rates are much lower than those found in flaming combustion (623-973K) [3.22] and smoldering can also survive on a much weaker air supply than what is required to support flames. Smoldering occurs more rapidly in flexible foams than in rigid foams because the cushioning application of flexible foams requires them to be permeable to air, while the insulating application of rigid foams requires the permeability to be close to zero to minimize convective heat transfer. However, the closed cells of rigid foams are like balloons and rupture at approximately 523K. Therefore, smoldering of rigid foams will remain on the surface until enough cells rupture to permit access to the interior. On earth, there are two possible categories of smolder propagation direction for 1-D cases: cocurrent smolder is propagation opposite to the direction of air flow (in the direction of gravity), countercurrent smolder is propagation in the same direction as that of the air flow. An expression for the mass loss rate of fuel, \dot{m} , has been determined for a 1-D cocurrent flow through a permeable bed based on the smolder front velocity, v_s , and the residue mass fraction of fuel, and it is given [3.15]:

$$\dot{m} = \rho v_s A (1 - \epsilon_p) \quad (3.10)$$

where

ρ = the density of the loose-fill insulation

A = the cross-sectional area of the smolder bed

ϵ_p = the residue mass fraction of fuel.

Since smoldering is greatly dependent on buoyancy forces on earth to supply oxygen, it is unknown whether smoldering in microgravity will more closely resemble cocurrent or countercurrent smoldering because of the lack of buoyancy-driven flows. Correlations, such as Eq. (3.10), may be valid in space, if smoldering progresses in a direction opposite to that of the forced flow of oxygen. However, if different behavior is recorded, new correlations may have to be formulated.

3.2.1.3 Smoke Release

This section deals with the investigation of the characteristics of smoke in microgravity. The hazards of smoke as well as the need for proper testing methods precedes a review of some of the existing models for the growth of smoke in a compartment. Light attenuation methods for the measurement of smoke particle concentration and size are presented along with the parameter known as the optical density, which is derived from attenuation measurements. An expression for the emissivity of smoke particles is also given.

In the event of a fire on-board a spacecraft, the rate of spread of smoke may be just as important as the spread of the fire itself. In addition to greatly decreasing visibility, smoke particles may damage sensitive electrical components. In space, the lack of gravitational forces may prevent the larger particles from settling out and a greater fraction would deposit on components. The type of atmosphere found aboard the spacecraft could greatly influence the damage done by smoke. In terrestrial experiments performed using a polystyrene sheet [3.24] it was found, not only that the rate of burn of the material increased with oxygen concentration and ambient temperature, but the size of the smoke particles also increased. This increase in size was due to the coalescence of smaller particles, which may partially explain the fact that the maximum optical density and the rate of increase to maximum obscuration decreased with increasing oxygen concentration and increasing temperature. These results may be particularly important in areas of the spacecraft with known high oxygen concentrations, such as airlocks, where oxygen may account for as much as 30 percent of the atmosphere.

In another set of experiments performed in a pressure chamber [3.25] it was found that the combustible and toxic properties of materials such as wood, wool fabrics and plastics depended on air pressure. The velocities of flame spread as well as material mass losses increased with pressure rise. The various effects of a spacecraft environment on the combustion of materials bears investigation. The volatile degradation products which are emitted during smoldering are not oxidized significantly. They represent a gaseous fuel which, in flaming combustion, would burn as a flame. These products are comprised of a complex mixture of high boiling point liquids and tars, quite different from smoke, which are flammable and toxic and may be extremely dangerous, if allow to accumulate in an enclosed space. This could be important in spacecraft, where ventilation flow patterns could create pockets where gases could accumulate.

The recognition that fire and smoke performance changes with changing environmental conditions has led to the concern that data from standard flammability and smoke tests does not reflect that which is actually observed in large fires. Correlations between full scale and standard smoke test data performed in References 3.26 and 3.27 were only satisfactory for materials which produced high levels of smoke in smoke tests. It was found that materials which produce low levels in smoke tests may produce high levels in large fires. This discrepancy in the data is directly due to the conditions under which materials burn in real fires compared to conditions found in standard tests. It has been observed that the fire performance of a material in a full scale fire is affected by properties other than those normally associated with fire tests, e.g., melting and the variation of the environment in terms of temperature and oxygen concentration (ventilation effects), both of which impact the rate of burning and smoke production. In contrast, the majority of fire tests use well-defined, static conditions including a fairly uniform oxygen concentration and perhaps a few different levels of incident heat flux.

Efforts to produce more meaningful fire tests include the development of a ventilated smoke test chamber [3.28] which has been utilized to obtain data on the physical characteristics of smoke particulates produced from flaming and nonflaming combustion of various materials. Ventilation gas compositions and radiant heating levels were varied to simulate real fire situations in tests of polyvinylchloride (PVC). It was found that smoke particle sizes measured tended to be larger with increases in radiant heating levels for nonflaming combustion. Particulate mass data showed also that the quantity of smoke was also substantially greater at heating rates of 6.2 W/cm² and 9.2 W/cm² than at 3.2 W/cm² (Figs. 3.1,3.2). Another experiment [3.29] found that during the combustion of thermoplastics such as polystyrene and nylon, the orientation of the specimen was very important with regard to the amount of radiant heat flux it received. It was observed experimentally that the smoke production of polystyrene was much less than that of PVC when burned in a vertical holder, although the opposite was true when the material was burned horizontally. This occurred as a result of the melting and dripping of polystyrene from the holder which prevented it from burning to completion. A trough was developed to catch the dripping material but it also blocked the material inside from the radiant source, therefore, the material was not completely pyrolyzed or was pyrolyzed under a less intense heat flux. The results of the test show that smoke generation depended on whether the sample remained intact and was exposed to the same heat flux for the duration of the test. Values of the maximum specific optical density for thermoplastics were up to six times greater when burned in the horizontal mode than when burned in the vertical mode. This points to the need to test materials in the configuration in which they will be found in real life applications. This is especially true for

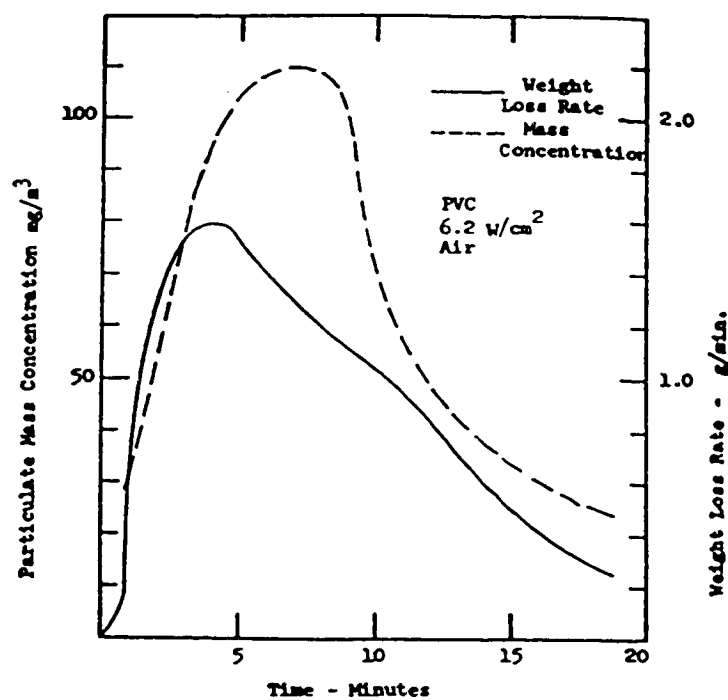


Figure 3.1. Comparison of Sample Weight Loss Rate with Particulate Concentration for PVC [3.28].

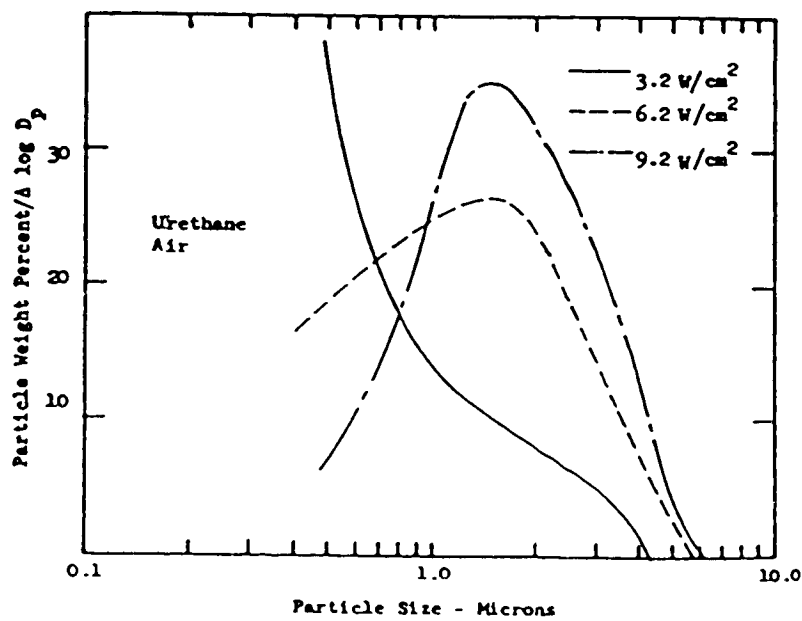


Figure 3.2. Particle Weight Distribution for Urethane Smoke in Air [3.28].

spacecraft materials in order to observe any additional effects of material separation while burning, such as secondary ignition. Extensive tests performed with electrical cables [3.30-3.33] have also shown that flame spread and extent of damage is extremely dependent on the configuration and spacing of the cable bundles, which is the reason why flammability tests on earth are required to be representative of the actual cable installation. This also confirms the need to test materials under conditions representative of those of the anticipated end-use hazard.

In the evaluation of the smoke generating properties of materials, particularly as pertains to risk, it is necessary to describe the variation of the quantity of smoke as a function of time. It is also necessary to relate the production of smoke to the fire in some way so that the amount of smoke produced by a given fire may be predicted. This is especially important in the development of damage models involving smoke (Section 3.4). A kinetic model [3.34] for smoke applicable to the burning of solid materials in controlled experiments assumes that the rate of smoke production is directly proportional to the rate of mass loss of the specimen and that the rate of smoke dissipation is proportional to the mass of smoke. Therefore, to model smoke as a dynamic system, the overall rate of smoke dissipation is the difference between the rate of dissipation and the rate of production:

$$dm_p/dt = k_1 m_i - k_2 m_p \quad (3.11)$$

where

m_p = the mass of airborne particulate matter (smoke)

m_i = the instantaneous mass of the burning sample

k_1 and k_2 = proportionality constants.

In Ref. [3.34], the sample mass is modeled as an exponential decay of the original mass, m_o , therefore, Eq. (3.11) becomes:

$$dm_p/dt = k_1 m_o \exp(-k_1 t) - k_2 m_p \quad (3.12)$$

which has the following solution:

$$m_p = m_o [k_1 / (k_2 - k_1)] (\exp(-k_1 t) - \exp(-k_2 t)) \quad (3.13)$$

The model from which Eq. (3.13) is derived made no assumptions regarding material or environmental variables, therefore, it is applicable in principle to experimental data obtained from

smoke tests in which the kinetic assumptions of the model, Eqs. (3.11) and (3.12), are valid. This means that Eq. (3.13) applies only to tests where smoke is accumulated in a closed chamber without ventilation, which may be valid in areas of a spacecraft such as an airlock. If the model were applicable, k_1 could be determined from the relationship between the original mass and the instantaneous mass (provided it was known) and k_2 could be determined from Eq. (3.13) given the mass of smoke particles. A test chamber in which air flows through the apparatus, carrying smoke with it, would have to account for the effect of ventilation in the smoke dissipation model and the above model Eq. (3.13), would not apply, therefore, an alternate model needs to be developed.

Concerning the issue of light obscuration, the primary means of smoke measurement are based on light attenuation measurements. The absorption of light due to smoke is measured in a variety of ways but all are based on the principle that the intensity of light transmitted through a certain apparatus decreases when smoke is present in the apparatus. All optical methods of smoke measurements are based on Bouguer's law:

$$I = I_0 e^{-\sigma L} \quad (3.14)$$

where

$\sigma =$ the attenuation coefficient [m^{-1}]

$I_0 =$ the intensity of the light source [kW/m^2]

$I =$ the intensity of the light at the end of the light path [kW/m^2]

$L =$ the light path length [m].

Smoke is assumed to consist of small solid particles of uniform size that can absorb and/or scatter light. Thus, as the beam traverses the smoke, the light intensity of the source, I_0 [W/m^2], is attenuated to a flux, I , at the end of the path length L . The results of this process are given in terms of the optical density, D , defined as:

$$D = \ln(I_0/I) \quad (3.15)$$

The attenuation coefficient, σ , is commonly used by investigators as a measure of smoke concentration. The "amount of smoke", S [m^2], is therefore defined in [3.35] as

$$S = \sigma V \quad (3.16)$$

where

$\sigma =$ the attenuation coefficient or "concentration of smoke" [m^{-1}]

$V =$ the volume in which the smoke is dispersed [m^3].

Although optical smoke measurements are useful in determining obscuration due to smoke, it is again necessary to express the amount of smoke in terms of the parameters of the fire so that a relationship between the fire and the smoke measurements may be determined. It has been found experimentally that the amount of smoke generated is proportional to the mass loss of the specimen, W :

$$S = kW \quad (3.17)$$

where

$k =$ an instantaneous smoke generation coefficient [m^2/kg], specific for a material.

By differentiation of Eq. (3.17) with respect to time, the rate of smoke generation, as shown in Fig. 3.3 over the entire combustion process, can be written as follows:

$$dS/dt = k dW/dt \quad (3.18)$$

where dW/dt is the mass loss rate, \dot{m} . Thus, the rate of smoke generation has two factors which have different characteristics. The mass loss rate is a function of ventilation or surface area, (Eqs. (3.7,3.8)). The smoke generation coefficient is specific for a material, independent of sample size, and is not a constant, but has been found by [3.36] to be a function of oxygen concentration as well as temperature (Figs. 3.4 and 3.5). It has been suggested that the two factors of the rate of smoke production be studied separately in order to obtain more basic data on the smoke-producing characteristics of materials [3.36].

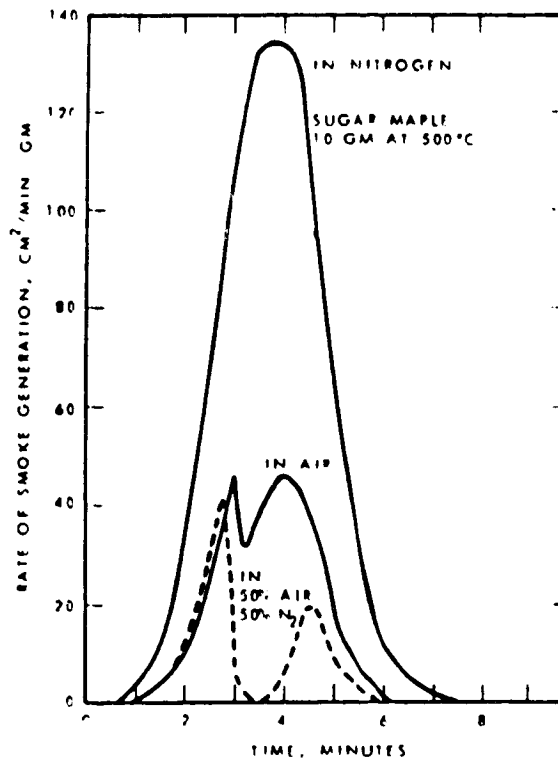


Figure 3.3. Rate of Smoke Generation During the Whole Combustion Process [3.36].

Rearranging Eq. (3.14), the attenuation coefficient may be expressed as

$$\sigma = (1/L)\ln(I_0/I) = D/L \quad (3.19)$$

where

D = the optical density as measured by light attenuation (Eq. (3.15)).

Furthermore, S may be determined by the expression:

$$S = \int \sigma v dt \quad (3.20)$$

where

v = the volumetric rate of smoke flow at the light path.

The overall smoke generating coefficient can then be calculated from:

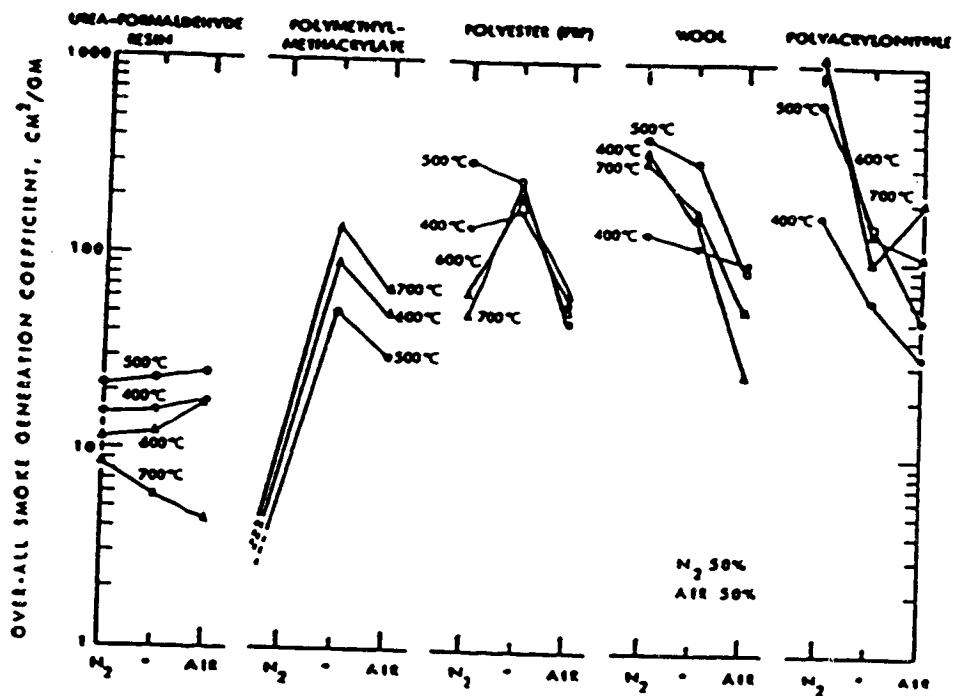


Figure 3.4. Overall Smoke Generation Coefficient of Various Materials [3.36].

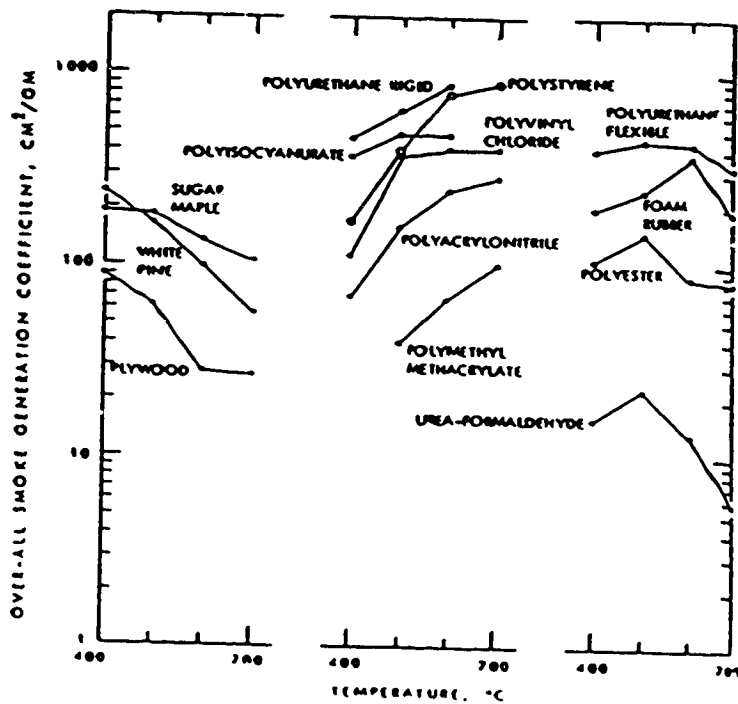


Figure 3.5. Effect of Temperature on Smoke Generation [3.36].

$$K = S/W \quad (3.21)$$

where

W = the mass lost by the sample.

Smoke measurements are most often expressed in terms of specific optical density, D_s , which can be obtained experimentally from light attenuation measurements and is defined as:

$$D_s = (V/AL)D \quad (3.22)$$

where

V = the chamber volume

A = the specimen area

L = light path length

D = optical density.

Much work has gone into the derivations of predictive parameters for full scale fires based on the measurement of D_s in smoke chambers. From work performed with the NBS smoke chamber, [3.37] two predictive parameters have been suggested: mass optical density (MOD) and particulate optical density (POD) which are defined as follows:

$$\text{MOD} = D_s A / m_s \quad [\text{m}^2/\text{kg}] \quad (3.23)$$

$$\text{POD} = D_s A / m_p \quad [\text{m}^2/\text{kg}] \quad (3.24)$$

where

m_s = mass loss of specimen

m_p = total mass of particles.

Experiments with wood and PVC [3.38,3.39] have shown, however, that the behaviors of MOD and POD seem to have limited application in modeling wood materials, with MOD especially varying with time and flux. The MOD is also found to vary for PVC and it is suggested that it is the concentration of smoke rather than m_s that should relate to the MOD, assuming that the POD remains constant.

The size of particles themselves are often measured by light scattering techniques. It is necessary, both in terms of obscuration and damage due to smoke, that the size of the smoke particles be known as a function of time. Differences will probably exist in the settling and coalescing properties of smoke particles in microgravity as compared to similar behavior in normal gravity. Since smoke particles are usually comparable to the wavelengths of visible light (0.3-5.0 μm) [3.40] the Mie scattering theory is applicable. In general, the total amount of light that a particle scatters follows the proportionality [3.41]

$$I_s \propto \lambda^2 f(\alpha) \quad (3.25)$$

where

$\lambda =$ the wavelength of the illuminating light.

and

$$\alpha = \pi d/\lambda \quad (3.25a)$$

where

$d =$ the particle diameter.

For the case of Mie scattering:

$$f(\alpha) = \alpha^n \quad (3.25b)$$

where $2 < n < 6$ (typically, $n = 5$ for smoke in terrestrial fires).

Light attenuation measurements, specifically the optical density, are also useful in calculating the total heat flux from the smoke due to gas and particle radiation using the following equation [3.42]:

$$\dot{q}''_{\text{tot}}/A = [1 - \exp(-k_3)D + \epsilon_{\text{go}}(1 - \exp(-2.3)D)/2.3D]\sigma T^4 \quad (3.26)$$

where

$T =$ the plume temperature [K]

$\sigma =$ the Stefan-Boltzmann constant [$5.67 \times 10^{-8} \text{ W/m}^2\text{K}^4$]

$\epsilon_{\text{go}} =$ the emissivity of the "soot-free" gas

$k_3 =$ an unknown constant which may be determined by the experimental determination of all other variables in the equation.

$\dot{q}''_{\text{tot}}/A =$ the heat flux from smoke which is equal to the following experimentally determined quantity, $(q/A)_2/F_{21}$, defined below.

The emissivity of the soot particles, ϵ_s , can be determined from the following equation, the right-hand side of which appears in Eq. (3.26):

$$\epsilon_s = 1 - \exp(-k_3)D \quad (3.26a)$$

The emissivity of the gaseous combustion products can be determined from the following equation:

$$\epsilon_{\text{go}} = (\dot{q}''/A)_2 / (F_{21}\sigma T^4) \quad (3.27)$$

where

$(\dot{q}''/A)_2 =$ the heat flux from the smoke measured by the radiometer

$F_{21} =$ the view factor, radiometer to plume reference surface.

After solving for " k_3 " using results from the experiments, the heat flux from smoke can be estimated from optical density, temperature and volume of smoke. The parameter k_3 is normally assumed to vary with temperature, however, the precise relationship has not been determined due to the limited amount of data available. Because of the small change in heat flux at

low burning temperatures, values of k_3 calculated at low temperatures and smoke concentrations could easily be 100 percent in error. This may pose a problem in space experimentation if the temperatures in the chamber remain low, which is possible given small sample sizes and lower burning temperatures in microgravity.

3.2.2 Objectives

The objectives of the proposed experiments are:

1. To develop numerical values for η so that \dot{Q} may be predicted.
2. To establish the functional dependency of the mass burning rate, \dot{m} , on air flow and/or surface area.
3. To establish the dependence of the amount of smoke production on the mass loss rate by determining a smoke generation coefficient K .
4. To predict the size of the smoke particles and verify the value of the exponent n , as well as the total amount of heat flux given off by smoke, by determining the constant k_3 .

The first objective will be accomplished by measuring the mass burning rates of heat release of several fuels and using Eq. (3.1) (Section 3.2.1).

The second objective will be accomplished by utilizing measured values of the mass burning rates. They will be plotted against known values of the air flow rate to determine the constant C_v in Eq. (3.2). The mass burning rates will also be plotted against experimental values of the external heat flux to determine \dot{m}_0'' in Eq. (3.3), (Section 3.2.1.2).

The third objective will be accomplished by measuring the amount of smoke by means of light attenuation measurements (determining the optical density) and comparing it to the amount of mass lost to determine the overall smoke generating coefficient in Eq. (3.16), (Section 3.2.1.3).

The fourth objective will be accomplished by measuring the sizes of the smoke particles and verifying the exponent in Eq. (3.25b). The heat flux from smoke will also be measured and the value of k_3 in Eq. (3.26) will be determined.

Sensitivity studies (Section 3.1.3) will be performed by varying the oxygen concentration, atmospheric pressure, fuel orientation, fuel geometry, air flow rate and ambient temperature because the mass loss rate and the amount of smoke produced may be greatly affected by any of these parameters, as stated in Sections 3.2.1.2 and 3.1.2.3.

3.2.3 Justification

Terrestrial risk assessments have found that the rate of heat release is extremely important in the characterization of fires. The mass loss rates of materials in space must, therefore, be determined, because fire in microgravity is controlled by different mechanisms than fire on earth. The amount of smoke produced by burning material must be determined in order to assess its risks as well as the overall smoke generating coefficient.

The experiments for determining the mass loss rate and, thus, the heat released, require more than thirty seconds of microgravity for completion; smolder experiments may take up to one hour. The fuel for flaming combustion must be burned to completion to determine the dependency of the mass burning rate. The material must also be burned to completion to determine the total amount of smoke produced. Therefore, these experiments must be performed in space.

3.2.4 Science Requirements

3.2.4.1 Mass Burning Rate

The mass burning rate of the fuel shall be measured as a function of time to a tolerance of (to be determined) kg/s. The mass loss rate shall be quantified for TBD fuels.

The size of the fuel samples to be burned shall be TBM cm x TBD cm x TBD cm. The configurations (e.g. rectangular, single sheet, parallel sheets) shall be TBD. The fuel samples shall be oriented at TBD degrees from the ignition source and TBD cm distance from the ignition source.

3.2.4.2 Rate of Heat Release

The rate of heat release shall be determined as a function of time to a tolerance of TBD kW. The rate of depletion of the concentration of oxygen shall be measured as a function of time and, when combined with the known value of the fuel-to-air mass ratio from the combustion reaction, the extent of the actual combustion reaction may be determined. The mass loss rate from this method may be multiplied by the heat of combustion of the fuel to find the actual rate of heat release. The rate of heat release shall be determined for TBD fuels.

3.2.4.3 External Heat Flux

The external heat flux onto the fuel shall be measured as a function of time to a tolerance of TBD kW/m².

3.2.4.4 Surface Temperature

The surface temperature of the fuel shall be measured as a function of time to a tolerance of TBD K.

3.2.4.5 Light Attenuation

The attenuation of light through smoke shall be measured as a function of time, to a tolerance of TBD kW/m².

3.2.4.6 Radiant Heat Flux

The total heat flux radiating from a volume of smoke shall be measured as a function of time to a tolerance of TBD kW/m².

3.2.4.7 Smoke Particle Size

The size of smoke particles shall be measured as a function of time at TBD points in the experimental chamber.

3.3 Heat Transfer Model

3.3.1 Model Description

This section discusses models for fire growth which deal with both the propagation of flame across the fuel and the transport of heat from a fire to a target at some distance from the fuel. Models for the propagation of the flame front in flaming and smoldering combustion are reviewed. Terrestrial models that describe the configurations of the flame and smoke patterns, which are related to their heat transfer properties, will probably not be valid in a space, therefore, some concerns dealing with the creation of new models will be discussed. Heat may be transported across space in two ways:

1. By convection from hot gases, and
2. By radiation from the fire, the wall and from the hot gases.

In order to determine the effects of heat transfer from hot gases, the pattern of hot gas flow must be determined in relation to the positions of the fuel source and the target. The relative size and shape of the hot gas is also necessary in determining the view factor for the radiation calculation. In order to produce a realistic fire scenario, the experiment must be scaled down from a realistic size to a model of a spacecraft compartment. An effort must be made to preserve the radiative effects in the model.

3.3.1.1 Flame Spread

The rate at which a fire grows is important in the determination of risk and it depends on how rapidly the flame can spread over the material. Flame spread acts both as a source of heat to the unburned material and as a source of piloted ignition. Several correlations exist to describe flame spread over solid surfaces, which is different in some aspects from flame propagation in smoldering combustion. Flame spread, as well as the propagation of a smolder wave, depend on pressure, oxygen concentration and air velocity and little is known about their behavior in micro-gravity, particularly with regard to smoldering.

In terrestrial fires, a distinction is made between propagation over thermally thick and thermally thin fuels with propagation being either in the horizontal, vertically upward or vertically downward directions. Under test conditions, transfer of heat through the gas phase is believed to be the dominant mechanism of flame spread for thin fuels [3.43,3.44] while conduction through the solid is believed to be the driving force for propagation over thick fuels [3.45,3.46]. In large scale flaming fires, radiation from the flames may dominate heat transfer to the unburnt fuel [3.47]. Flames propagate much faster in the vertically upward direction than in the horizontal or vertically downward directions. Flame propagation in the downward direction is steady almost from the outset while propagation in the upward direction reaches a steady state after an extended period of time, if at all. Limited investigation of flame spreading in reduced gravity has shown that low-gravity flames are similar to downward spreading flames in normal gravity [3.48,3.49]. Flame propagation is dependent to a great extent on pressure, oxygen concentration [3.50], and air currents. Flame spread usually increases with increasing oxygen concentration, see Fig. 3.6, and pressure and air velocities past the flame have varying effects on flame spread from enhancement to extinguishment.

The basic equation for the propagation speed is a simple energy conservation equation given by [3.51]:

$$V = \dot{q}'' / \rho \Delta h \quad (3.28)$$

where

V = the rate of spread

\dot{q}'' = the net energy flux across the surface of the flame front

ρ = the bulk density of the fuel.

Δh = the enthalpy change due to the temperature increases in a unit of mass fuel.

In practice, however, several correlations and mathematical models exist which correlate experimental results in dimensionless form [3.52-3.55]. In these correlations, the measured spread rate is most often expressed in the form [3.56]:

$$V_f = f(B) \quad (3.29)$$

where

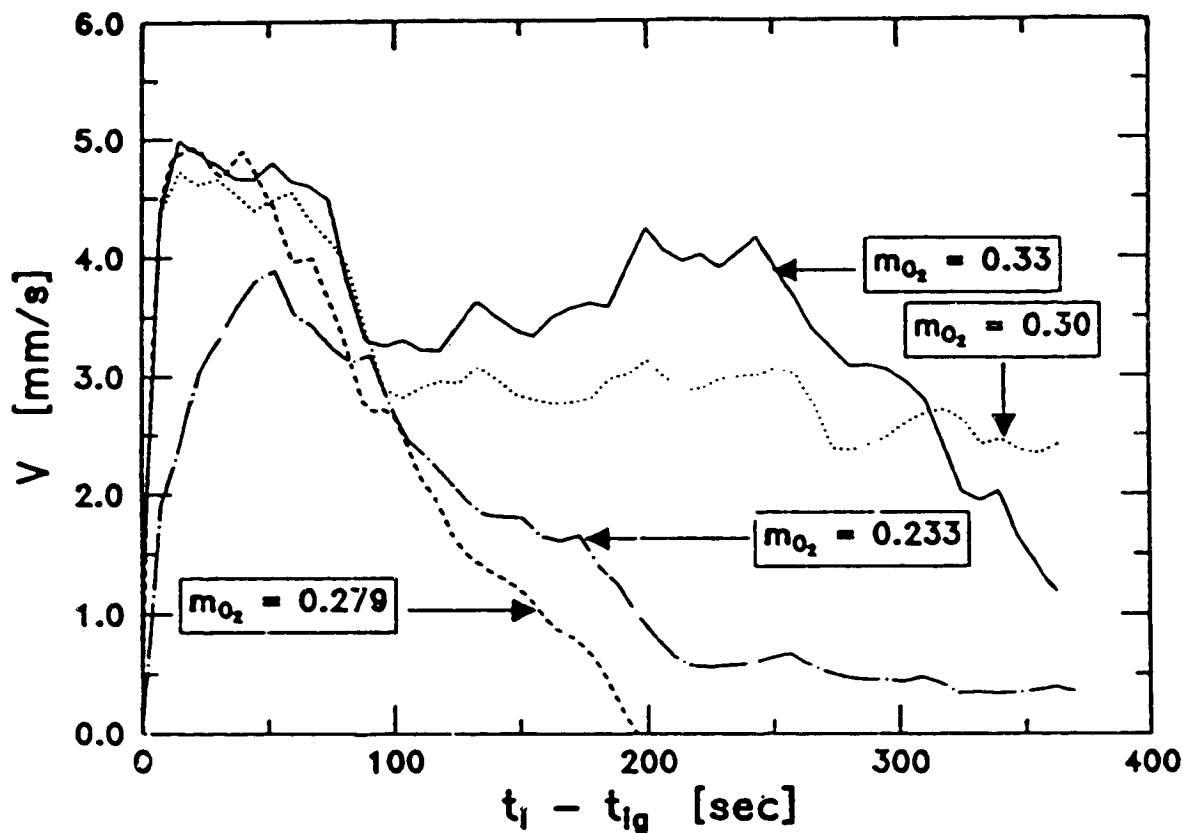


Figure 3.6. Increase in the Fire Propagation Rate Due to Increase in Oxygen Concentration for a Vertical, 1.29 m (4 ft) Long Cable. m_{O_2} Represents Mass Fraction of Oxygen [3.30].

V_f = a dimensionless spread rate which is a measure of the amount of heat transferred forward of the flame

B = Damkohler number which is the ratio of a fluid mechanical (residence) time to a chemical (reaction) time.

This correlation shows the existence of the two regimes of heat transfer mentioned above: one thermally controlled at large Damkohler numbers and one controlled by gas phase kinetics at small Damkohler numbers.

The propagation of flame in smoldering combustion is different from ordinary flaming combustion because the flame propagates through the material instead of on top of it, however, Eq. (3.28) still applies. A study of smoldering in cellulosic rods [3.57] has identified three distinct regions of the smoldering wave (Fig. 3.7):

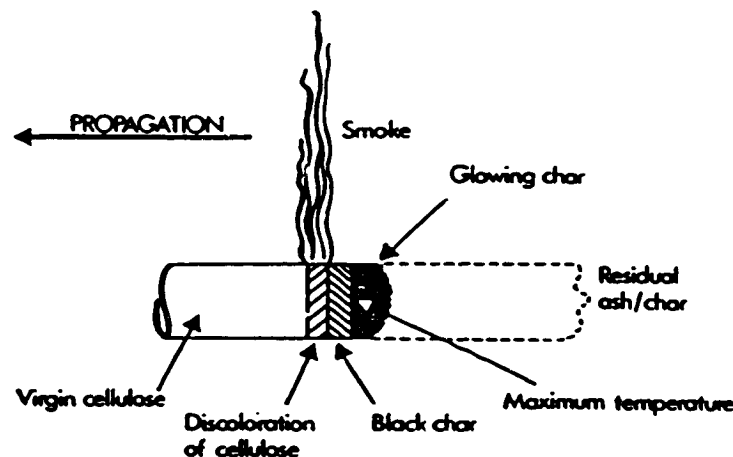


Figure 3.7. Representation of Steady Smoldering Along a Horizontal Cellulose Rod [3.50].

- Zone 1: Pyrolysis zone in which is is a sharp temperature rise and an emission of smoke and other gaseous products.
- Zone 2: A charred zone where the temperature reaches a maximum, smoke production stops and glowing occurs.
- Zone 3: A zone of porous residual char which is no longer glowing and whose temperature is falling slowly.

The mechanism of propagation of smoldering combustion is not as well understood as other types of combustion. However, it has been shown experimentally that the propagation speed depends strongly on oxygen mole fraction and partial pressure, as is the maximum temperature (Fig. 3.8). Smoldering combustion is an oxygen-limited phenomenon and the amount of oxygen received by the smolder wave depends on the magnitude of the buoyancy forces relative to the

drag forces. Experiments studying the effects of the buoyancy forces [3.58] found that, in the absence of gravity, diffusion of oxygen to the reaction zone is not a sufficient transport mechanism to support the combustion process, which suggests that for smolder combustion to occur in a microgravity environment, the flow of oxidizer must be forced through the fuel. This makes the convection of air by forced ventilation extremely important to smoldering combustion in space.

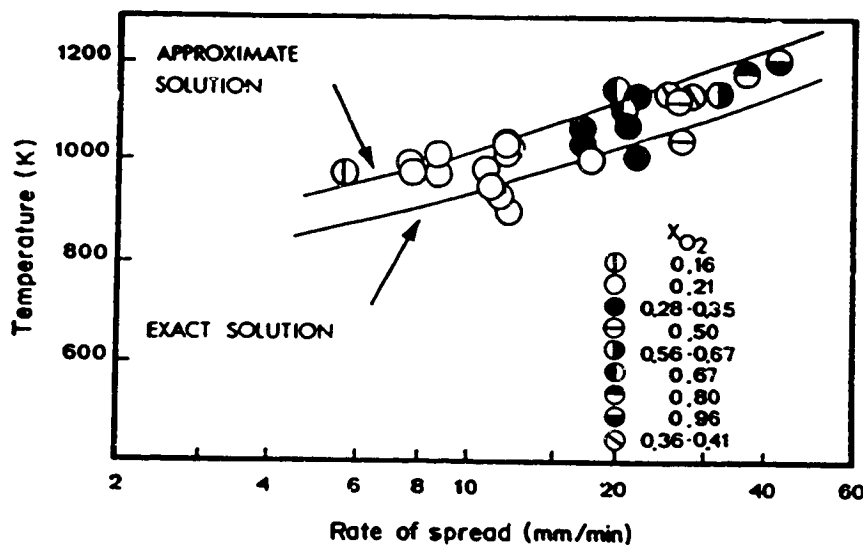


Figure 3.8. Data Showing the Correlation Between Rate of Spread and the Maximum Temperature in Zone 2 for Smoldering Along Horizontal Cellulose Rods. The Various Symbols Refer to Different Proportions of Oxygen in Nitrogen, Except for the Symbol O Which Refers to Oxygen/Helium Mixtures [3.50].

3.3.1.2 Heat Transfer to Secondary Sources

Terrestrial models for the transfer of heat to secondary fuel elements are well defined in terms of flame shape, plume shape and hot gas layer. Since these models will not be valid in space, other models must be developed, especially for the pattern of smoke flow. This also requires experimentation in a reduced scale apparatus so that the actual behavior of the fire in a spacecraft can be represented and measured. Several types of scaling procedures are reviewed for this purpose (Section 3.3.1.3).

In earth-based compartment fires, the hot gases rise and accumulate near the ceiling, forming a hot gas layer (see Fig. 2.2). Because of this buoyancy effect, approximate terrestrial fire models are composed of two layers, the upper hot gas layer (HGL) and the lower, cooler fresh air region. The fire itself is depicted as a vertical cylinder, possibly inclined at some angle,

from which a vertical smoke plume rises. The doorway mixing jet and the wall jet are usually combined with the plume flow model to form the air entrainment model, since they all take part in the entrainment of fresh air into the HGL (Section 2.2). They are the only mechanisms that allow mass exchange between the two regions and are considered part of the HGL. The lower region is often assumed to be thermally inert. Heat transfer to the target is thus the combination of convective transfer if the target is in the HGL, and the radiative transfer from the fire and hot gases with the view factors being well defined.

This two-layer model will not be valid in microgravity and its importance on earth suggests that an effort should be made to determine what will be present in space. If the assumption is made that the forced ventilation system will carry out some of the hot gases, then a pattern of hot gas flow throughout the module will be created that may leave pockets of hot gases trapped in certain areas of the module. This could be an extremely important aspect of fires and fire damage in microgravity. The patterns of hot gas flow created by a combustion source and the flow of ventilation in a spacecraft module, as well as the flame shape, must therefore, be determined through experimentation and modeling. In order to determine realistic scenarios for the combustion and spread of hot gases in a space station or Spacelab module, the experiment must attempt to duplicate all of the important parameters that exist in the actual module. Since a full-scale experiment in space is not possible, a scaling effort must be made to create a model of the module in which to conduct the experiment. In this way, meaningful results may be obtained that may correlate to the actual fire scenarios.

3.3.1.3 Scaling Methods

The study of fire phenomena in reduced-scale systems, based on the governing laws of physics, is both an essential and practical means of obtaining general results. The study of a fire phenomenon at a scale suitable for laboratory observation can also give insights into the mechanisms and behavior of the system, even if it does not give exact quantitative results. The use of dimensional analysis leading to the significant dimensionless parameters is a well-known technique for the generalization of experimental results and for establishing the laws of scaling for a system. Uses of dimensional analysis include the establishment of the governing parameters of the phenomena to be modeled and the reduction and rearrangement of the independent parameters into nondimensional form. This analysis is often carried out by the method of similitude in which: (1) important forces of the problem are expressed in terms of parameters by physical or dimensional arguments, and (2) pertinent nondimensional groups (often called pi groups)

are constructed by forming ratios of these forces (including enough length ratios to ensure geometric similarity). The basis for this method can be expressed by the following quotation [3.59]: "Two systems will exhibit similar behavior if geometric, kinematic and dynamic similarity are all guaranteed; furthermore, these conditions will be fulfilled if the two systems are made geometrically similar and if the ratios of all the pertinent forces are made the same in the two problems." Examples of common force ratios include, the Reynolds number, the Froude number and the Grashof number which are defined in Table 3.1 [3.2].

Similar behavior of two systems can generally be guaranteed if the two systems obey the same set of governing equations and boundary conditions and if all parameters in these equations and conditions are made the same. Fundamental governing equations used in fluid mechanics and combustion dynamics include: Conservation of Mass, Conservation of Momentum, Conservation of Energy, and the Radiative Heat Transfer Equation. These equations are presented in their dimensionless form (one-dimension) along with their corresponding pi's in [3.60]. There is no practical strategy currently in existence for matching all of the pi groups that define a system. However, partial scaling techniques exist that have produced good quantitative results and insight into fire phenomena at reduced scale and cost. Three such strategies have been used with success in fire research and they are referred to as analog modeling, Froude modeling and pressure modeling. In analog modeling, different fluids, such as water, can be used to simulate the buoyancy effects of fire in air, an unimportant concern in microgravity.

Froude modeling (also known as atmospheric, geometrical or proportional modeling) involves experiments performed in air at normal ambient conditions with the Froude number being preserved. However, since it is impossible to preserve both the Froude and Reynolds numbers at atmospheric pressure, Froude modeling assumes negligible solid boundary effects to justify ignoring the Reynolds number. This method is often used with success for purely natural convection conditions. Quarter-scale tests performed for the National Bureau of Standards [3.61] with different interior finish materials from low density foam plastics to high density cellulose, exhibited similarities in both the maximum temperatures reached and the times to flash-over for the full-scale and model rooms, but usually slightly longer times and lower temperatures were observed in the model. Problems encountered with the scaling include: (1) the lateral flame spread rates and flame heights did not scale, (2) the convective heat transfer coefficient in the model was too low since air velocities were proportional to the square root of the scale, and (3) the flame radiation was very scale dependent. Tests conducted at Factory Mutual Research

Table 3.1: Dimensionless Groups [3.2].

Group		Physical Interpretation
Froude	$Fr = \frac{u_{\infty}^2}{lg}$	$\frac{\text{inertia forces}}{\text{gravity forces}}$
Grashof	$Gr = \frac{g l^2 \beta T}{\rho v^2}$	$\frac{\text{buoyancy forces} \times \text{inertia forces}}{(\text{viscous forces})^2}$
	$= \frac{g l^3 \Delta \rho}{\rho v^2}$	$= Re \cdot \frac{\text{buoyancy forces}}{\text{viscous forces}}$
Reynolds	$Re = \frac{\rho u_{\infty} l}{\rho v^2}$	$\frac{\text{inertia forces}}{\text{viscous forces}}$

where

u_{∞} = final value of the flow velocity [m/s]

l = flame height or length [m]

g = gravitational acceleration constant [m/s^2]

β = coefficient of expansion

T = temperature [K]

ρ = density [kg/m^3]

v = linear flow rate [m/s]

[3.62] for various fuels (including wood cribs, alcohol, parafin oil and plastics) exhibited overall fire behavior which conformed well with the modeling hypothesis. However, some nonconformity between the temperatures of the thermal properties of the walls and the porosities of the fuel piles were not conserved. These last conditions are due to the fact that the re-radiation and convective exchange at the walls have to be forced to scale. Figure 3.9 shows higher temperatures in the larger model due to improper scaling of the wall thickness.

The most exact form of physical modeling is pressure modeling. If all of the lengths are scaled as a negative $2/3$ power of the pressure, both the Reynolds number and the Froude number are preserved, in which case the Navier Stokes equations take on the same dimensionless form for all scales. If radiation can be neglected or can be assumed to be proportional to the burning rate and if the fuel can be assumed to be a simple evaporating solid, such as PMMA, then the heat and mass transfer will also scale properly. However, the presence of radiation and char forming solids has caused some problems with pressure modeling. Experiments performed at Factory Mutual Research involving the burning of plexiglass cylinders [3.63] demonstrated that not only the gas phenomena, but also the solid-phase heat and mass transfer, fire spread, and other transient phenomena can be modeled by appropriately defining two time scales, one for the gas-phase and one for the solid phase. It was noted that, in general, the gas-phase times were reduced by the negative $1/3$ power of the pressure ratio, while the solid-phase times were reduced by the negative $4/3$ power of the pressure ratio. Steady burning rate measurements for both plexiglass and pine cylinders were shown to be correlated by the suitably defined Grashof number (Fig. 3.10), despite the fact that the re-radiation from heated surfaces does not scale properly. This may indicate that radiation is proportional to the burning rate.

The calculation of the radiative transfer to a secondary fuel source is extremely important in space as radiation is the primary mode of heat transfer, however, radiation is very difficult to scale. Radiation from flames, which typically represents 80 percent of the heat feedback in large scale fires, is generally dominated by external heat fluxes in small-scale fires. With regard to pressure modeling, re-radiation from solid surfaces is invariant with pressure if temperatures are preserved as required by modeling, however, other heat fluxes increase as $p^{2/3}$ at any given Grashof number. Although pressure modeling does not preserve radiative effects as it does convective heat transfer, it has been have found [3.64] that, despite this limitation, pressure modeling appears to work well for PMMA for wall fires up to 3.6 m or pool fires of less than 0.5 m in diameter. The successful modeling of wall burning rate and mass flux for a significant range of Grashof numbers implies that some radiative transfer processes must also scale. Figure 3.11

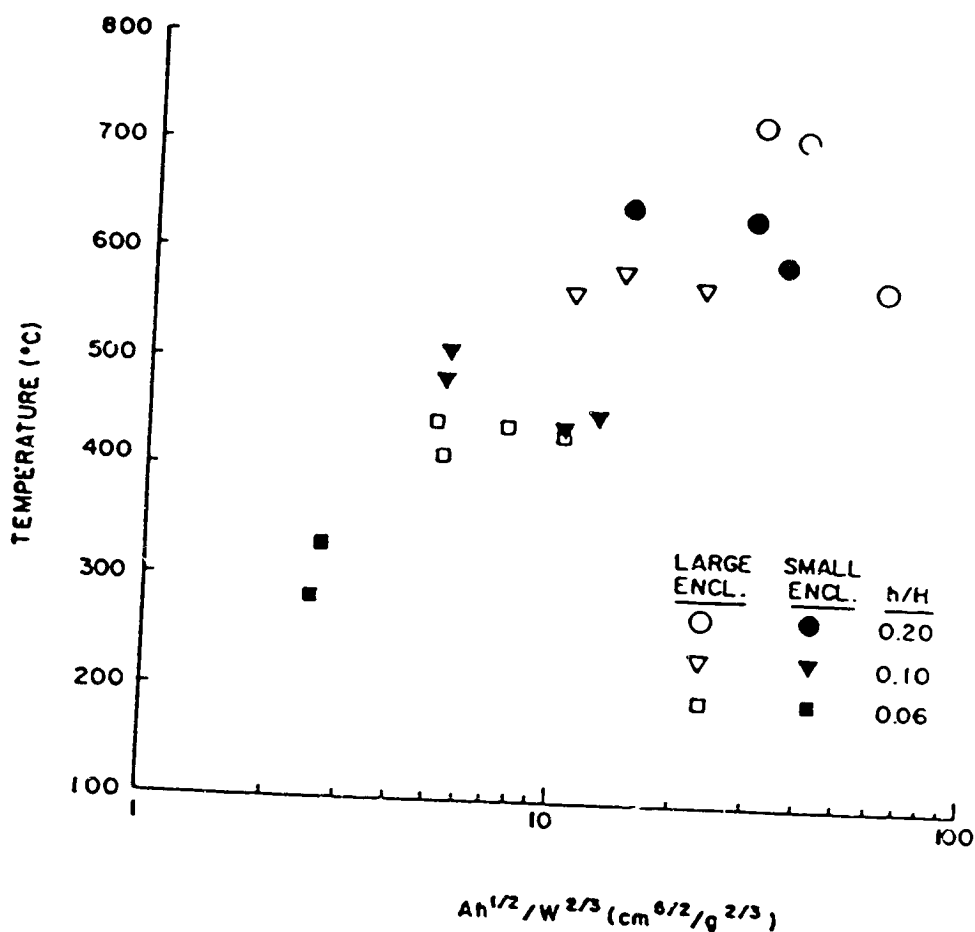


Figure 3.9. Temperatures; Average of Readings at Sampling Point and Image near Opposite Vent [3.62].

indicates that while the separate radiative components do not always increase sufficiently with ambient pressure, their difference does seem to attain the proper magnitude for a large range of Grashof numbers. This difference between the flame radiant flux and surface re-radiation is simply the net radiant feedback to the fuel surface and thus the driving force for PMMA vaporization. Results of pool burning rate as a function of Grashof number are given in Fig. 3.12. The model results can be seen to diverge beginning with pool sizes of about 0.4 m in one atmosphere. The burning rates for larger fires are lower in the models due to an insufficient increase in flame radiation with pressure. The model burning rates are greater at low Grashof number due to the low surface re-radiation at elevated pressures. The significance of this modeling technique seems to be its determination of broad trends due to changes in size and geometry.

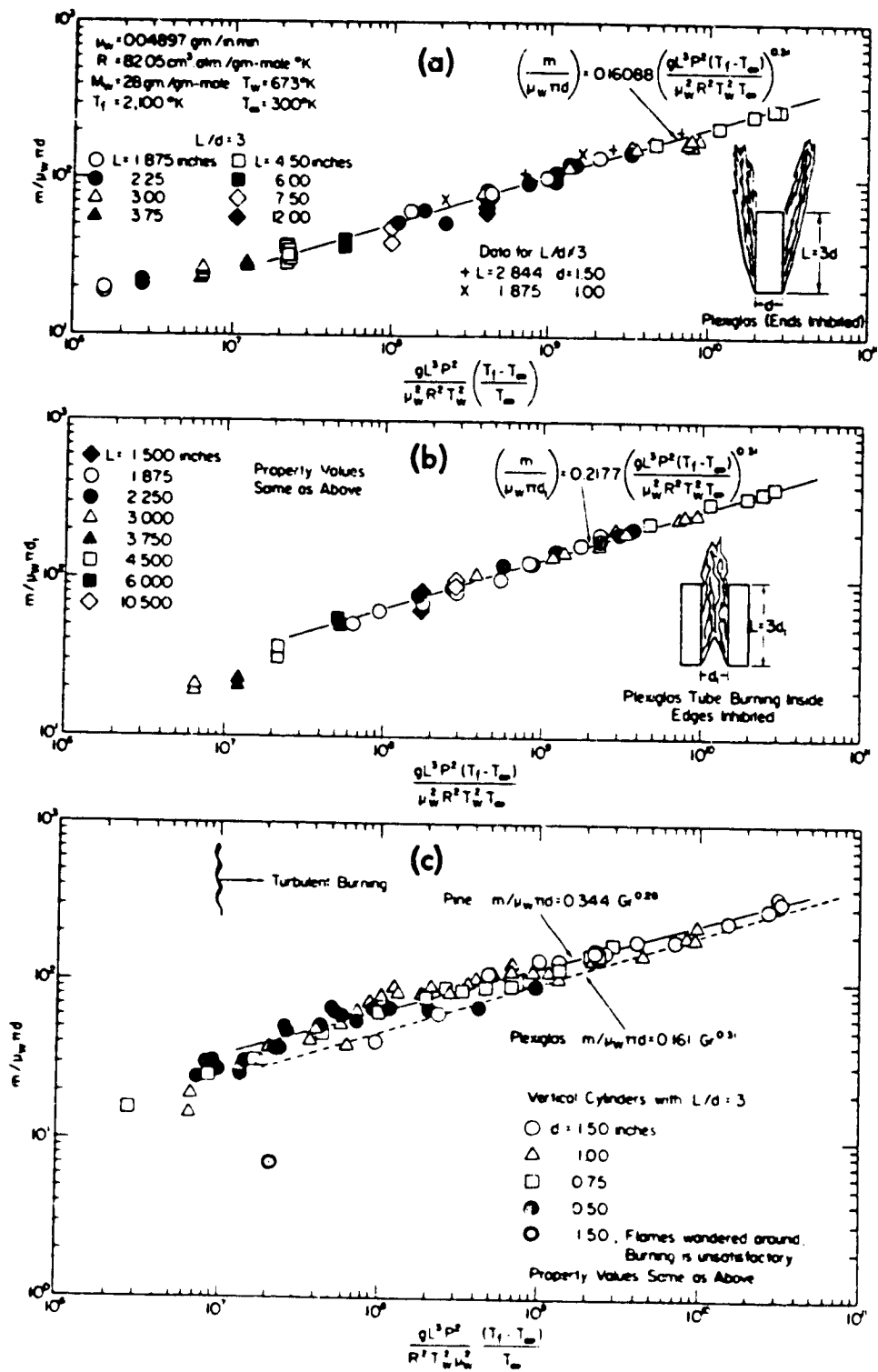


Figure 3.10. Burning Rate versus Grashof Number Correlation. (a) for Plexiglas Cylinder Burning; (b) for Plexiglas Tube Burning Inside; (c) for Pine Wood Cylinder Burning [3.63].

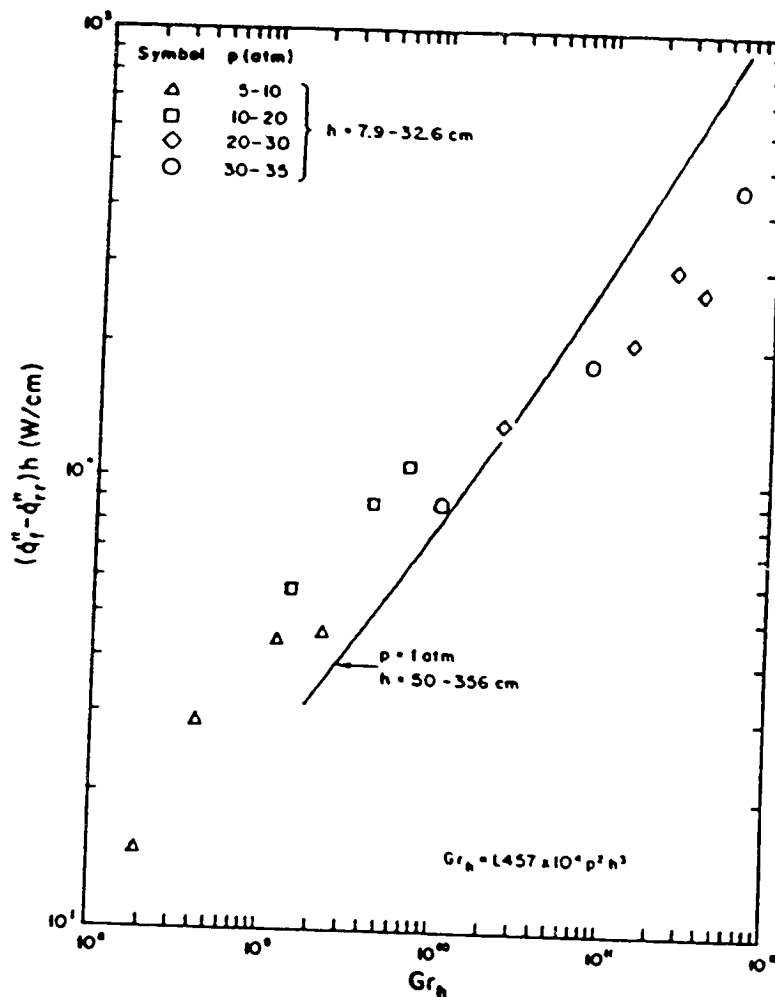


Figure 3.11. Behavior of the Net Radiant Flux Back to the PMMA Wall Surface with Grashof Number Based on Distance from the Bottom of the Wall. Symbols Correspond to $d = h/10$ [3.64].

3.3.2 Objectives

The objectives of these experiments are:

1. To determine the type of flame spread present in microgravity for both flaming and smoldering fires (Section 3.3.1.1).
2. To examine the transport paths of heat from a fire to another fuel source in a spacecraft module and/or electrical rack by attempting to determine the pattern of hot gas flow using a scaled model of a spacecraft module (Section 3.3.1.2).

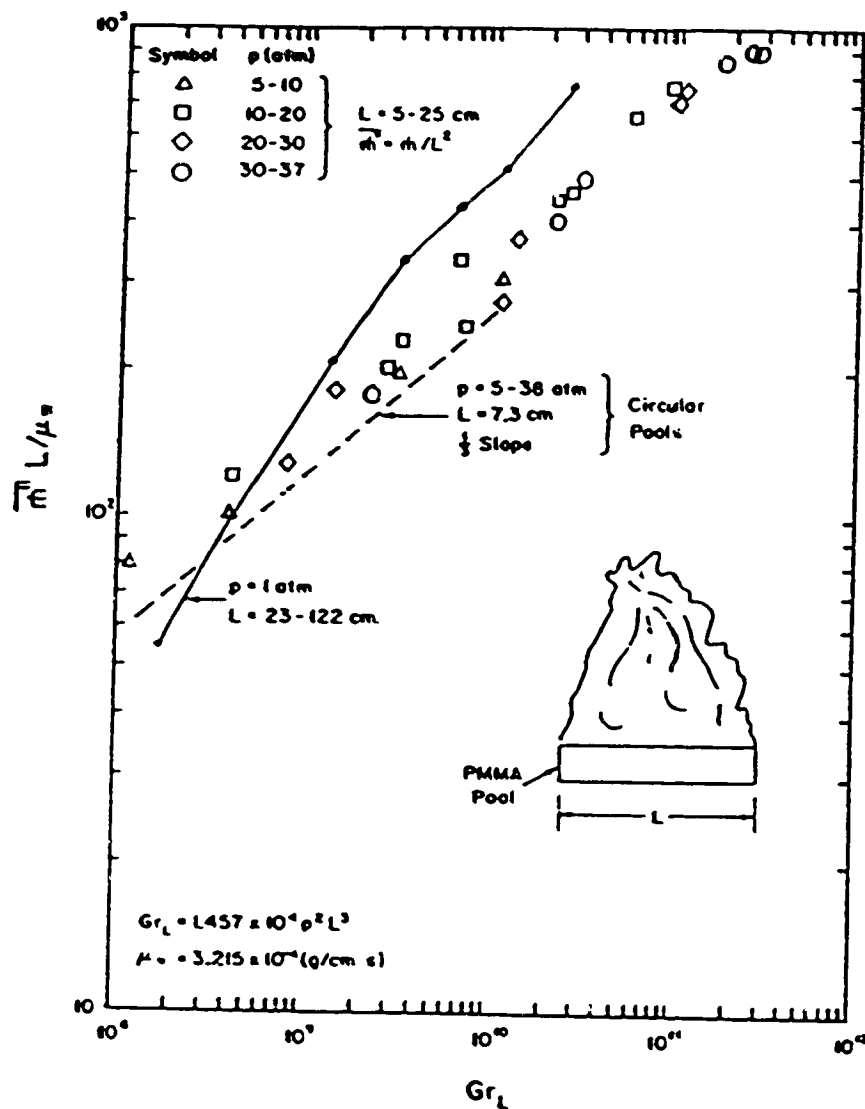


Figure 3.12. Variation of Nondimensional Pool Burning Rate with Grashof Number Based on PMMA Width [3.64].

The first objective will be accomplished by measuring the rates of flame spread for flaming and smoldering fires and comparing them to known terrestrial models.

The second objective will be accomplished by using scaling methods to duplicate the behavior of an actual fire in a spacecraft. The shape of the flame and the patterns of hot gas flow will be determined and their importance in the heat transport model evaluated.

Sensitivity studies (Section 3.1.3) will be performed by varying the oxygen concentration, atmospheric pressure, fuel orientation, fuel geometry, air flow rate and ambient temperature. The flame spread rate is affected by oxygen concentration, pressure and air flow rate (Section 3.3.1.1) and may be affected by fuel geometry, as in the case of electrical cable bundles (Section 3.2.1.3). The pattern of hot gas flow may be affected by fuel orientation relative to the ventilation pattern, air flow rate and ambient temperature.

3.3.3 Justification

To determine the risks due to fire in microgravity, a fire growth model must be determined for microgravity as it has been on earth (Section 2.2). One of the first stages of fire growth is the spread of flame over or within the fuel, therefore, models for the spread of flame in space must be determined, including the assessment of the validity of terrestrial models. The importance of the two-layer heat transport model on earth suggests a need to examine the same phenomenon (flame shape and smoke pattern) in space, especially given the relative importance of radiative heat transport in space.

Experiments to determine the flame spread behavior of a material require more than thirty seconds of microgravity, especially in the case of smoldering combustion, because the material must be burned to completion and flame spread occurs much slower in microgravity than on earth. Experiments to determine the pattern of gas flow must also allow the material to burn to completion as well as allow time for the smoke to spread throughout the chamber, which also requires more than thirty seconds of microgravity. Therefore, these experiments must be performed in space.

3.3.4 Science Requirements

3.3.4.1 Flame Spread Rate

The rate of flame spread shall be determined for TBD fuels by measuring the temperature of the fuel at various points as a function of time (3.3.4.2) and by visual recordings (3.3.4.6) to a tolerance of TBD m/s.

3.3.4.2 Temperature

The surface temperature of the fuel at the experiment chamber walls and the temperature of the chamber atmosphere (air and gases) at TBD points, including the outlet gases, shall be measured as a function of time to tolerances of TBD without disturbing the flow pattern.

3.3.4.3 Gas Flow Rate

The flow rates of the chamber gases shall be measured at TBD points throughout the experiment chamber as a function of time to a tolerance of TBD.

3.3.4.4 Species Concentration

The species concentrations of TBD gases shall be measured at TBD points throughout the experiment chamber as a function of time to a tolerance of TBD.

3.3.4.5 Smoke Concentration

The concentration of smoke shall be measured through light attenuation measurements at TBD points in the experiment chamber as a function of time to a tolerance of TBD.

3.3.4.6 Visual Record

A visual record of the distribution of gases and smoke in the chamber shall be made for the duration of the experiment.

3.4 Damage Model

3.4.1 Model Description

This section deals with predicting the ignition or damage of a known target, which may be another fuel source or, for example, sensitive electronic equipment. Existing terrestrial models deal only with the heat flux to the target, identifying damage or ignition when a critical heat flux is reached, e.g., in Ref. [3.32]. These models may also be used in space, provided that the temperatures and heat fluxes can be determined, however, another source of damage may be the presence of smoke particles and/or corrosive gases in an otherwise sterile atmosphere. The potential for damage due to smoke has been recognized and must be assessed.

In terrestrial models, which are primarily concerned with large flaming fires, all of the heat fluxes incident on a damage target are calculated and damage or ignition is predicted to occur when the temperature or heat flux of the target exceeds a prescribed limit. For example, studies involving the ignition of upholstered furniture [3.65] have shown that ignition of furniture padding tends to occur at radiant fluxes higher than 5 kW/m^2 ; typical ignition curves based on irradiance are shown in Fig. 3.13. Many models have been used, an example of which [3.2] utilizes one-dimensional conduction through a semi-infinite slab. The time-dependent surface temperature may be calculated by solving the transient heat conduction equation using the Crank-Nicholson finite difference scheme:

$$\delta T / \delta t = \alpha \delta^2 T / \delta x^2 \quad (3.30)$$

$$-K[\delta T / \delta x]_{x=0} = h(T_{\text{env}} - T_t) + \epsilon \sigma (T_{\text{env}}^4 - T_t^4) + \dot{q}_{\text{ext}}'' \quad (3.31)$$

where

- α = thermal diffusivity (m^2/s)
- K = thermal conductivity ($\text{W/m}^2\text{K}$)
- h = convective heat transfer coefficient ($\text{W/m}^2\text{K}$)
- T_{env} = the temperature of the environment (K)
- T_t = the damage target temperature (K)
- ϵ = emissivity of element
- σ = Stefan-Boltzmann constant ($\text{W/m}^2\text{K}$)
- \dot{q}_{ext}'' = the external heat flux (W/m^2).

This analysis is independent of gravity and, therefore, holds for microgravity applications, where radiation transfer is the primary mode of fire-related heat transfer. However, the temperature of the target, the external heat flux and the temperature of the environment may be affected by the combination of microgravity and forced ventilation found in the spacecraft modules. The type of

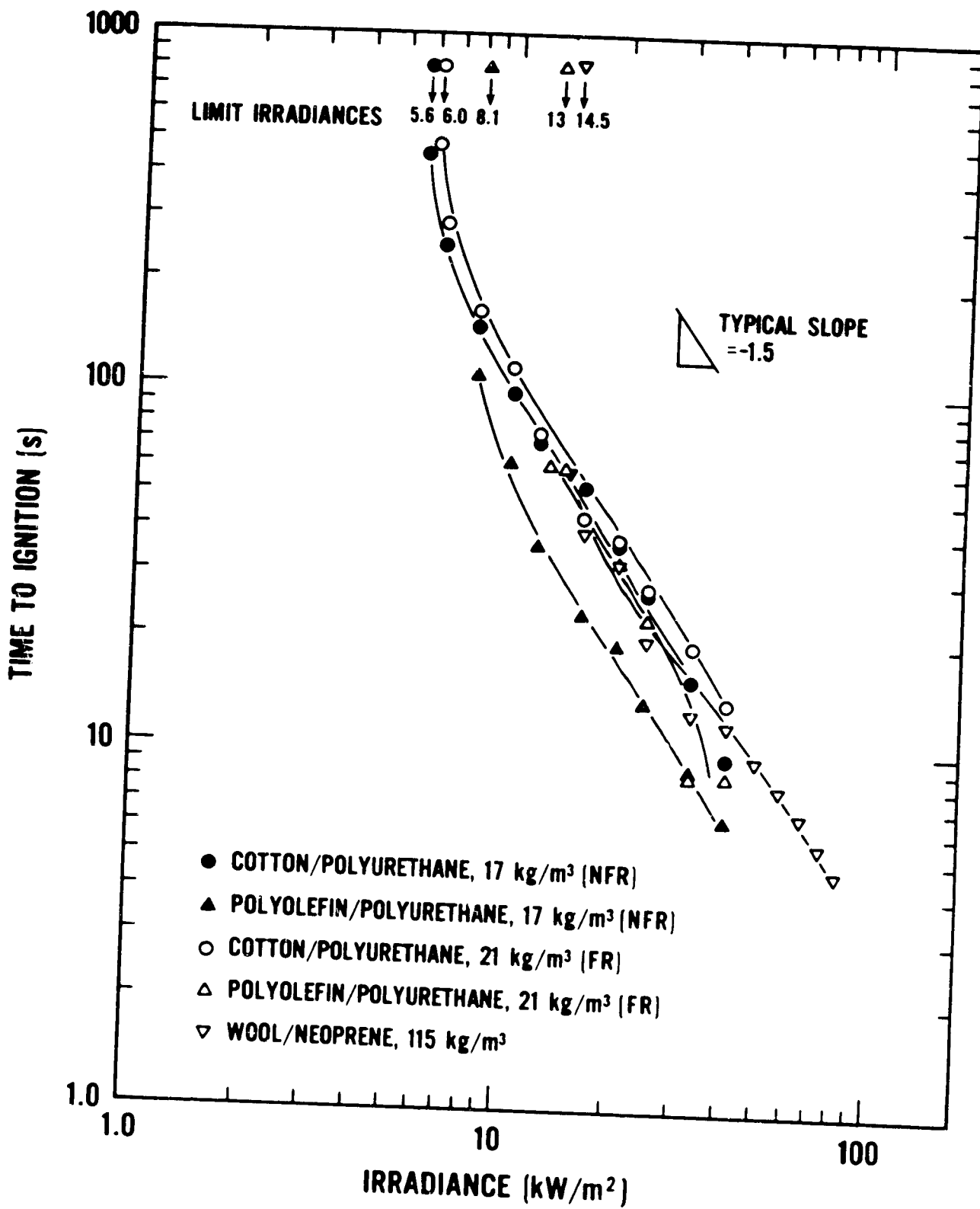


Figure 3.13. Typical Ignition Curves for an Range of Upholstered Furniture Fabric/Padding Combinations. The Abbreviations NFR and FR Refer to Non-fire-retardant Fabric and Fire-retardant Fabric Respectively [3.65].

damage target should also be considered when choosing a model. The heat transfer model used for cylindrical cable bundles may be different from the model needed when dealing with small pieces of electronic equipment and the surfaces to which they are attached.

Damage caused by smoke may be just as important as damage due to excessive temperatures. In addition to greatly decreasing visibility, smoke particles may damage sensitive electrical equipment by shorting circuits, causing open circuits or corroding the material itself. Smoke particles with high emissivity (typical of microgravity combustion) could also increase heat transfer to adjacent surfaces. Corrosion of electronic materials may occur uniformly or locally at a continuous or discontinuous rate but it eventually leads to material failure. The high levels of reliability required in spacecraft, even with redundant components, are achievable only if failures from corrosion are essentially eliminated. The structural elements involved in electronic devices are often very small, with separations and other distances measured in micrometers, therefore, even small amounts of corrosion or small particles, of the order of nanograms or less, can cause problems to unprotected devices and even device failure. Particularly when corrosion is localized, the structural elements themselves can be altered by the corrosion and the electrical properties of the adjacent regions can be changed [3.67]. The corrosion behavior of any material or structure is determined by its local environment (oxygen, pressure). The amount of damage caused to sensitive components by the presence of smoke and other corrosive products must be determined as a function of the atmosphere present.

3.4.2 Objectives

The objectives of these experiments are to develop the various damage models applicable to the specific scenarios found in space in terms of damage or ignition due to heat flux and damage due to smoke or corrosive gases. In addition to determining the rate of temperature increase of the target, the deposit rate of smoke particles and their size distribution must also be determined and the damage caused by them assessed.

Sensitivity studies (section 3.1.3) will be performed by varying oxygen concentration, atmospheric pressure, target orientation, air flow rate and ambient temperature. Orientation of the target with respect to the fire source and the air flow rate may have an effect on the pattern of hot gas flow seen by the target, which would affect its impinging heat flux, as would the ambient temperature. Corrosion of electronic materials is sensitive to the type of atmosphere present, for example, oxygen concentration and pressure.

3.4.3 Justification

The risk due to the secondary ignition of fuel elements and/or the damage of sensitive electronic components must be determined from a damage model which predicts the time to damage, given a fire, based on a specified temperature of ignition or a specified rate of smoke particle deposit. Experiments to determine these damage and ignition limits must allow time for the fire to grow, the heat or smoke to reach the target, the target to heat up to the point of ignition or exhibit damage from smoke particles. This scenario will require more than 30 seconds of microgravity, therefore, these experiments must be performed in space.

3.4.4 Science Requirements

3.4.4.1 Smoke Particle Deposit Rate

The rate of deposit of smoke particles on TBD damage targets shall be measured.

3.4.4.2 Temperature

The surface temperature of the damage target shall be determined as a function of time.

3.4.4.3 Smoke Particle Size

The size of the smoke particles deposited on the target shall be determined.

3.4.4.4 Heat Flux

The heat flux to the damage target shall be measured as a function of time to a tolerance of TBD kW/m².

3.5 Fire Protection in Microgravity

Current designs of spacecraft fire protection systems (Figs. 3.14-3.15 provide examples of systems designed for Spacelab and the space shuttle [3.68]) are generally based on terrestrial technology and experience. Since full scale testing of these systems in their working conditions is impractical and virtually impossible, the development of physical models that lead to the quantification of the response of various fire detectors and suppression systems is essential in order to perform a risk analysis to evaluate the performance of fire protection systems in manned

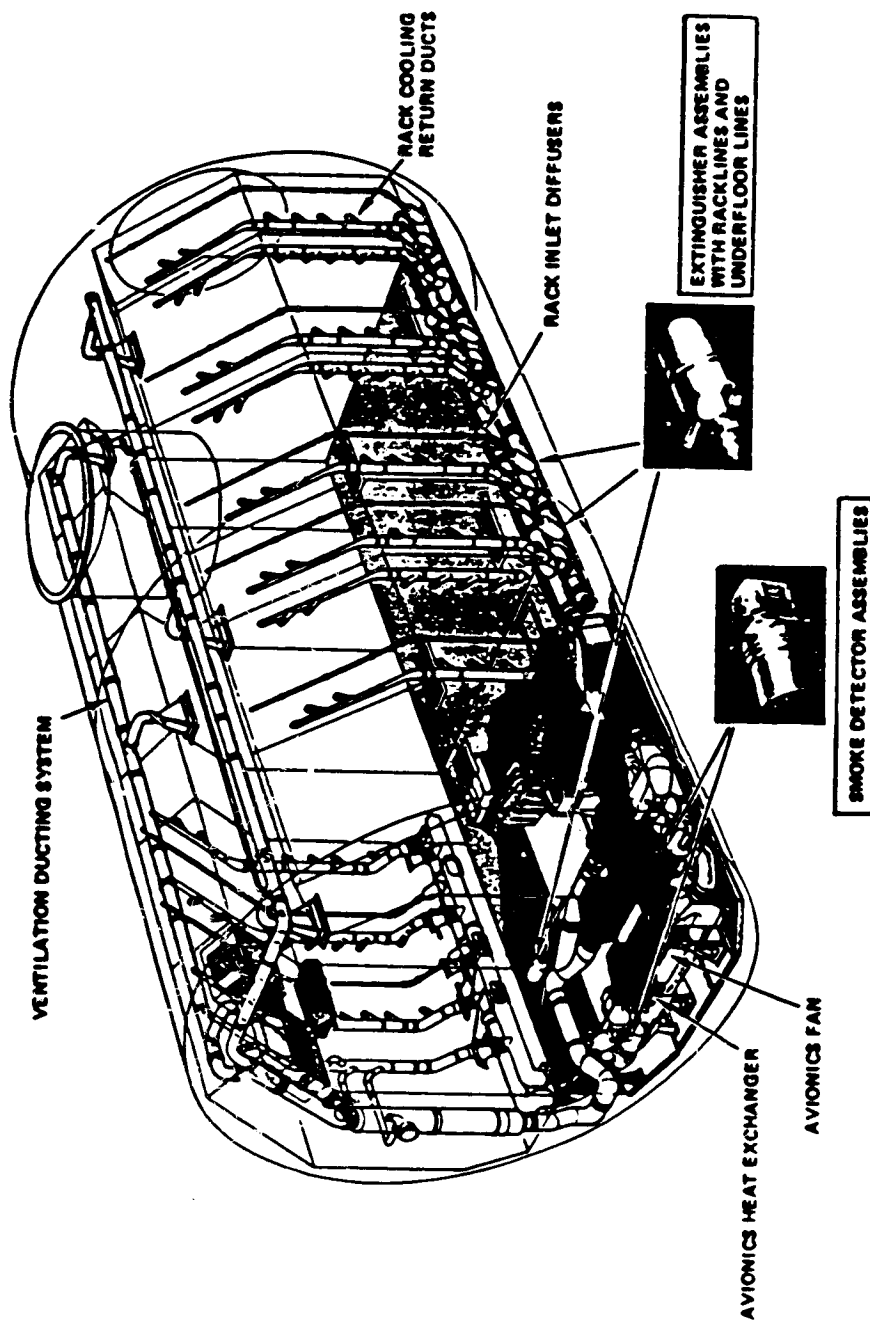


Figure 3.14. Fire Protection System for the Spacelab [3.68].

ORIGINAL PAGE
BLACK AND WHITE PHOTOGRAPH

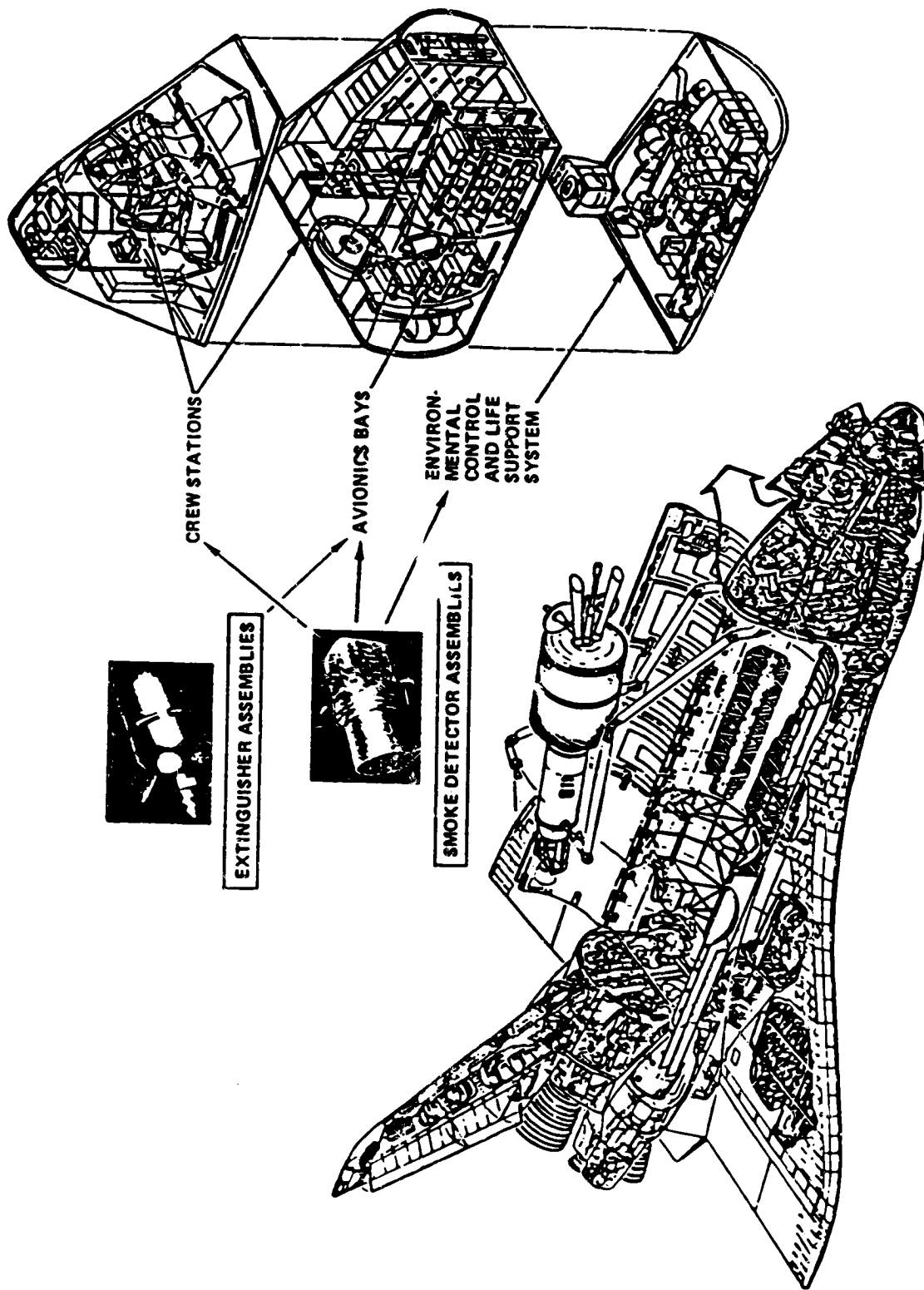


Figure 3.15. Arrangement of Fire Protection System for the Space Shuttle [3.68].

BLACK AND WHITE PHOTOGRAPH

spacecraft. This development requires substantial knowledge of fire detection and suppression processes in microgravity environment. Because the knowledge of fire phenomena and smoke transport in microgravity, which is essential to the development of the risk models, is limited, concern for fire protection in space has introduced new research and development challenges.

3.5.1 Purpose

Various models have been developed to predict the response of detectors and sprinklers for terrestrial facilities. The applicability to a microgravity environment is uncertain. This leads to the need for in-space fire detection and suppression experiments to verify the applicability of these terrestrial risk models in microgravity, and to identify unknown or uncertain elements.

The simulation of ignition-detection-suppression processes will help to identify any unaccounted for scenarios, and will provide information about the interaction between detection and suppression processes. The results will be useful in the development of risk models for the processes in microgravity.

3.5.2 Scope

Unlike fire protection strategies employed in terrestrial facilities, concerns for fire protection equipment in space include not only its ability to detect and suppress a fire, but also to decontaminate the module from combustion products and to remove spent suppressant. However, a quantitative decontamination model is not presently available, therefore, the models investigated in this Chapter are limited to detector and fire-suppressant interaction models. These models estimate the essential time competing factors that are identified from the fire detection and suppression processes. The physiological effects of the suppressants on the astronauts require long term monitoring, and is not within the scope of the present work.

In this section, the various fire protection models that may be applicable in microgravity are presented; the justification for the need for in-space experiments to verify these models is discussed; the objectives of the required experiments are identified; and the science requirements of these objectives are provided. Functional requirements and experiment designs will be presented in the following chapters.

3.5.3 Time Characteristics of Fire Detection and Suppression Processes

Prompt fire detection and suppression can protect life and property from the heat and by-products (e.g., smoke or toxic fumes) released from a fire. For example, the installation of smoke detectors and automatic sprinkler systems in buildings often provides early warning for safe evacuation of personnel and reduces property damage resulting from fires [3.69].

As discussed in Section 2.2, the fire growth, detection, and suppression processes are time-competing processes and can be summarized by the characteristic time factors T_G and T_H . A component X is damaged by fire if $T_G < T_H$, where T_G is the fire growth time and is defined as the time it takes for the fire to propagate to X and damage it. T_H is the hazard time and is defined as the total fire exposure time during which X can be damaged by the fire. The conditional frequency that X will be damaged, given that the fire occurs, is given by Eq. (2.1), which, for convenience, is repeated here:

$$Q_X = \text{Fr}\{T_G < T_H/\text{fire}\} \quad (2.1)$$

Equation (2.1) simply says that the damage frequency of X , given that a fire has occurred, equals the frequency by which the growth time is smaller than the hazard time, i.e., the time to damage a component, given a fire, is shorter than that time it takes to detect and suppress the fire.

Since a component can be damaged not only by the heat effect of a fire, but also by the smoke generated from the fire source, the estimation of the frequency of damage should be conditioned to smoke, as well as fire. Various models have been developed to simulate T_G for terrestrial fires. These models, including heat release, smoke generation, and component damage models, are investigated by experiments defined in the previous subsections. The following section describes the models developed to estimate T_H .

3.5.4 Hazard Time Model

The hazard time T_H is determined by the interaction of fire protection systems such that:

$$T_H = T_D + T_S \quad (3.32)$$

where

T_D = the detection time, which is defined to include not only the time to acknowledge the presence of the fire, but also the time interval following acknowledgment but prior to initiation of suppression efforts

T_S = the suppression time, i.e., the time required to extinguish the fire after the actuation of the suppression systems.

Estimation of T_D and T_S for terrestrial fires usually relies on generic data. This practice may be suitable for terrestrial fire risk analyses when plant experience is considered to be abundant, and benchmark tests are generally available to verify the applicability of the data. However, terrestrial generic data are questionable in the estimation of the response times in microgravity, not only because the fire protection systems to be used in space are different from those in terrestrial facilities, but the characteristics of fire phenomena in space are unlike those on earth. A new data base has to be developed before this generic data approach can be employed for fire risk analysis for spacecraft. It is presently impossible to develop such a data base when the fire experience in space is virtually nonexistent. Physical models are needed to estimate the response time characteristics.

In the following sections, the various detector response time models and the effectiveness of various suppressants are described. The derivations and assumptions of these models are given. The feasibility of applying these models to processes in microgravity is discussed.

3.6 Fire Detection Experiment

Reliable fire detection is an essential aspect of fire protection. Prompt fire detection can provide early warning of the outbreak of an unwanted fire so that appropriate actions to mitigate the consequences of the fire can be taken. Fire detection is influenced by various factors, including the type of detector, the location of the detectors, the room ventilation flow rate, the configuration of the room, and the items contained in the room.

Different types of detectors are designed to respond to different changes in their local environment that indicate the presence of a fire. These changes in ambient conditions are called fire signatures. Each of the different fire types (e.g., smoldering, flaming fire, etc.) will produce its own characteristic set of fire signatures. These characteristic sets may consist of either one or more of the following environmental conditions: heat, smoke, and light. Therefore, the optimal

detection system selected to guard an area must be the one that provides the earliest response to the signatures that may be created by the potential fire hazards. Fire detection is considered to be successful if the detector can sense the presence of a fire in its early stages so that mitigating measures can be initiated to minimize the damage effects of the fire. Detailed discussions of the different fire signatures and descriptions of detector types are given in [3.70-3.73].

Different types of fire detectors have different pre-determined thresholds for sensing the fire signatures. Once the intensity of the fire signature exceeds the threshold, the detector will acknowledge the presence of a fire with an alarm. Four kinds of detectors are studied in this section, thermal detectors, smoke detectors, gas detectors, and flame detectors. Detailed descriptions of the applications and, advantages and disadvantages of different detectors are given in [3.73].

Response models have been developed to estimate the time required by different detector types to recognize the fire signature that they are sensing. Therefore, the detection time T_D is the time at which the detector response parameter is larger than the pre-determined criterion of the detector.

It is noted that in some terrestrial fire studies, some detector response models are often called sprinkler actuation or sprinkler response models (e.g., in [3.74-3.75]). This terminology is suitable only when the sprinkler in consideration has its own detector unit, e.g., a liquid-filled bulb sprinkler. To avoid misunderstanding, the detector response models described in this subsection are those used to estimate the time to the recognition of a fire hazard.

3.6.1 Thermal Detector Response Model

Thermal detectors provide low false alarm rates, however, for most fire types, they are usually the slowest to provide warning compared to other detector types. These detectors respond either at a pre-determined temperature (typically, 330 K), or at a specific rate of environment temperature change (typically, 0.14 K per second) [3.73]. Figure 3.16 illustrates several types of heat detectors: bimetal snap-disk, pneumatic-type, and a rate of rise fixed-temperature detector using a bimetal element.

For a given fire situation, the detector response time is determined by the thermal responsiveness of the detector, and the hot gas temperature and gas flow rate at the detector location. In terrestrial modeling of heating of thermal sensing elements, net radiative effects during early fire growth were found to be less than 20 percent of convective heating [3.76]. Therefore, most of the terrestrial detector response models are based on convective heating only [3.74-3.78]. Following these references, the balance on the heat sensing element is:

$$mc \frac{dT_e}{dt} = hA(T_g - T_e) \quad (3.33)$$

where

m = mass of the detector element

c = specific heat of the element

T_e = temperature of the element, alarm will activate when $T_e > T_{\text{threshold}}$

t = time; the time when $T_e > T_{\text{threshold}}$ is T_D

h = convective heat transfer coefficient

A = surface area of the detector element

T_g = hot gas temperature

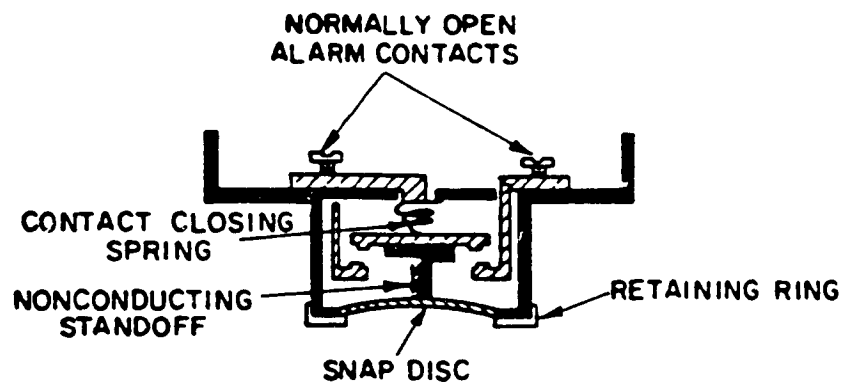
In terrestrial practice, Eq. (3.33) is usually expressed in the form of

$$\frac{dT_e}{dt} = \tau^{-1}(T_g - T_e) \quad (3.34)$$

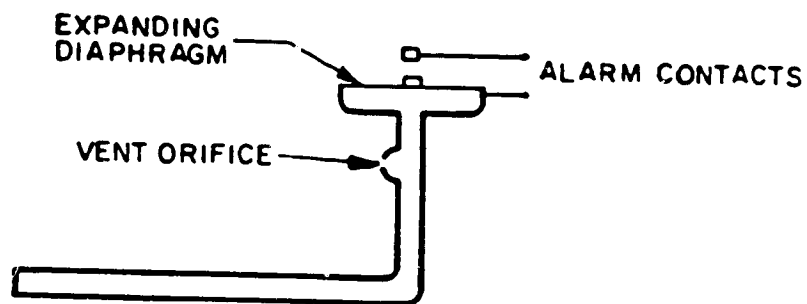
where

$\tau = mc/hA$, a time constant used to relate the properties of the sensing element to the convective heating of the gas flow to which it is exposed.

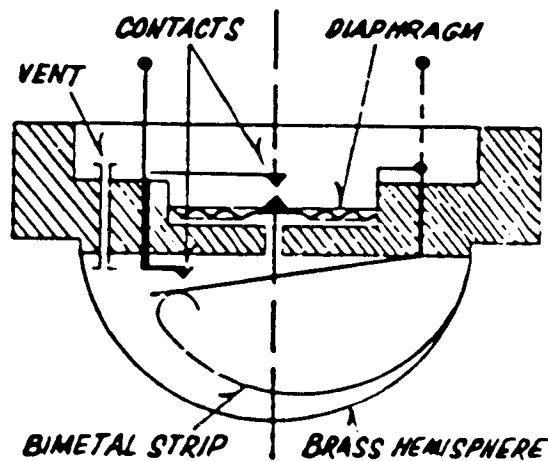
It was also found that the variation of the convective heat transfer coefficient is proportional to the square root of gas flow rate and is independent of the gas temperature [3.76]. Therefore, the time constant of a detector can be estimated based on a set of known τ_0 and v_0 :



Bimetal Snap-Disk Heat Detector



Pneumatic-Type Heat Detector



Rate of Rise Fixed-Temperature Detector Using a Bimetal Element

Figure 3.16. Illustration of Typical Thermal Detectors [3.73].

$$\tau = \tau_0(v_0/v)^{1/2} \quad (3.35)$$

A detector-specific response time index, RTI, is used to measure the performance of detectors based on the time constant, such that

$$RTI = \tau_0 v_0^{1/2} \quad (3.36)$$

For a given temperature, the smaller the index, the earlier the detector will respond. The customary unit for the RTI is $m^{1/2}s^{1/2}$. The response time of different detector designs can be obtained from a tabulated RTI data base [3.76, 3.79].

The RTI and detector temperature rating are sufficient to predict the response of conventional detectors. Our interest is to develop a RTI table for the thermal detectors used in microgravity to facilitate the selection of detectors for different locations based on the allowable T_D . However, since the derivation of Eqs. (3.33-3.36) is based on terrestrial approximations, modification of the models is necessary before their application in microgravity.

Since radiative heat transfer may play a significant role in microgravity heat transfer, an additional radiative heat transfer term is added in Eq. (3.33) to model the response of a thermal detector in microgravity.

Assuming that the detector is a gray body with emissivity of ϵ (see Eqs. (3.26) and (3.27)), Eq. (3.33) can be rewritten as:

$$mc \frac{dT_e}{dt} = hA(T_g - T_e) + \epsilon\sigma A(T_g^4 - T_e^4) \quad (3.37)$$

where

$\sigma =$ the Stefan-Boltzmann constant ($5.6697 \times 10^{-8} \text{ Wm}^{-2}\text{K}^{-4}$).

Using Eq. (3.34), Eq. (3.37) can be expressed as:

$$\frac{dT_e}{dt} = \tau^{-1}(T_g - T_e) + \gamma^{-1}(T_g^4 - T_e^4) \quad (3.38)$$

where

$\tau =$ time constant of the detector as described in Eq. (3.34)

$\gamma =$ $mc/A\epsilon\sigma$, radiative time constant.

Since the relative importance of the convective and radiative terms in Eq. (3.38) is uncertain, the applicability of Eqs. (3.34) and (3.38) will have to be verified by an in-space experiment.

3.6.2 Smoke Detector Response Model

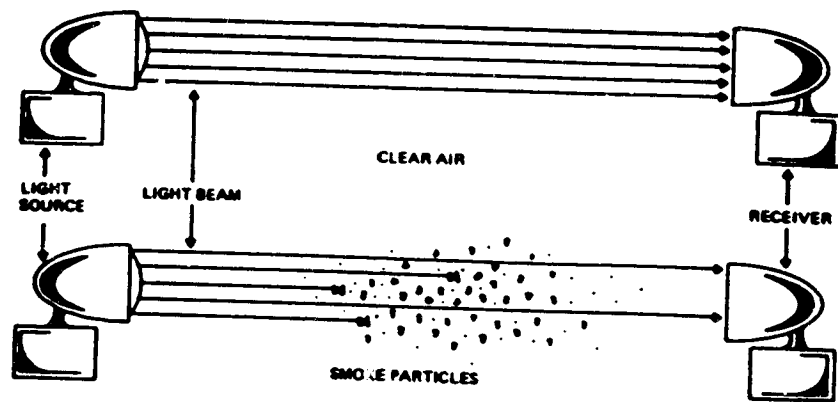
Smoke detectors generally provide a faster detection time than the thermal detectors because smoke release always occurs in the early stages of a fire [3.71-3.73, 3.80]. Transport of smoke has been discussed in an earlier part of this chapter. This section concentrates on the description of smoke detector response models.

Similar to thermal detectors, smoke detectors are designed to send out alarm signals once the fire signature they measure (smoke density) is detected to be higher than a predetermined threshold. There are generally two kinds of smoke detectors: photoelectric and ionization smoke detectors. Photoelectric smoke detectors are best used in locations with potential for smoldering fires or fires involving low temperature pyrolysis. Ionization smoke detectors are useful where flaming fires are a possibility [3.8]. Figures 3.17 and 3.18 provide the schematics for the two types of smoke detectors [3.8].

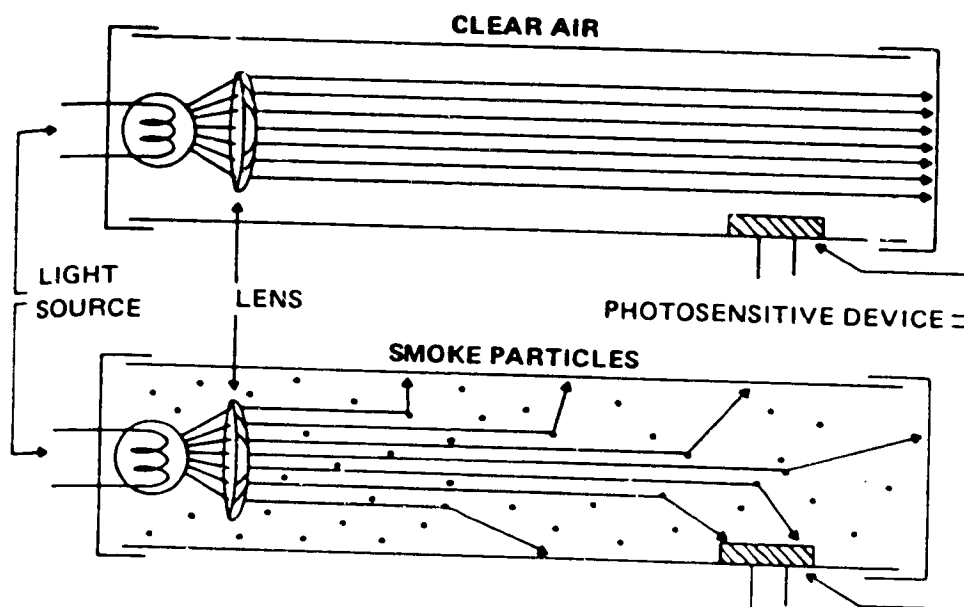
Most of the current smoke detector designs employ a duct type network to draw air into a sampling chamber for measurement of the smoke density. Thus, the design of the duct network may delay the response of a detector. This time lag is a significant factor in determining the sensitivity of a smoke detector. Figure 3.19 depicts an example of an ionization detector that is used for space applications [3.68]. The response models of the two types of smoke detectors are given in the following subsections.

3.6.2.1 Photoelectric Smoke Detector Response Model

The presence of suspended smoke particles generated during the combustion process affects the propagation of a light beam through the air. The effect can be utilized to detect the



Principle of Operation for Photoelectric Obscuration Smoke Detector



Principle of Operation for Photoelectric Scattering Smoke Detector

Figure 3.17. Illustration of Photoelectric Smoke Detectors [3.8].

IONIZATION DETECTOR

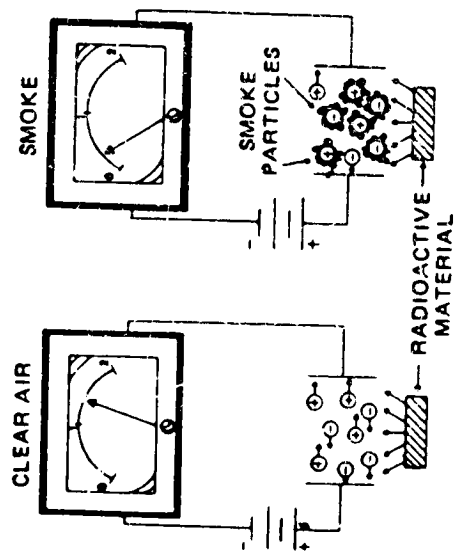
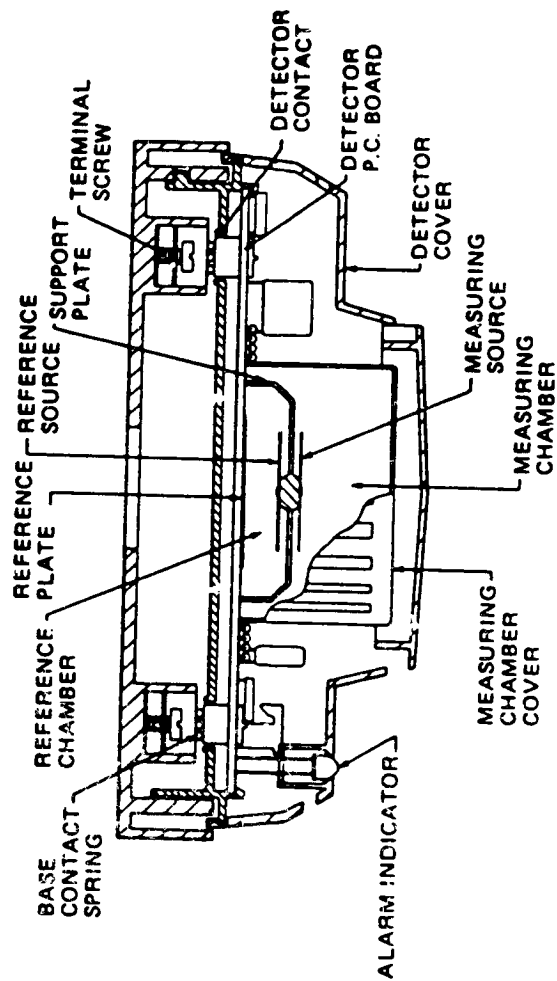


Figure 3.18. Illustration of a Ionization Smoke Detector [3.8].

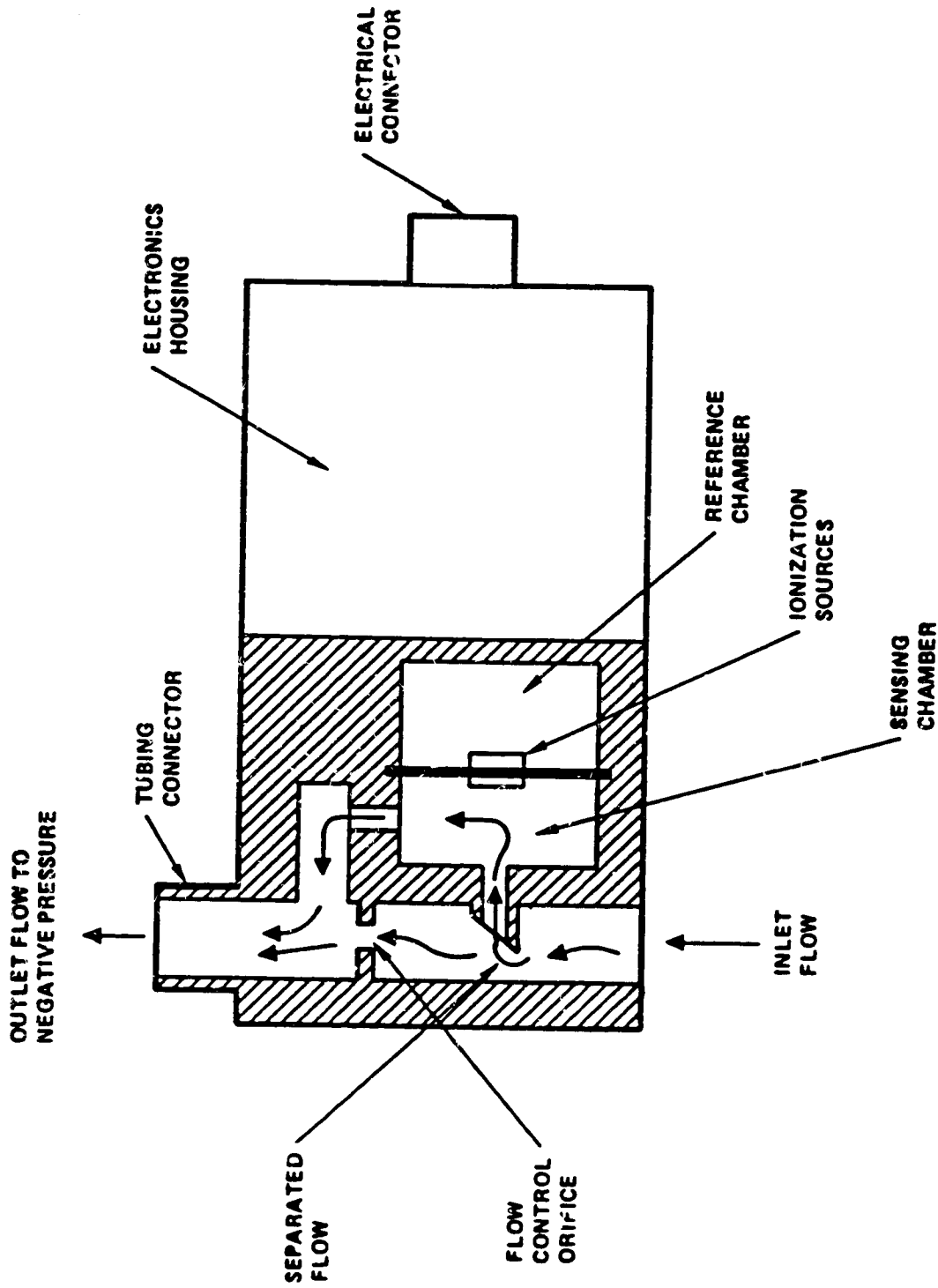


Figure 3.19. Illustration of a Typical Ionization Detector Used in Space Applications [3.68].

presence of a fire in two ways: obscuration of light intensity over the beam path, or scattering of the light beam. Figure 3.17 depicts the principle of the two different kinds of photoelectric smoke detectors.

In either of the two kinds of photoelectric smoke detectors (as shown in Fig. 3.17), the smoke density is usually measured in terms of the optical density of the sampling gas. Response models developed for smoke detectors use optical density as the variable (as contrasted with temperature in thermal detectors). The following relationship is developed [3.77-3.78]:

$$\frac{d(D_g)}{dt} = \frac{v}{L} (D_D - D_O) \quad (3.39)$$

where

D_O = optical density needed in the environment to trigger the smoke detector

D_D = actual optical density inside the detector that triggers the detector

L = characteristic length. This parameter is related to the ease of smoke entry into the sensing volume of the detector, and depends on the geometry of the detector. If $L = 0$, it indicates that there is no entry delay

v = the local flow rate of the smoke at the detector

$\frac{d(D_g)}{dt}$ = the rate of growth of smoke as measured in optical density.

If L/v is defined as τ_s , Eq. (3.39) can be rearranged as:

$$\frac{d(D_g)}{dt} = \tau_s^{-1} (D_D - D_O) \quad (3.40)$$

where

τ_s = smoke detector time constant (as contrasted with τ of thermal detector in Eq. (3.33)).

3.6.2.2 Ionization Smoke Detector Response Model

Ionization detectors utilize a small amount of radioactive material that ionizes the air in a sensing chamber, rendering the air conductive and permitting a current through the air between two charged electrodes (as shown Fig. 3.18). This gives the sensing chamber an effective electrical conductance. When smoke particles enter the chamber, they decrease the conductance of the air by attaching themselves to the ions, causing a reduction in ion mobility. When the conductance is below a predetermined level, the detector responds.

Ionization detectors generate different ionization currents as a function of the absolute concentration of smoke, and the type of smoke (i.e., the structure, particle size and distribution, etc.). A response model is developed for the ionization detectors [3.77]:

$$\ln(I_0/\Delta I) \approx a f_v = \frac{7.0 a}{\lambda(D_\lambda)} \quad (3.41)$$

where

$I_0/\Delta I$ = ratio of initial current to the change in current

a = detector material sensitivity factor (an empirical factor)

f_v = the particulate volume fraction

D_λ = the optical density at a specific wavelength, λ , of light absorption.

Since the effects of microgravity on smoke transport is uncertain, the applicability of Eqs. (3.40) and (3.41) in microgravity will be tested in the in-space experiment.

3.6.3 Gas Detector Response Model

Several species of gas (e.g., CO, CO₂) are released in the earliest stages of a fire [3.80]. The detection of these gases will provide the earliest warning of a fire. The principle of gas detectors is similar to that of the smoke detectors, except that gas detectors measure the concentration of specific species of gases. Similar to Eq. (3.40), the response model of gas particle detectors can be expressed as [3.77-3.78]:

$$\frac{dC_s(t)}{dt} = \tau_g^{-1}(C_{o(t-t_l)} - C_s(t)) \quad (3.42)$$

where

$C_s(t)$ = the instantaneous concentration of gases as measured by the detector at time t

$C_{o(t-t_l)}$ = the actual concentration of gases in the environment near the detector at time $t - t_l$

t_l = the lag time of the detector, i.e., the time required by the gases to travel to the sensing area via filters, sampling lines, etc

τ_g = time constant for the gas detector.

3.6.4 Flame Detectors

Since flame detectors (infrared or ultraviolet sensors) detect the presence of fire by sensing the infrared or ultraviolet radiation at specific range of light spectrum emitted by combustion flames (as illustrated in Fig. 3.20), the response of these detectors depends on the actual light spectrum of fires emitted at microgravity, and the attenuation of light by smoke generated from fires. Since the smoke transport in microgravity is uncertain, the attenuation of light in a fire scenario is also uncertain. No quantitative response model is available in the literature. The response time of the flame detectors used to detect microgravity fires can be compared to that of a terrestrial fire to examine the difference, if it exists, in the performance of the detectors under the different environments.

3.6.5 Objectives

The objectives of the fire detection experiment can be summarized as follows:

1. Evaluate the feasibility of applying the models as described by Eqs. (3.38), (3.40-3.42) in microgravity.
2. Evaluate the detection time of various types of detectors to various fire signatures.
3. Investigate the applicability of using a time constant to measure the effectiveness of detectors in microgravity.

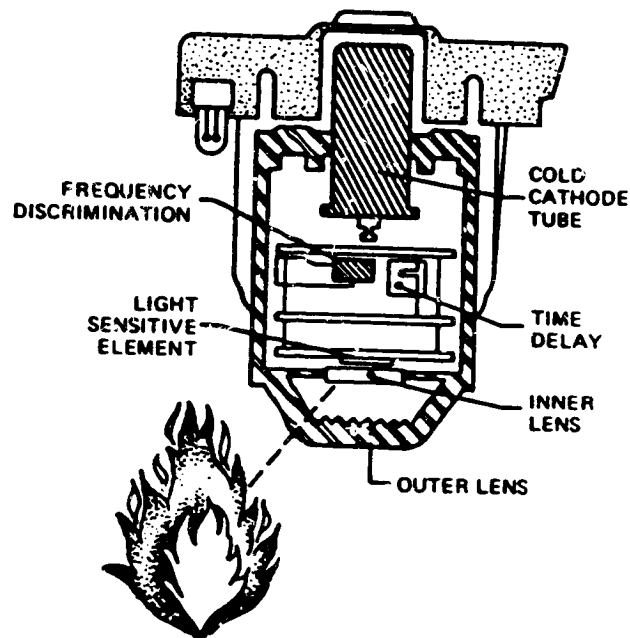


Figure 3.20. Illustration of a Flame Detector [3.8].

4. Study the effects of microgravity on the relationship of different detector types to air flow rate, fire types, location of fire and the detectors, magnitude of fire, and orientation of the compartment.

3.6.6 Justification

The detector time constants have been used as convenient indices to compare the effectiveness of different detector design in earth-based facilities. The models (Eqs. (3.38), (3.40-3.42)) provide a quantitative basis for the modeling of the time constants in a microgravity environment. The proposed experiment may confirm the adequacy of these terrestrial models in microgravity.

The results of the proposed experiment may facilitate the selection of the optimal type and location of installation of detectors in an area where there is a dominant fire hazard.

3.6.7 Science Requirements

The science requirements of the experiments designed to verify the detector response models as described in this section are summarized as follows:

3.6.7.1 Hot Gas Flow Rate

The local gas flow rate, v , at the thermal detector locations shall be measured as a function of time to a tolerance of TBD ms^{-1} . This includes the initial ventilation flow rate.

3.6.7.2 Local Hot Gas Temperature

The local hot gas temperature, T_g , at the thermal detector locations shall be measured as a function of time to a tolerance of TBD K. This includes the initial temperature of the experiment chamber.

3.6.7.3 Hot Gas Temperature

Distribution of the hot gas temperature inside the chamber shall be measured as a function of time to a tolerance of TBD K (Section 3.3.4.2).

3.6.7.4 Pressure

The fluctuation in air pressure, P , in the experiment chamber due to fire shall be measured as a function of time to a tolerance of TBD Torr.

3.6.7.5 Detector Temperature

The surface temperature of the thermal sensing elements of the thermal detectors, T_e , shall be measured to a tolerance of TBD K. This includes the initial surface temperature of the elements.

3.6.7.6 Detector Response Time

The response time of the various detectors, T_D , shall be measured to a tolerance of TBD s.

3.6.7.7 Gas Concentration

The local concentration of various species of gases (e.g., CO and CO₂) at the gas detector locations shall be measured as a function of time to a tolerance of TBD ppm. This includes the initial gas concentrations in the experiment chamber (Section 3.3.4.4).

3.6.7.8 Optical Density

The local optical density of hot gases, D_λ , at a specific wavelength, λ , of light absorption at the smoke detector locations shall be measured as a function of time to a tolerance of TBD m^{-1} .

3.7 Fire Suppression Experiment

Three factors must co-exist before combustion can occur. As shown in Fig. 1.1, these factors are the fuel, oxidant, and ignition source. Except for fires due to gas leaks, most uncontrolled fires involve surfaces (e.g., liquid and solid). For a fire to be sustained on these surfaces, a feedback mechanism (Fig. 3.21) must be established. The fire triangle (either combustible or oxidant) and the feedback mechanism are essential for the existence of a flaming fire. The fundamental principle of fire suppression is, therefore, to remove an element from the fire triangle and to interrupt the feedback mechanism [3.80]. Since it is difficult to remove the fuel element in the fire triangle (Fig. 1.1) from a confined environment, such as a space station, a more rational tactic to suppress a fire is either to restrict the supply of oxidant, or to lower the temperature or the amount of free radicals in the combustion zone.

One of the objectives of the proposed fire suppression experiment (to be defined in this section) is, then, to investigate the feasibility of various approaches in applying the above principles of suppression in microgravity environment. The problems involved with suppressant

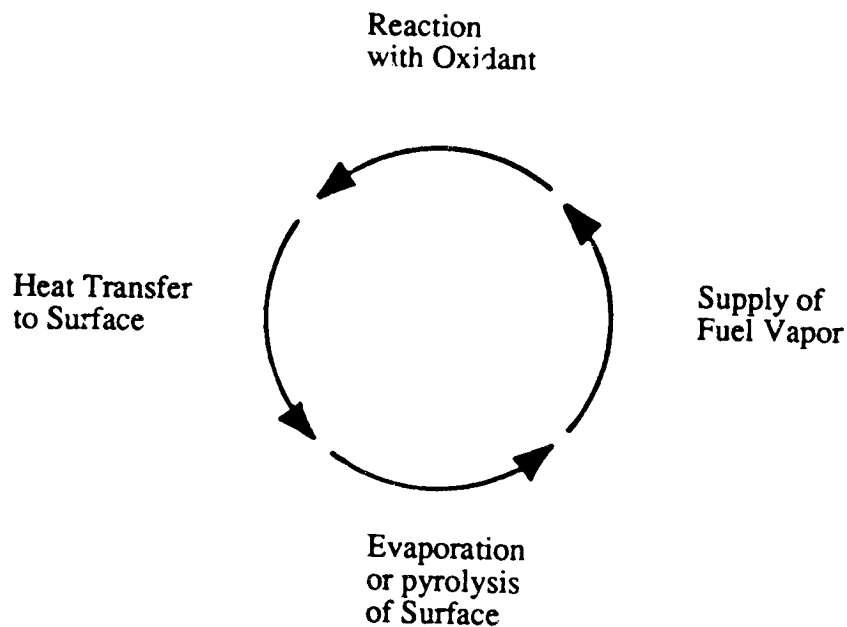


Figure 3.21. Feedback Mechanism in Fire [3.80].

application, such as flame augmentation due to oxygen entrainment and solid surface fragmentation, possibly leading to secondary ignition, will also be investigated. Most of the fire suppression techniques proposed for spacecraft have been employed on earth, therefore, another objective is to study the reactions of various suppressants to different types of fire in microgravity.

This section presents a description of the suppressants selected for the suppression experiment and the models developed to measure the effectiveness of these suppressants relative to various types of fire. The results from the proposed experiment will be valuable in selecting the optimal suppressant for a particular fire hazard.

3.7.1 Suppressant Selection

Candidate suppressants to be used in the suppression experiment are discussed in this subsection. These agents are selected in terms of their roles in the interruption of the fire triangle and the feedback mechanism (as shown in Figs. 1.1 and 3.21): oxidant restriction, temperature reduction, and free radical reduction.

3.7.1.1 Oxidant Restriction

One way to break the fire triangle is to restrict the availability of oxidant to the combustion zone, thus, the thermal feedback from the flame to the fuel surface can be interrupted. Several methods have been suggested in [3.81-3.83] to restrict the availability of oxidants by either sealing the fire source from oxygen diffusion, or by inerting the atmosphere such as reducing the partial pressure of oxygen in the atmosphere, or partial vacuuming of the area.

The feasibility of inerting the atmosphere by changing the partial pressure of oxygen requires substantial research as to its physiological effects in the crew [3.21, 3.82]. This effort is beyond the scope of this work. However, the influence of the partial pressure of oxygen on fires and other suppressants will be investigated.

Among the various oxygen suffocating methods (to seal the fire source from oxidants), nitrogen flooding seems to have definite potential since it introduces fewer long term physiological effects to the crew, requires a relatively easy cleanup effort, and is less corrosive to the electronic equipment [3.82]. Furthermore, nitrogen also provides a cooling effect to lower the temperature of the fire source. The applicability of using nitrogen flooding as a suppressant to extinguish fires in microgravity will be investigated.

Carbon dioxide, another commonly used inerting gas in terrestrial suppression, will also be considered in the proposed experiment although it has been considered to impose a much higher weight penalty to the spacecraft [3.82-3.83].

The use of foam as a suppressant in spacecraft has been proposed [3.83-3.84]. Foam will adhere to the surfaces to which it is applied and act as a barrier to restrict the diffusion of oxygen into the combustion zone. It is generally believed that the adhesiveness of foam will increase in microgravity [3.83]. Different types of foam, e.g., water-based foam, foam generated with compressed nitrogen, etc., will be considered. The performance of these suppressants will be investigated in the suppression experiment.

3.7.1.2 Temperature Reduction

Cooling of the fuel element surface, in the case of a liquid fuel, reduces the vapor pressure and, in the case of a solid fuel, reduces the rate of pyrolysis interrupting the supply of fuel vapor.

Liquid water extinguishes fires primarily by cooling the fuel (to retard pyrolysis), the combustion zone, and the surroundings (to reduce heat flux received by the target components). The performance of water as a suppressant in various modes of application to various types of fires in microgravity environment will be studied.

3.7.1.3 Free Radicals Reduction

The flame zone can be inhibited by removing the free radicals that are essential for combustion (e.g. the OH radical). Once the radicals are removed, the reaction with the oxidant is interrupted. This can be achieved by introducing a material that acts as a 'sink' for the free radicals.

Halon 1301 which is an effective inhibitor for the flame zone, extinguishes fires by chemically impeding combustion by releasing bromine atoms that can repeatedly remove OH radicals necessary for combustion [3.82]. It is known that Halon is ineffective against deep seated fires. It does not cool solid fuel, nor chemically inhibit glowing smolder-type combustion reactions.

3.7.2 Fire-Suppressant Interaction Modeling

The general approach in modeling the fire-suppressant interaction is statistical in nature, and is used to compare the effectiveness of different suppressants [3.75-3.76]. This approach is based on the determination of whether the amount of suppressant applied to the combustion zone is sufficient to extinguish a fire [3.75], rather than the physics of fire extinguishment. Although empirical correlations have been developed to model the effects of water spray on burning fuels, based on heat transfer between the water droplets and the fire [3.11, 3.85-3.86], generalized quantitative models for the interaction between different types of fires and various suppression agents are not available.

Although the statistical approach seems to be rudimentary, it can be applied directly to any environment, including microgravity, without major modification, since it relies only on whether the suppressant can put out the fire.

The parameters that characterize the effectiveness of a suppression system have been identified in earlier studies [3.11, 3.75, 3.80]. These parameters are: the individual (liquid) suppressant droplet size, the required quantity of the suppressant released, the quantity of the suppressant actually delivered to the fire source, the rate of application, the burning characteristics of the fires, and the geometric arrangement and ventilation conditions associated with the fuel.

The individual droplet size is important because it determines the surface area available for evaporation. If the droplet is too small, it will evaporate before reaching the flame zone and cannot cool the combustion. If the droplet size is too large, the total surface area available for cooling is less than that of several smaller droplets that have the same total mass of suppressant, once the droplet reaches the flame zone. Thus, the effectiveness of the suppressant is decreased. Therefore, an optimal droplet size is desired.

The time taken to suppress a fire is proportional to the inverse of the rate of application. As shown in Fig. 3.22, a minimum critical rate of application, R_c , exists for different fire sizes, below which suppression can not be achieved. If the rate is too small, the suppressant will be consumed as fast as it is applied. Although it might seem that a very high rate of application may achieve faster suppression, the quantities required should be considered, especially when the suppressants must be transported must be to orbit at great expense. An optimal application rate, R_{opt} , usually exists such that a minimum quantity of suppressant can achieve extinguishment with the least weight penalty. This optimal rate must be about twice the critical rate [3.80]. Figure 3.23 illustrates a typical quantity curve for a fire suppressant [3.80].

3.7.3 Objectives

The objectives of the fire suppression experiments can be summarized as follows:

1. Study the effectiveness of different fire suppressants used to extinguish different types of fires in microgravity.

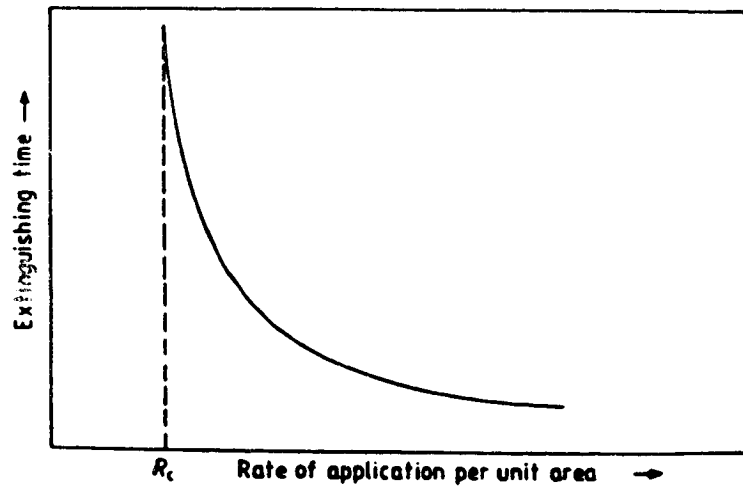


Figure 3.22. The Critical Fire Rate Curve for Fire Suppressant [3.80].

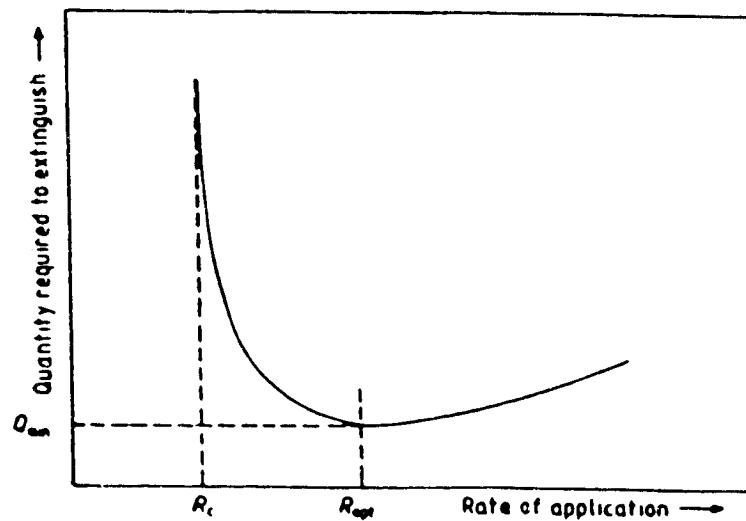


Figure 3.23. Quantity Curve for Fire Suppressant [3.80].

2. Investigate the differences in the relevant parameters of different fire-suppressant interactions between terrestrial experience and microgravity.
3. Study the effects of microgravity on the requirements of the application rates of different suppressants.

4. Simulate the time-competing detection and suppression processes involved in a fire in microgravity.

3.7.4 Justification

The experiment will identify the most effective suppressant to be used for the fire types investigated in this work. The results of the experiment can be helpful in the selection of an optimal suppressant release rate and provide a basis to determine an optimal suppressant for a particular fire type based on the amount and time required to extinguish the fire.

3.7.5 Science Requirements

The science requirements of the suppression experiments are summarized as follows:

3.7.5.1 Drop Size

The drop size, D_s , of various liquid suppressants shall be measured in term of the mean diameter and as a function of time and distance from the release mechanism to a tolerance of TBD m.

3.7.5.2 Suppression Time

The time to suppression, T_s , of various suppressants to various fire types shall be measured to a tolerance of TBD s.

3.7.5.3 Suppressant Discharge Pressure

The discharge pressure, P_d , of various suppressants shall be measured as a function of time to a tolerance of TBD Torr.

3.7.5.4 Suppressant Discharge Rate

The discharge rates of suppressants to the fire source, shall be measured as a function of time to a tolerance of TBD ms^{-1} .

3.7.5.5 Suppressant Flow Rate

The flow rate distribution of the suppressants shall be measured as a function of the distance between the suppressant release mechanism, the time from release, and the temperature of the chamber to a tolerance of TBD ms^{-1} .

3.7.5.6 Suppressant Temperature

The release temperature of the various suppressants, T_s , shall be measured to a tolerance of TBD K.

3.7.5.7 Flame Temperature

The flame temperature shall be measured with and without the presence of suppressants as a function of time to a tolerance of TBD K.

References

- 3.1. *Spacecraft Fire Safety*, Proceedings of A Workshop held at NASA Lewis Research Center, Cleveland, OH, Aug. 20-21, 1986, NASA Conference Publication 2476, Scientific and Technical Information Branch.
- 3.2. D. Drysdale, *An Introduction to Fire Dynamics*, John Wiley and Sons, 1985.
- 3.3. C. Huggett, "Estimation of Rate of Heat Release by Means of Oxygen Consumption Measurements," *Fire and Materials* 4, 61-65, 1980.
- 3.4. W.J. Parker, *Calculations of the Heat Release Rate by Oxygen Consumption for Various Applications*, National Bureau of Standards, NBSIR 8-2427, 1982.
- 3.5. G. Holmstedt, "Rate of Heat Release Measurements with the Swedish Box Test," *Fire and Materials*, 8, 20-27, 1984.
- 3.6. V. Babrauskas, "Development of the Cone Calorimeter - A Bench-scale Heat Release Rate Apparatus Based on Oxygen Consumption," *Fire and Materials*, 8, 81-95, 1984.
- 3.7. I.G. Svensson and B.A. Östman, "Rate of Heat Release by Oxygen Consumption in an Open Test Arrangement," *Fire and Materials*, 8, 206-216, 1984.

- 3.8. *Fire Protection Handbook*, National Fire Protection Assoc., 16th Edition, Quincy, MA, 1981.
- 3.9. F. Tamanini, "Direct Measurements of the Longitudinal Variation of Burning Rate and Product Yield in Turbulent Diffusion Flames," *Combustion and Flame*, 51, 231-243, 1983.
- 3.10. A. Tewarson and R. F. Pion, "Burning Intensity of Commercial Samples of Plastic", *Fire Technology*, 11, 274-281, 1975.
- 3.11. R.S. Magee and R.D. Reitz, "Extinguishment of Radiation Augmented Plastic Fires by Water Sprays", *Fifteenth Symposium (Intl.) on Combustion*, 1974.
- 3.12. National Fire Protection Association, *NPFA Fire Protection Handbook*, 14th edition, Boston 1976.
- 3.13. D. Burgess and M. Hertzberg, "Radiation from Pool Flames," *Heat Transfer in Flames*, N.H. Afgan and J.M. Beer, eds., Scripta Book Co., Washington D.C., 413-430, 1974.
- 3.14. A. M. Kanury, "The Science and Engineering of Hostile Fires," *Fire Research Abstracts and Reviews*, 18, 72-96, 1976.
- 3.15. D.B. Spaulding, *Some Fundamentals of Combustion*, Butterworths, London, 1955.
- 3.16. G. Lengelle, "Thermal Degredation Kinetics and Surface Pyrolysis of Vinyl Polymers," *AIAA Journal*, 8, 1989-1996, 1970.
- 3.17. R.F. Chaikem, W.H. Andersen, M.K. Brash, E. Mishuck, G. Moe and R.D. Shultz, "Kinetics of Polymethylmethacrylate," *J. Chem Phys.*, 32, 141-146, 1960.
- 3.18. J.H. Kimzey, *Skylab Experiment M-479, Zero Gravity Flammability*, Final Report, NASA, JSC 22293, 1986.
- 3.19. K. Sacksteder, "Microgravity Combustion Fundamentals," *Spacecraft Fire Safety Workshop*, 57-60, 1986.
- 3.20. J.R. Lawson and J.G. Quintiere, "Slide Rule Estimates of Fire Growth," *Fire Technology*, 21, 4, 267-292, 1985.

- 3.21. D.R. Knight, "Fire Related Medical Science," *Spacecraft Fire Safety Workshop*, 31-42, 1986.
- 3.22. T.J. Ohlemiller and F E. Rogers, "A Survey of Several Factors Influencing Smoldering Combustion of Flexible and Rigid Polymer Foams," *Journal of Fire and Flammability*, 9, 489-509, 1978.
- 3.23. G. Mulholland and T.J. Ohlmiller, "Aerosol Characterization of a Smoldering Source," *Aerosol Science and Technology*, 1, 59-71, 1982.
- 3.24. R. McIlhagger, B.J. Hill and A.J. Brown, "Effect of Environmental Conditions on Smoke Propagation," *Fire and Materials*, , 1, 19-24, 1988.
- 3.25. J. Trezeszczywski, D. Wlodaszczak and T. Bojko, "The Influence of Pressure on Combustible and Toxic Properties of Materials," *Fire and Materials*, 11, 3, 1987.
- 3.26. K.T. Paul, "Relationship Between Smoke in Large Scale Fire Tests and in Standard Smoke Tests," *2nd Int'l Conference: Flame Retardants '85*.
- 3.27. K.T. Paul, "Characterization of the Burning Behaviour of Polymeric Materials," *Fire and Materials*, 8, 3, 137-147, 1983.
- 3.28. C.P. Bankston, R.A. Cassanova, E.A. Powell and B. Zinn, "Initial Data on the Physical Properties of Smoke Produced by Burning Material under Different Conditions," *Fire and Flammability*, 7, 1976.
- 3.29. L.H. Breden and M. Meisters, "The Effect of Sample Orientation in the Smoke Density Chamber," *Fire and Flammability*, 7, 1976.
- 3.30. A. Tewarson and M.M. Khan, *Electrical Cables-Evaluation of Fire Propagation Behavior and Development of Small-Scale Test Protocol*, FMRC J.I.OM2E1.RC, 1989.
- 3.31. S.J. Grayson and S. Kumar, "Assessing Electrical Cable Performance Under Fire Conditions," *International Progress in Fire Safety*, 89-99, 1987.
- 3.32. L.W. Hunter, "Models of Horizontal Electric Cables and Cable Trays Exposed to a Fire Plume," *Combustion and Flame*, 35, 311-322, 1979.

- 3.33. M.M. Khan and A. Tewarson, "Parameters for the Assessment of Fire Hazard from Electrical Wires and Cables," *33rd Int'l. Wire and Cable Symposium*, 1984.
- 3.34. J.M. Schwarcz, W.M. Malone and S. Blinder, "Rate of Smoke Evolution from Burning Polymeric Materials," *Journal of Fire and Flammability*, 6, 554-567, 1975.
- 3.35. F. Saito "Smoke Generation from Building Materials," *15th Symposium (Intl) on Combustion*, 269-279, 1974.
- 3.36. Y. Tsuchiya and K. Sumi, "Smoke Producing Characteristics of Materials," *Journal of Fire and Flammability*, 5, 64-75, 1974.
- 3.37. J.D. Seader and W.P. Chein, "Physical Aspects of Smoke Development in an NBS Smoke Density Chamber," *Journal of Fire and Flammability*, 6, 294-310, 1974.
- 3.38. H.C. Tran, "Smoke Generated From Wood in the NBS Smoke Chamber," *Journal of Fire Sciences*, 6, 163-180, 1988.
- 3.39. K.G. Martin and L.S. Burn, "Studies on the Measurement of Smoke Propensity of UPVC," *Fire and Materials*, 7, 3, 101-110, 1983.
- 3.40. F.R.S. Clark "Assessment of Smoke Density with a Helium-Neon Laser," *Fire and Materials*, 9, 1, 30-35, 1985.
- 3.41. P. Lilienfeld, "Optical Detection of Particle Contamination on Surfaces: A Review," *Aerosol Science and Technology*, 5, 145-165, 1986.
- 3.42. P. Chung and E.E. Smith, "Emissivity of Smoke," *Fire and Flammability*, Vol 13, 104-113, 1982.
- 3.43. W.J. Parker, "Flame Spread Model For Cellulostic Materials," *Journal of Fire and Flammability*, 3, 254-269, 1972.
- 3.44. T. Hirano, S.E. Noreikis and T.E. Waterman, "Postulations of Flame Spread Mechanisms," *Combustion and Flame*, 22, 353-363, 1974.
- 3.45. A.C. Fernandez-Pello and R.J. Santoro, "On the Dominant mode of Heat Transfer in Downward Flame Spread," *17th Symposium (Intl) on Combustion*, 1201-1209, 1980.

- 3.46. A.C. Fernandez-Pello and F.A. Williams, "Laminar Flame Spread over PMMA Surfaces," *15th Symposium (Intl) on Combustion*, 217-231, 1974.
- 3.47. E. Braun and P.J. Allen, *Flame Spread on Combustible Solar Collector Glazing Materials*, NBSIR 84-2887.
- 3.48. R.A. Altenkirch, D.C. Winchester and R. Eichhorn, "Buoyancy Effects on the Temperature Field in Downward Spreading Flames," *ASME J. of Heat Transfer*, 104, 560-563, 1982.
- 3.49. A. Fernandez-Pello and F.A. Williams, "A Theory of Laminar Flame Spread Over Flat Surfaces of Solid Combustibles," *Combustion and Flame*, 28, 251-277, 1977.
- 3.50. R.S. Magee and R.F. McAlevy, "The Mechanism of Flame Spread," *Journal of Fire and Flammability*, 2, 271-297, 1971.
- 3.51. F.A. Williams, "Mechanisms of Fire Spread," *16th Symposium (Intl) on Combustion*, 1281-1294, 1977.
- 3.52. J. Quintiere, M. Harkleroad and D. Walton, "Measurement of Material Flame Spread Properties," *Combustion Science and Technology*, 32, 67-89, 1983.
- 3.53. J.G. Quintiere, *Significant Parameters for Predicting Flame Spread*, NBSIR 85-3109.
- 3.54. J.G. Quintiere and M. Harkleroad, *New Concepts for Measuring Flame Spread Properties*, NBSIR 84-2943.
- 3.55. R.A. Altenkirch and M. Vedha-Nayagam, *Gravitational Effects in Flame Spreading*, University of Kentucky for NASA, 1985.
- 3.56. J.N. de Ris, "Spread of a Laminar Diffusion Flame," *12th Symposium (Intl) on Combustion*, 241-252, 1969.
- 3.57. N.A. Mousa, T.Y. Toong and C.A. Garris, "Mechanism of Smoldering of Cellulostic Materials," *16th Symposium (Intl) on Combustion*, 1447-1455, 1976.
- 3.58. S. Dosanjh, J. Peterson, A.C. Fernandez-Pello and P.J. Pagni, "Buoyancy Effects on Smouldering Combustion," *36th International Astronautical Congress*, 1985.

- 3.59. S.J. Kline, *Similitude and Approximation Theory*, Springer-Verlag, New York, 1986.
- 3.60. J.G. Quintiere, *Scaling Applications in Fire Research*, Center For Fire Research, NBS, 1988.
- 3.61. W.J. Parker, *An Assessment of the Correlations between Laboratory and Full-Scale Experiments for the FAA Fire Safety Program, Part 6: Reduced-Scale Modeling of Compartments of Atmospheric Pressure*, Center for Fire Research, NBS 82-2598.
- 3.62. G. Hekestad, "Modeling of Enclosure Fires," *14th Symposium (Intl) on Combustion*, 1972.
- 3.63. J. De Ris, A. Murty Kanury and M.C. Yuen, "Pressure Modeling of Fires," *14th Symposium (Intl) on Combustion*, 1972.
- 3.64. R.L. Alpert, "Pressure Modeling of Fires Controlled by Radiation," *16th Symposium (Intl) on Combustion*, 1976.
- 3.65. V. Babrauskas and J. Krasny, *Fire Behavior in Upholstered Furniture*, NBS Monograph 173, 1985.
- 3.66. V. Ho, N. Siu and G. Apostolakis, "COMPBRN III-A Fire Hazard Model for Risk Analysis," *Fire Safety Journal*, 13, 137-154, 1988.
- 3.67. R.B. Comizzoli, R.P. Frankenthal, P.C. Milner and J.D. Sinclair, "Corrosion of Electronic Materials and Devices," *Science*, 234, 340-345, 1986.
- 3.68. E.C. Thomas, *Space Station Incipient Fire Detector Concept*, 1428-398, Brunswick Corporation Defense Division, Costa Mesa, California, 1989.
- 3.69. J.P. Barris and D.L. Conte-Russian, "Sprinkler Trade-Offs: Are They Justified?," *Fire Safety Journal*, May, 63-70, 1980.
- 3.70. B.P. Botteri, "Aircraft Fire Protection Technology," *Aircraft Fire Safety*, AGARD, CP-166, 18.1-18.15, 1975.
- 3.71. M. Rieber, "Why it is Difficult to Measure the Burning Characteristics of Materials and Products," *Fire and Materials*, 7, 180-184, 1983.

- 3.72 D.J. Rasbash and D.D. Drysdale, "Theory of Fire and Fire Processes," *Fire and Materials*, 7, 79-88, 1983.
- 3.73 R.W. Bukowski, "Techniques for Fire Detection," *Spacecraft Fire Safety*, NASA Conference Publication 2476, August, 1987.
- 3.74 D.D. Evans, *Thermal Actuation of Extinguish Systems*, NBSIR 83-2807, National Bureau of Standards, Washington, DC, March 1984.
- 3.75 C. Yao, "FMRC Sprinkler Research," presented at the Ninth Meeting of the U.S./Japan Panel on Fire Research and Safety, May 1987.
- 3.76 G. Heskestad and H.F. Smith, *Investigation of a New Sprinkler Sensitivity Approval Test: The Plunge Test*, FMRC, Factory Mutual Research Corporation, Norwood, Massachusetts, December 1976.
- 3.77 J.S. Newman, "Prediction of Fire Detector Response," *Fire Safety Journal*, 12, 205-211, 1987.
- 3.78 J.S. Newman, "Principle for Fire Detection," *Fire Technology*, May, 116-127, 1988.
- 3.79 D.W. Stroup and D.D. Evans, "Use of Computer Fire Models for Analyzing Thermal Detector Spacing," *Fire Safety Journal*, 14, 33-45, 1988.
- 3.80 P.F. Thorne, "The Physics of Fire Extinguishment," *Physics and Technology*, 16, 263-268, 1985.
- 3.81 H.W. Carhart, "Inerting and Atmospheres," *Spacecraft Fire Safety*, NASA Conference Publication 2476, August, 1987.
- 3.82 J. de Ris, "Fire Extinguish and Inhibition in Spacecraft Environments," *Spacecraft Fire Safety*, NASA Conference Publication 2476, August, 1987.
- 3.83 R.L. Smith and T. Kashiwagi, *Expert System Applied to Spacecraft Fire Safety*, NASA Contractor Report 182266, NASA, June 1989.
- 3.84 M.B. Cole, "Space Station Internal Environment and Safety Concerns," *Spacecraft Fire Safety*, NASA Conference Publication 2476, August, 1987.

- 3.85 R.L. Alpert, "Calculated Interaction of Sprays with Large- Scale Buoyant Flows," *ASME Journal of Heat Transfer*, 106, 310- 317, 1984.
- 3.86 R.L. Alpert, "Calculated Spray Water-Droplet Flows in a Fire Environment," *FMRC RC86-BT-6 Technical Report*, Factory Mutual Research Corp., Norwood, MA, October 1986.

4.0 EXPERIMENT SYSTEM DESCRIPTION AND MISSION PLAN

4.1 Introduction

4.1.1 Purpose

As discussed in Chapter 3, Probabilistic Risk Assessment (PRA) uses several models to define and quantify the characteristics of fire, including heat release models, heat transfer models, detection and suppression models, and damage models. Each of these models possesses its own set of science requirements from which functional requirements will be derived. The purpose of this chapter is to relate science requirements of the Risk-based Fire Safety Experiment to engineering functional requirements. These derived functional requirements will be used to select or design the appropriate Experiment System equipment to perform the microgravity experimentation. The Experiment System is defined as the overall flight hardware and software required to perform the experimentation.

Chapter 4 also defines a plan by which one mission will be used to acquire the required science data. Although not described in this report, current planning calls for examination of a multi-mission approach using a series of simple, precursor experiments which build toward the more complex Experiment System. The precursor experiments would be flown on earlier missions and gather science and engineering performance data which could be used to improve the design and utility of the ultimate hardware of the Experiment System. This option will be explored during the development phase.

4.1.2 Scope

In Section 4.2, the summarized science requirements on the Experiment System are gathered in one location to aid in visualizing the overall functional requirements definition. A preliminary list of experimental sample materials and suppressant approaches is also presented. Section 4.3 presents the engineering approach and types of equipment associated with acquiring science data for each PRA model. Section 4.4 contains the overall system and subsystem description. Section 4.5 summarizes the approach to establishing system interfaces. Section 4.6 presents a listing of support equipment requirements documentation to be developed in the development phase. The project safety philosophy is presented in Section 4.7. The approach to system design verification is described in Section 4.8. The mission plan is presented in Section 4.9 with an operations approach.

A number of TBDs (to be determined) are scattered throughout this document and are indicative of the typical conceptual design stage. TBDs indicate that additional information/data/analyses must be developed or obtained. During the development phase of the project, we will establish a log of TBDs. A log will be located at the beginning of each associated document (e.g., Science Requirements Document, Functional Requirements Document) and will establish a plan for elimination of each TBD, including the steps to be taken, the date of closure, and the responsible individual.

4.1.3 Applicable Documents

The following documents serve as key sources of information in defining engineering requirements for the Experiment System and in shaping the fundamental system design. A more extensive list of references is located in Section 4.10.

- A. Engineering Handbook for STS Payloads, Parts 1-5, NASA Headquarters, September 1982.
- B. Safety Policy and Requirements for Payloads Using the Space Transportation System (STS), NSTS 1700.7B.
- C. STS Payload Ground Safety Handbook, KHB 1700.7/SAMTO HBS-100.
- D. Space Shuttle Payload Accommodations, NASA Lyndon B. Johnson Space Center, JSC 07700, Volume XIV.
- E. Space Transportation System User Handbook, NASA Headquarters, MOP-6, June 1977
- F. Shuttle Payload Interface Definition Document for Middeck Accommodations, NSTS 21000-IDD-MDK.

4.2 Science Requirements on Fire Safety Experiment System

A number of experimental fuel samples are under consideration for selection as final flight samples (Table 4.1). The objective is to select combustible samples which are indicative of those which commonly appear, or will appear, in inhabited spacecraft (e.g, shuttle, Spacelab, space station, Spacehab) and include paper, cable and other insulations, cloth, rubber, waste

materials, and several others. This list has been shaped to some extent by the experience derived from Skylab combustion experiments, and is subject to change during the development phase. These materials were also selected after a review of MSFC-HDBK-527 (JSC 09604), "Materials Selection List for Space Hardware Systems." Additionally, several suppressants for fire extinguishment are under consideration for experimentation and are listed in Table 4.1.

Table 4.1. Preliminary Experiment Combustible Materials and Suppressants

Combustible Materials	
Wiring/cable insulation and clamps (Teflon, Tefcel, Kapton, rubber, nylon)	Thermal insulation
Foam rubber	Space suit materials
Velcro	Astronaut clothing samples
Paper of various thicknesses & types	Rubber materials
Plastics of various thicknesses & types	Sealants
Composite structural materials	Waste materials (trash)
Paints & other coatings	Fiberglass
Circuit board materials	Straps (cloth, plastic)
Electronic components	Metal alloys
Suppressants	
Nitrogen	Water
Carbon dioxide	Halon 1301
Foam	

The science requirements for each of the models of Chapter 3 are consolidated in Table 4.2 to provide quick reference in deriving the functional requirements.

Table 4.2. Science Requirements and Associated Models

Science Requirements	Model
Mass Loss Rate	Heat and Smoke Release
Rate of Heat Release	Heat and Smoke Release
Heat Flux	Heat and Smoke Release, Damage
Sample and Target Temperature	Heat and Smoke Release, Damage
Chamber, Wall, Atmosphere, and	Heat Transfer,
Inlet/Outlet Gas Temperature	Fire Detection and Suppression
Fire Detector Local Hot Gas Temperature	Fire Detection and Suppression
Fire Detector Temperature	Fire Detection and Suppression
Suppressant Temperature	Fire Detection and Suppression
Flame Temperature	Heat and Smoke Release,
Light Attenuation	Fire Detection and Suppression
Smoke Particle Size	Heat and Smoke Release, Heat Transfer,
Suppressant Drop Size	Fire Detection and Suppression
Flame Spread Rate	Heat and Smoke Release, Damage
Species Concentration	Fire Detection and Suppression
Visual Record	Heat Transfer
Smoke Particle Deposit Rate	Heat Transfer,
Gas Flow Rates	Fire Detection and Suppression
Suppressant Discharge Rate	All
Suppressant Flow Rate	Damage
Chamber Pressure	Heat Transfer,
Suppressant Discharge Pressure	Fire Detection and Suppression
Fire Detector Response Time	Fire Detection and Suppression
	Fire Detection and Suppression

4.3 Engineering Approach

The approach taken to conceptualize the Experiment System has been to use the science requirements to establish the Instrumentation Subsystem. Extensive research was required to determine what equipment would acquire the science data. Combustion diagnostics instrumentation for use in a microgravity environment is at an embryonic stage of development which necessitated the selection of equipment designed for ground-based usage. This equipment will be modified to meet our requirements, as well as the launch vehicle and host spacecraft requirements. Once the Instrumentation Subsystem was laid out, the remaining support subsystems were conceptually designed. To assist the reader in understanding the configuration, Figures 4.1 and 4.2 are presented here to indicate the basic concept which consists of three modules: Combustion, Fluids, and Command and Power. These are discussed in detail later in this chapter.

4.3.1 Mass Loss Rate and Heat Release Rate

Both the mass loss rate and heat release rate determinations are a function of oxygen concentration depletion during combustion.

The same types of instrumentation used in the Lewis Research Center (LeRC) Modular Combustion Facility (MCF), which is now in the concept definition stage, will be used to determine the mass loss rate in the Experiment System. However, the MCF documentation currently on hand [4.1] does not mention a method of measuring mass. In the event that the MCF instrumentation definition has not matured by the time our design decisions must be made, we will choose among three approaches to determining mass loss rate. The three methods of estimating mass loss rate are: 1) measuring oxygen and other species concentration depletion rates and correlating them to the mass loss rate; 2) direct observations from video photography; and, 3) changes in vibration frequency response of the sample support assembly. The method, or methods, to be employed in the actual experiment is TBD, although the oxygen concentration depletion rate method appears to be a strong candidate.

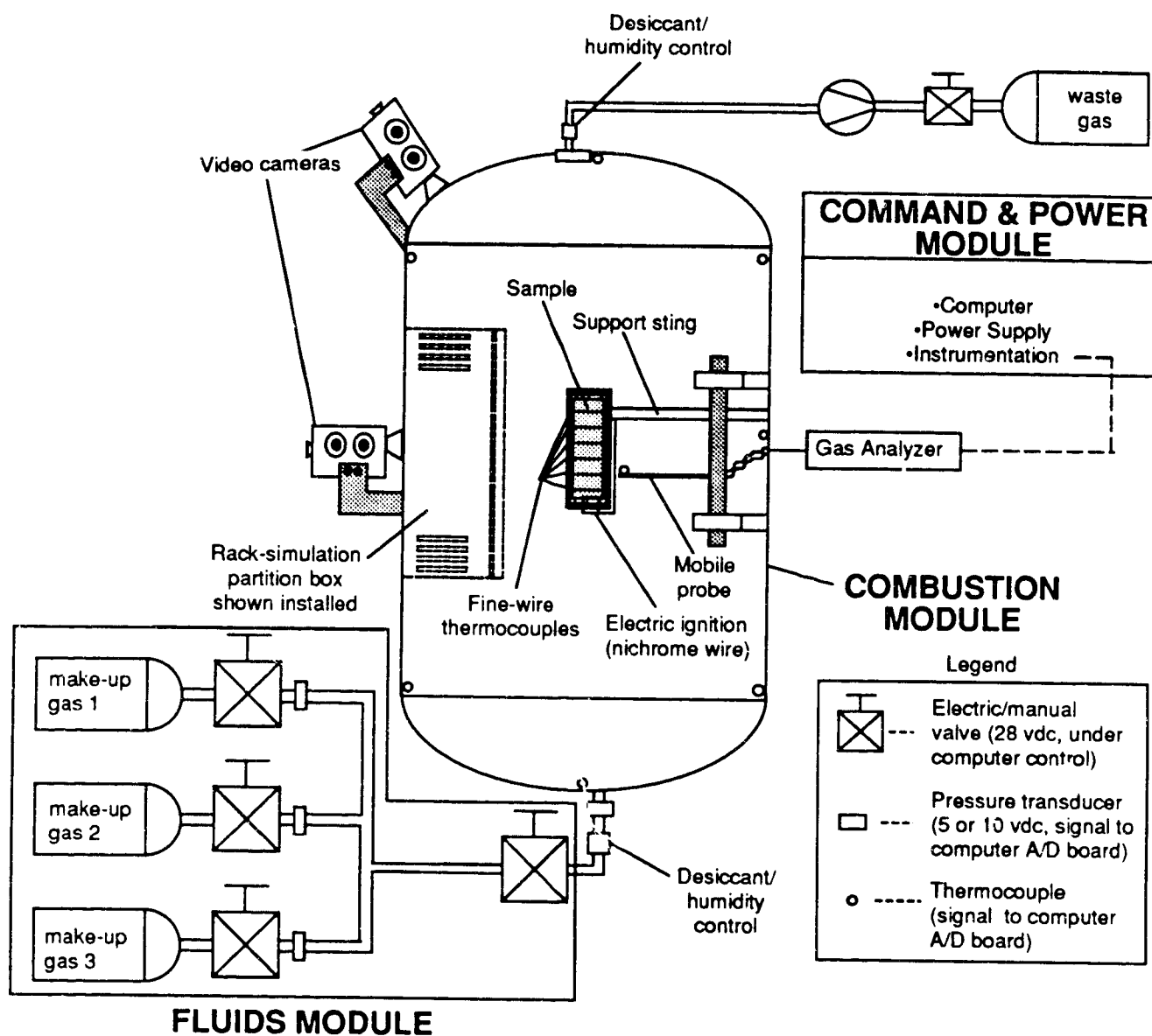


Figure 4.1. Combustion Chamber with Sample Holder.

4.3.1.1 Changes in Oxygen Concentration

The first method under consideration involves analysis of the on-orbit-determined change in oxygen concentration during combustion. This variation in oxygen concentration will be compared to the ground-determined pre-burn and post-burn weights of the sample. It appears reasonable to assume that the sample mass loss rate is equivalent to the combustion chamber oxygen content depletion rate. The oxygen (and other gases) concentration in the combustion chamber will be measured as a function of time. After burning the sample, its remains will be

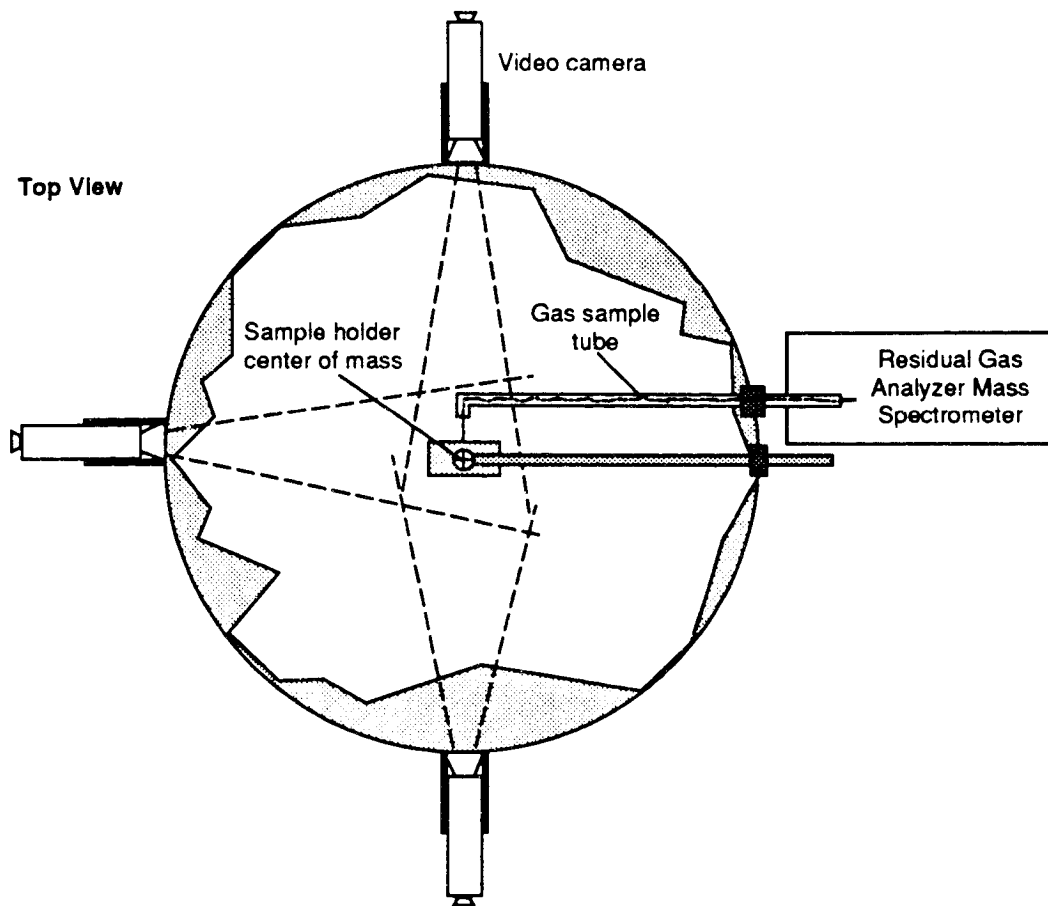


Figure 4.2. Top View of Combustion Chamber Configuration.

packaged and returned for ground analysis, including weighing. This further assumes that none of the oxygen is absorbed or reacts with anything in the combustion chamber other than the sample. The intent is to select combustion chamber materials which do not absorb or react with oxygen.

The rate of heat release will be indirectly determined by measuring the rate of depletion of oxygen concentration in the combustion chamber as a function of time. Measurement of the oxygen concentration depletion rate is the underlying technique in three experimental set-ups for determining the rate of heat release for terrestrial applications. The three methods (discussed below) are:

1. Ohio State University box modified for oxygen consumption;
2. Swedish Forest Products Research Laboratory open arrangement; and,
3. National Bureau of Standards (NBS) cone calorimeter.

These terrestrial approaches have provided background information which was used to formulate the experiment approach.

Early methods of measuring rate of heat release (RHR) used the temperature of exhaust gases. More recent methods use oxygen consumption for simplicity and detect almost 100 percent of the energy released. The heat released per unit mass of oxygen consumed during complete combustion is almost constant for most fuels in common fires at about 13,100 kJ per kg of oxygen consumed with an accuracy of ± 5 percent or better. The volume flow of gases in the exhaust duct and the decrease in oxygen concentration when a material is burned are both measured. See Section 3.2.1.1 for a more detailed discussion of the physical principles concerning oxygen concentration depletion measurements.

If exhaust duct volume flow measurements are made, they must be corrected for chemical reaction mole increases. In all three experimental set-ups discussed below, the formation of carbon monoxide was neglected with a resulting error increase estimated to be less than one percent. The Experiment System will measure carbon monoxide and other gases so that the accuracy should be improved over the three methods presented in Reference 4.6, in addition to their potential risk significance. Several important sensitivities were noted during testing which will be given careful consideration in the experiment development: sampling time must be relevant to the fuel; oxygen concentration measurements are vital; gas-flow measurement (use orifice plate); gas temperature; keeping moisture content in the sample low; specimen size; on earth, vertical and horizontal orientations correlate well and absolute heat release rate is higher in the horizontal orientation of the specimen.

The three experimental set-ups (not to be confused with the three approaches to measuring mass loss rate) are discussed in the following three sections.

4.3.1.1.1 Ohio State University Set-up

Oxygen concentration measurements are made on dried and cooled exhaust gases and flow of gases entering the apparatus (Figure 4.3). This is a more closed system than the Swedish open arrangement described below. Air supply into the exhaust system was sealed since it acts only as a diluent. The air flow was thus reduced to $0.011 \text{ m}^3/\text{s}$. A longer stack was used and gas sampled 0.430 m from the bottom. The oxygen concentration in pre-dried gases was measured with a high-temperature zirconium oxide analyzer (MSA 803 P). Some experiments were run with a paramagnetic instrument (Siemens Oxymat 2). The combustion chamber was insulated for the comfort of the operator.

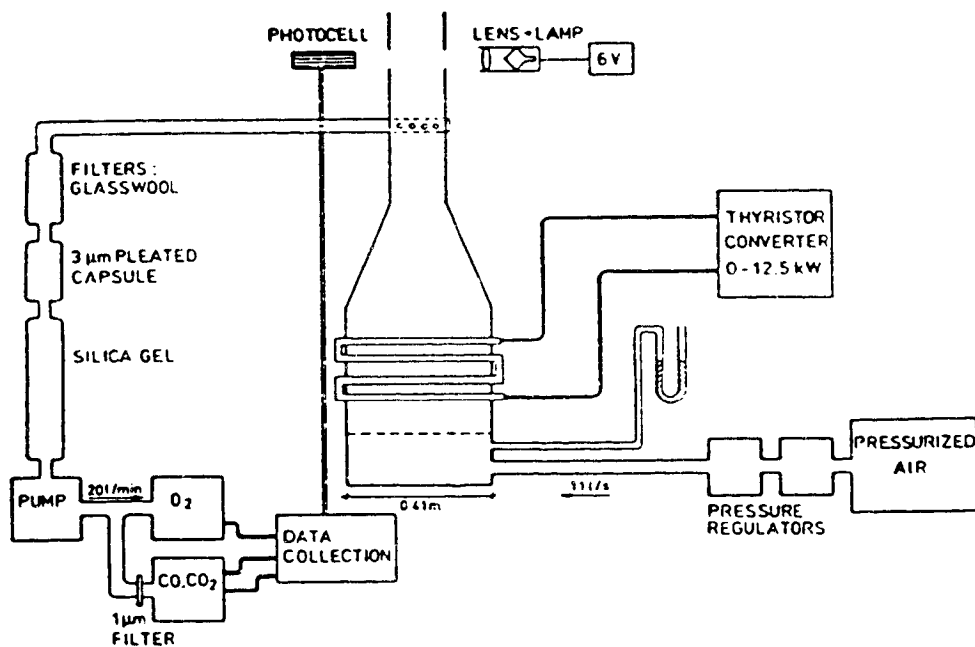


Figure 4.3. OSU Apparatus with Instrumentation for O_2 [4.6].

4.3.1.1.2 Swedish Forest Products Research Laboratory Set-up

Both the oxygen concentration and the flow were measured on hot and wet gases in the exhaust duct. The equipment consists of a vertical radiation panel and a sample holder placed under an open hood (Figure 4.4). The oxygen concentration was measured directly in the exhaust duct by a high-temperature cell with zirconium oxide as the solid electrolyte (Thermox

WDG-P). The gas flow in the duct was measured with an averaging pressure tube flow meter, i.e., a set of pitot static tubes, and kept at about $0.02 \text{ m}^3/\text{s}$. Approximately 95 percent of the heat released can be detected in this manner.

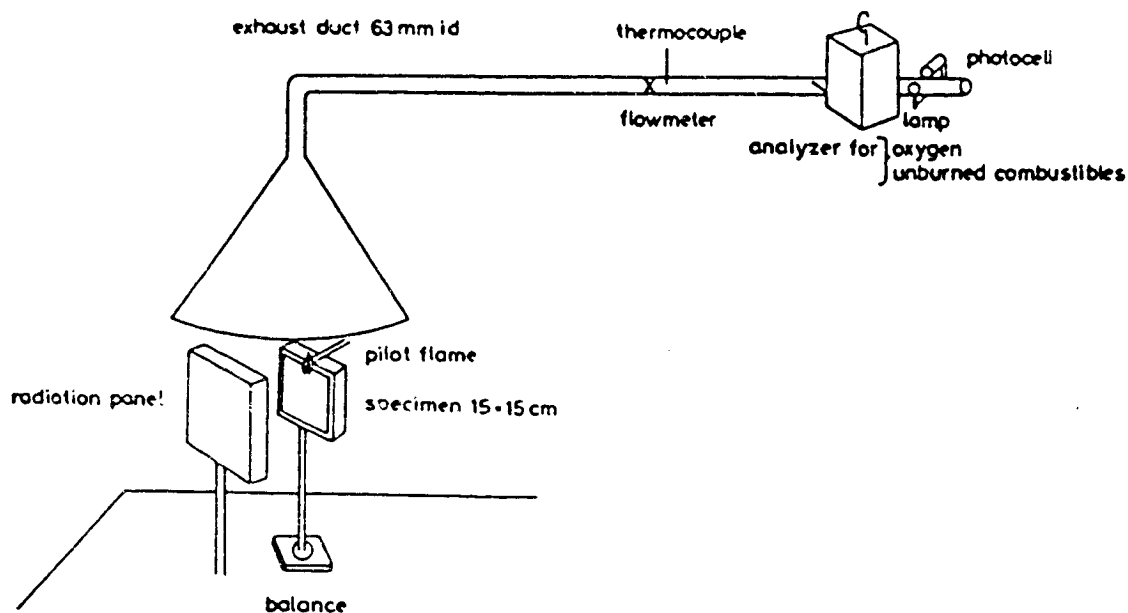


Figure 4.4. Swedis' Open Arrangement [4.6].

4.3.1.1.3 NBS Cone Calorimeter Set-up

The oxygen concentration of the dried and cooled gases from which the carbon dioxide had been trapped and the flow was measured in the exhaust duct. A radiant cone heater similar to that used in the ISO ignitability test is used. Samples were tested vertically and horizontally.

4.3.1.1.4 Equipment Approach

Nominal oxygen concentration will be TBD and will be controlled to within \pm TBD percent of nominal. The oxygen concentration will be sampled TBD times per second. The oxygen concentration will be measured at TBD locations around the interior of the combustion chamber. No non-sample material will absorb oxygen or react with oxygen.

A quadrupole mass spectrometer is planned as the initial oxygen/gas species concentration measuring device (see Section 4.4.3.1 for a more detailed discussion). A VG Instruments mass spectrometer (residual gas analyzer) has been examined and is a candidate for being modified to meet our requirements. Devices with both 5 percent and 1 percent accuracies are available and have selectable atomic mass unit (amu) settings. The more accurate devices are more costly. The amu of interest here is 32 for oxygen. Of course, it has the typical quadrupole problem in resolving species compounds which have the same amu. However, the software which is supplied with the system provides the concentration level and calculates the probability that it has identified the correct compound. Given some knowledge of the combustion chamber gases (such as nitrogen), the probability of identifying the compound correctly is greatly increased.

Alternatively, the use of a mass spectrometer/gas chromatograph, as planned for the LeRC Modular Combustion Facility, will be considered. The characteristics of the envisioned LeRC MCF mass spectrometer/gas chromatograph follow [4.1]:

- a. Mass range limited to approximately 12 to 200 amu.
- b. Resolution of the mass range determination is approximately 10 percent.
- c. The mass spectrometer will be a two-stage double-focusing, electrically scanned instrument, with a 90x electric sector followed by a 90x magnetic sector. The gas stream is pumped into the analyzer by a 500 cm/sec ion vacuum pump and is ionized by 45 and 70 eV electron-bombardment ion sources. The accelerated heavier molecules have trajectories which are not deflected as much as the lighter molecules and strike detector targets at different locations thus permitting the sensing and counting of different molecules.
- d. The gas chromatograph is envisioned as a micropacked column with a 0.75 mm inner diameter and 2 m long.
- e. The combined volume and mass estimates are 23 to 46 kg and 0.03 to 0.06 m³, respectively. Power requirements are estimated at 150 to 300 W.

The NASA Johnson Space Center (JSC) Gas Analyzer Mass Spectrometer was reviewed for applicability and availability for this experiment with JSC personnel. Although it appears that the equipment may perform the appropriate functions, it will not be available during the required time frame. Thus, unless it becomes unexpectedly available in a timely manner, we will modify a residual gas analyzer to meet the experiment requirements.

In hopes of reducing the mass, power, and volume requirements, we will attempt to use instrumentation which is more focused on the experiment requirements rather than the broader requirements of the MCF.

Oxygen concentration may be controlled via a closed-loop (automatic) approach using feedback from the mass spectrometer to open or close an electric valve between the oxygen supply and the combustion chamber, or by having a crew member make manual valve adjustments.

4.3.1.2 Video Image Analysis

The second method of determining mass loss rate involves manual analysis of video images of the sample taken during combustion. The equipment providing the imaging will be a charge coupled device (CCD) video camera. The images will be taken at a rate of TBD frames/s and will have a TBD resolution. The rate of advance of the charred area of the sample (Figure 4.5) would be manually measured, frame by frame using a film motion analyzer connected to a personal computer. Previous experimenters at LeRC have used this technique (with photographic film) with the ability to consistently position video measurement crosshairs (from the film images) to within ± 0.03 cm [3]. Thus, one could manually measure (from the video images) the variation in flame front propagation rate and relate that to the ground-determined initial and final sample masses to determine the mass loss rate. Admittedly, this may be somewhat less accurate and more tedious.

4.3.1.3 Change in Frequency Response

The third method under consideration involves the determination of the mass loss rate by measuring the change in frequency response [4.2] of the sample support sting to a small step function force applied to the external extension of the sample support sting as a function of time when the sample is burning. The step forcing function will be periodically applied to the external sting extension (using a hammer specifically designed outside of the natural frequency range

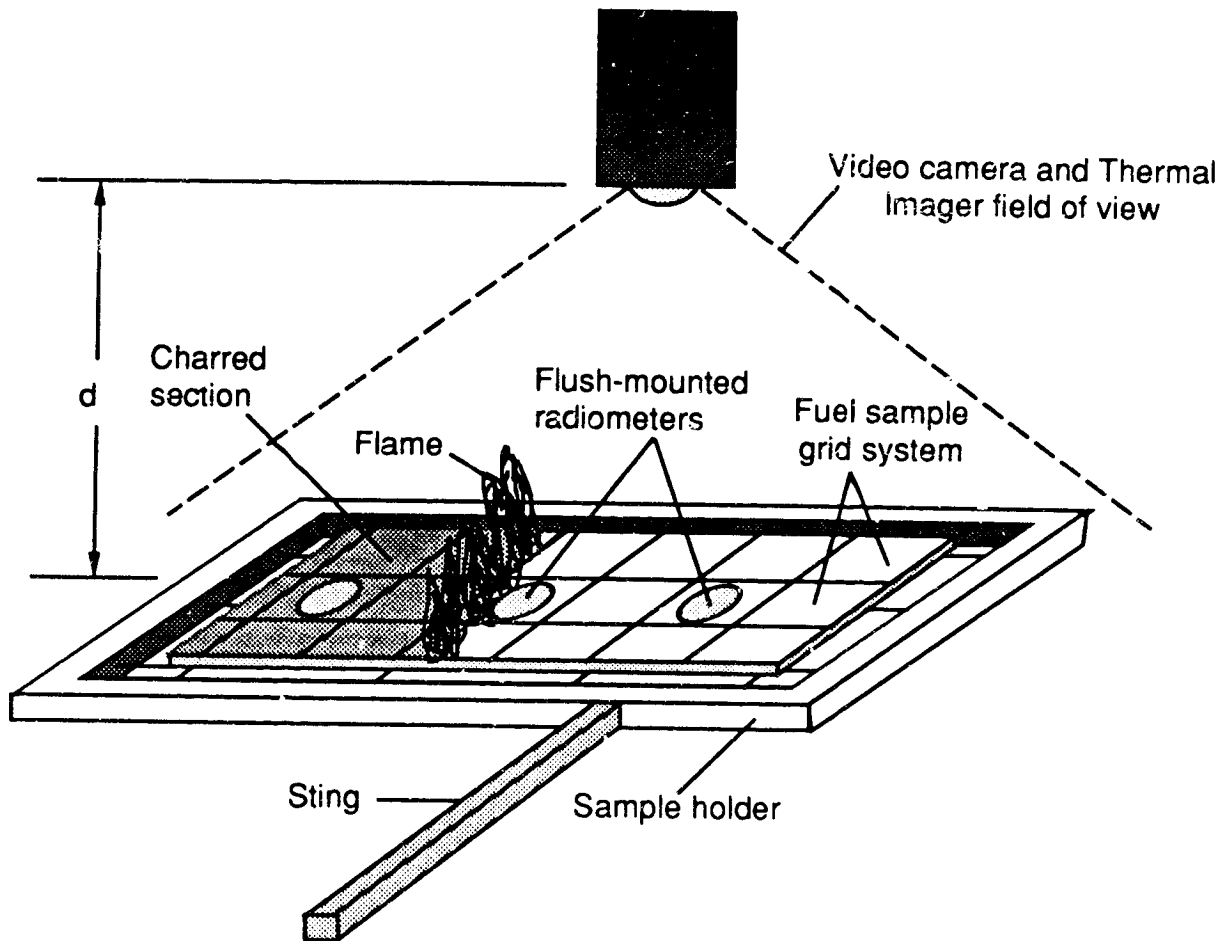


Figure 4.5: Optical Mass Loss Rate and Heat Flux Detection.

of the sample support sting) at a rate of TBD cycles per minute. The resulting small acceleration measured by an accelerometer located on the sample support sting will vary as a function of the fuel sample mass change. The accelerometer signal data could be input to a vibration spectrum analyzer on the ground to determine the frequency of vibration. Given the frequency, the mass can be determined. Further work is required to determine whether the vibration induced into the sample is a source of major disturbances to the combustion process and whether a frequency can be selected (tuned) which will not disturb the combustion process.

4.3.2 Heat Flux

4.3.2.1 External Heat Flux

The external heat flux impinging on a fuel sample and on a remote damage target will be measured TBD times per second to a tolerance of TBD kW/m^2 . The anticipated range is TBD kW/m^2 .

The approach will be to use several radiometers, of known field of view, flush-mounted to the sample and target, and possibly by radiometers mounted on the sample and target holder, to obtain heat flux data as a function of time. The total heat flux on the fuel sample (radiometer) will, thus, be measured. Medtherm radiometers, type Schmidt-Boelter, are strong candidates for use in the experiment. If available, we will use the same type of radiation detector as used by the LeRC MCF. See Section 4.4.3.2 for a more detailed discussion of the use of radiometers.

4.3.2.2 Radiant Heat Flux

The radiant heat flux of the smoke will be determined by the use of several radiometers with a field of view of TBD portions of the smoke [4.10]. In the referenced work, an OSU release rate apparatus was fitted with a calibrated radiometer. An auxiliary gas burner was added to the environmental chamber to produce higher temperatures in the outlet stream than could be obtained by the electrically powered radiant heating rods. The air flow through the environmental section was increased and controlled to vary temperature and smoke concentration of the effluent gas plume. The plume section monitored was immediately above the stack. The radiometer location and view angle was selected so that neither the surface of the stack, nor any other hot surface could be "seen." The radiometer was also protected from convective heating by an air-cooled enclosure. The view factor from the radiometer to the plume boundary was determined and the flux at the plume boundary calculated from the radiant flux to the radiometer. The optical density and temperature of the plume were monitored as is normally done in a release rate test. Because the optical density was determined through the long dimension of the plume, i.e., perpendicular to the plume depth viewed by the radiometer, the optical density was corrected for a light path equal to the plume depth. Care must be taken in the use of the results of this approach due to the possible errors obtained at low temperatures and low smoke concentrations [4.10].

The experiment will incorporate a number of radiometers which target various portions of the smoke within the combustion chamber to obtain the smoke's radiant heat flux. Radiometers will be shielded from direct view of the flame and other hot surfaces. Radiometers will be hard-mounted on each end of the sample holder, several locations around the combustion chamber, and on the mobile probe (Figure 4.6).

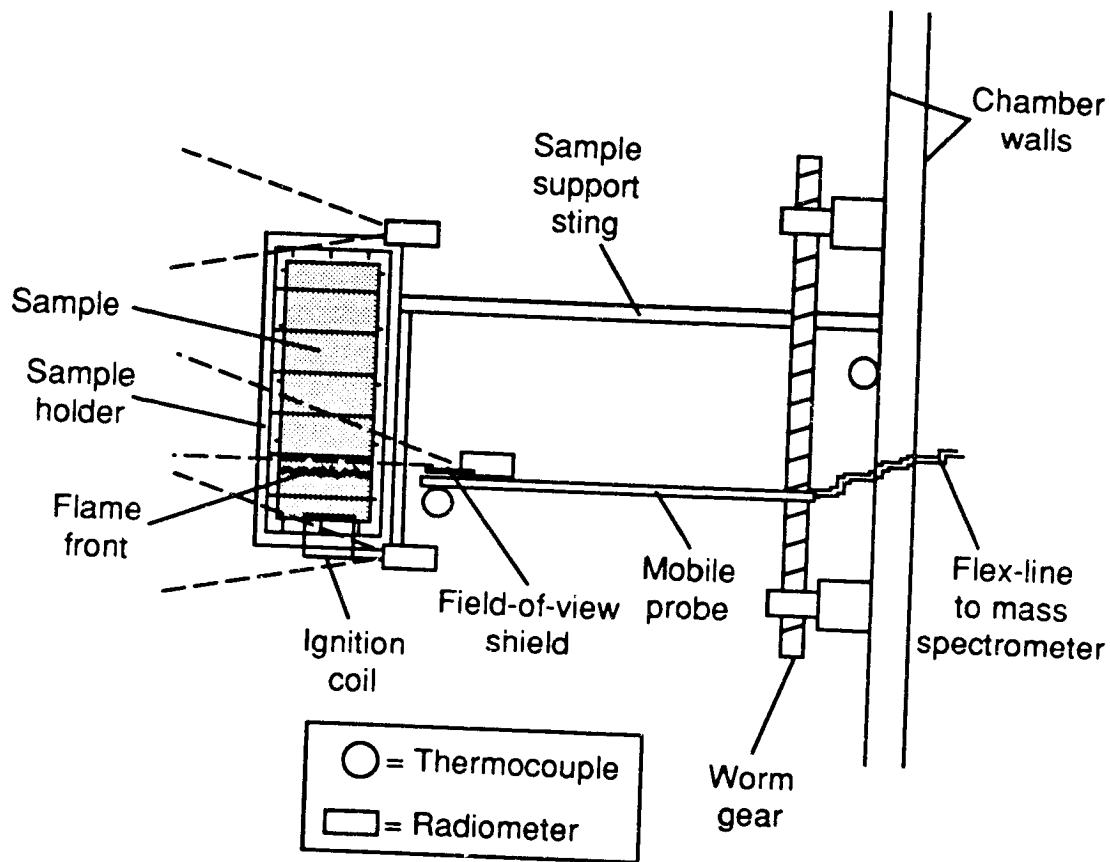


Figure 4.6. Sample Support Assembly.

4.3.3 Temperature

4.3.3.1 Sample and Target Surface Temperature

Embedded, fine wire thermocouples at surface level [4.3] and thermocouples contacting the sample and target surfaces [4.11] are both under consideration for determining surface temperature. In the first experimental case, thin paper fuel samples have had the thermocouple bead placed into a carved-out cavity with the leads at the surface level. Near term future LeRC

experimentation using thicker plexiglass fuel samples will have the leads and the bead embedded in a small hole drilled through the long length or width dimension (as opposed to the thickness dimension).

Sample surface and flame temperature profiles may be further quantified using an Inframetrics Thermal Imager modified to meet our requirements. The Thermal Imager instrument produces a color video tape showing different temperatures as different colors. The instrument software also incorporates graphical plot capability for selectable sample or flame zones of interest so that temperature versus time plots can be displayed. Otherwise, frame-by-frame variation in the temperature profile colors can be manually plotted for other zones of interest.

The surface temperature of the damage target will be determined from thermocouples embedded at the particular locations whose temperature is desired. The number and placement of the thermocouples depends largely on the type of damage targets employed. When the target is another fuel sample, the sensors will be attached just as on the main sample, with the thermocouples being placed in pre-drilled locations equally spaced throughout the sample. If the target is a piece of equipment or a less uniformly-shaped object, the location of the thermocouples will be determined according to the unique nature of the target.

4.3.3.2 Chamber Wall, Atmosphere, and Inlet/Outlet Gas Temperature

Thermocouples and the Thermal Imager will be used to provide chamber wall temperatures non-intrusively. Thermocouples will be used to measure the chamber ambient gas temperatures throughout the chamber, including one at the end of the mobile probe, as a function of time and distance from the fire source and the suppressant injection port. Thermocouples will be used to measure the chamber inlet and outlet gas temperatures to a tolerance of TBD K.

4.3.3.3 Fire Detector Local Hot Gas Temperature

Three types of fire detectors will be tested in the Experiment System: thermal fire detectors which sense temperature; infrared fire detectors which sense visible (flame) and infrared light wavelengths; and ion smoke detectors which sense certain smoke ions, as well as photoelectric detectors which sense light obscuration. The fire detectors will be attached to the external wall of the combustion chamber. Their sensing elements will be exposed to the internal chamber environment through ports which penetrate the chamber wall.

The ambient temperature will be measured by thermocouples mounted at each thermal fire detector. Many of the thermocouples used for general purposes will be close enough to thermal fire detectors to be utilized for this purpose as well. Multiple usage of thermocouples will be employed in many locations to reduce the amount of instrumentation.

4.3.3.4 Fire Detector Temperature

The surface temperature of the thermal sensing elements of the thermal fire detectors will be measured by fine-wire thermocouples in each location. The thermocouples will be placed unobtrusively so that they will not disrupt air flow or heat transfer within the thermal fire detectors.

4.3.3.5 Suppressant Temperature

The release temperature of various suppressants will be measured by thermocouples with liquid probes at each discharge point, as well as the Thermal Imager. The size and placement of the wire probes will be determined by the requirement to minimize suppressant flow disruption.

4.3.3.6 Flame Temperature

The flame temperature will be measured throughout the experiments with thermocouples and the Thermal Imager. Thus, this measurement will probably be accomplished solely with equipment necessary for other parts of the experiment.

4.3.4 Light Attenuation

The preliminary means of measuring light attenuation will be by the use of a helium-neon laser and associated photo-diode detectors [4.7]. The detectors will be screened from extraneous light and calibrated using neutral density filters. Optical density of the smoke will, thus, be recorded as a function of time, TBD times per second. A modular laser light scattering instrument capable of making both dynamic and static light scattering measurements is being developed at LeRC for eventual use on the MCF [4.8]. The technology should be available in time for use by the project. Other potential applications include miniature laser Doppler velocimeters and photon correlation spectroscopy systems (which would allow us to identify gas concentrations with a simple system) [4.9]. The laser light scattering instrument consists of the following main elements:

- a. Light sources
- b. Light detection
- c. Receiving optics
 - 1. Simultaneous multi-angle arrays
 - 2. Fiber optics probes
 - 3. 2-d charge coupled devices (CCDs) for low angles
- d. Signal processing
 - 1. Maximum likelihood correlators
 - 2. Polydispersity algorithms

The light sources are expected to be single longitudinal and transverse mode continuous wave laser diodes with powers of 30-50 mW. These will have a wavelength of 780 or 830 nm and will be current regulated and Peltier cooled for wavelength control. Drive currents are typically 40-100mA at approximately 2 volts. The laser and drive circuitry can occupy a volume as small as a few cubic centimeters. The laser diodes are vertically polarized. One percent or better stability is expected.

Signal detection will be accomplished through the use of avalanche photo diodes (APDs) with dark counts of less than 100-200 cps at 273 Kelvin. Their quantum efficiency will be between 15-20 percent. After-pulsing will be negligible for photon correlation spectroscopy time scales. Active quenching is employed to ensure dead times of less than 30-40 nanoseconds and count rates exceeding 10 MHz. The APDs are mounted in a 16.4 cm³ power supply cube.

The windows in front of each laser and each photodiode will be kept clean by small attached heaters which will keep smoke particles from building up and obscuring the instruments' view.

4.3.5 Particle and Droplet Size

4.3.5.1 Smoke Particle Size

The smoke particle sizes will be measured using a helium-neon laser-based Particle Dynamics Analyzer. The Particle Dynamics Analyzer manufactured by Dantec Electronics, Inc. is a candidate for modification to meet the requirements of this experiment. The Dantec Particle

Dynamics Analyzer can measure particles in the size range 1-10,000 μ m. See Section 4.4.3.3 for a more extensive discussion of the Particle Dynamics Analyzer components and its operation.

The lasers will be mounted on the outside of the chamber wall, and their associated photodiodes will be similarly mounted directly across the chamber. All will have windows in the chamber wall which will be kept clean through the use of attached heaters to keep soot from being deposited. Also, some smoke may be carefully injected into storage vials and stored following certain experiments for later ground analysis to further determine the smoke particle size. Additionally, the use of witness plates stored after each experimental run will assist to some extent in identifying particle sizes.

4.3.5.2 Droplet Size

The droplet size of various liquid suppressants will be measured as a function of time and distance from the release mechanism by the Particle Dynamics Analyzer laser-scattering technique identical to that used in other parts of the experiment. The video cameras will also record the droplet sizes and dispersion, but the ability to resolve the smaller droplets will be determined during the development phase. Rapid, stop-action, still photography is also under consideration and will be made by a high-resolution camera taking pictures of the released suppressant TBD times every second. The size of the drops would be measured from the photographs in post-flight analysis.

4.3.6 Flame Spread Rate

The flame spread rate will be measured using temperature data collected by thermocouples embedded in the sample, the Thermal Imager, and by video camera recordings.

4.3.7 Species Concentration

The same instrumentation (mass spectrometer) used to measure oxygen concentration will be used to measure other combustion species concentrations. See Section 4.4.3.1 for a more detailed description of the approach and instrumentation. Gas samples will be taken from a number of locations using probes mounted in the chamber wall, as well as in the flow path upstream and downstream of the sample, and through the mobile probe.

4.3.8 Visual Record

A visual record of all experimental runs will be made using miniature color and monochrome video cameras mounted on the external wall of the chamber with adjustable fields of view through window ports. These window ports will also be heated to reduce smoke particle build-up which could obscure the view, and will be wiped clean before each new experiment run. The required window temperature will be determined through analysis and test, and traded against power requirements, laser interface temperature requirements, and the rate of smoke particle deposit. Additionally, a still-photography camera will be used for selected experiment runs.

Flame shape will be characterized by using the video cameras and the Thermal Imager, and this information will be used in the evaluation of the thermal environment of the chamber.

4.3.9 Smoke Particle Deposit Rate

The smoke particle deposit rate will be measured with a helium-neon laser and a photodiode situated on opposite sides of the chamber. As with all other lasers used, this laser's window will be kept clear with a small attached heater, but the associated photodiode will not be heated, allowing smoke to be deposited on the window in front of it. As the field of view of the photodiode becomes obscured, less of the laser's light will enter it. The resulting decrease in the output signal of the photodiode will correspond directly to the smoke deposit rate. Additionally, the use of witness plates stored after each experimental run will assist to some extent in identifying particle deposition rates.

4.3.10 Flow Rates

4.3.10.1 Chamber Gas Flow Rates

The air flow rate will be measured to within a tolerance of \pm TBD m/s and controlled to \pm TBD m/s so that the volumetric flow rate (m^3/s) can be calculated. Flow rates will be set at, or scalable to, those of the space station modules and racks, Spacelab, and the shuttle. Turbulence and stagnant air spaces to match the spacecraft open volume flows and patterns will be simulated in the combustion chamber (Figure 4.7). The actual flow patterns which will be observed in the chamber are currently unknown, thus, the flows indicated in Figure 4.7 are representative only. Rack flows and patterns will also be simulated using a wall partition box on the inside of chamber. The partition box is removable to provide for open volume flow simulations. Slots

and louvers within the walls of the partition box can be opened and closed individually for sensitivity studies. We recognize that the time scales associated with flow are different from those of combustion and thermal processes. These differences will be accommodated by modeling. The flow rate and pressures will be sampled TBD times per second within the chamber and the partition box. Different combinations of vent openings will be used to vary the flow.

The flow may be measured and controlled by a fully automated (closed-loop) means using a non-intrusive diagnostic instrument (as a goal) such as laser Doppler velocimetry. If a non-intrusive diagnostic instrument is not available, a flow meter or pressure differential standard orifice will be used. Feedback from the flow sensor shall be used to drive the make-up atmosphere. The use of computational flow dynamics analysis is anticipated to assist in predicting the flow patterns, as well as visualization of the flow.

4.3.10.2 Hot Gas Flow Rate

The hot gas flow rate will be monitored by flowmeters at each thermal detector location. To minimize air flow disturbance, as many as possible of the flowmeters used for general air velocity monitoring (see Section 4.4.3.6) will be used also for this purpose. This will be accomplished by adjusting the placement of the flowmeters and thermal detectors in such a way that many of the thermal detectors will be sufficiently close to flowmeters planned for other purposes. In this way, the number of extra flowmeters necessary will be reduced, although some may be added specifically to monitor thermal detector areas.

4.3.10.3 Suppressant Discharge Rate

The discharge rates of suppressants to the fire source will be measured by flowmeters at each point of discharge. The flowmeters will be located at the suppressant port to the chamber to eliminate chamber air flow disturbance and will be oriented to minimize disruption of the suppressant flow.

4.3.10.4 Suppressant Flow Rate

The flow rate of the released suppressant will be measured by liquid flowmeters, the Particle Dynamics Analyzer laser-scattering technique, and video imagery.

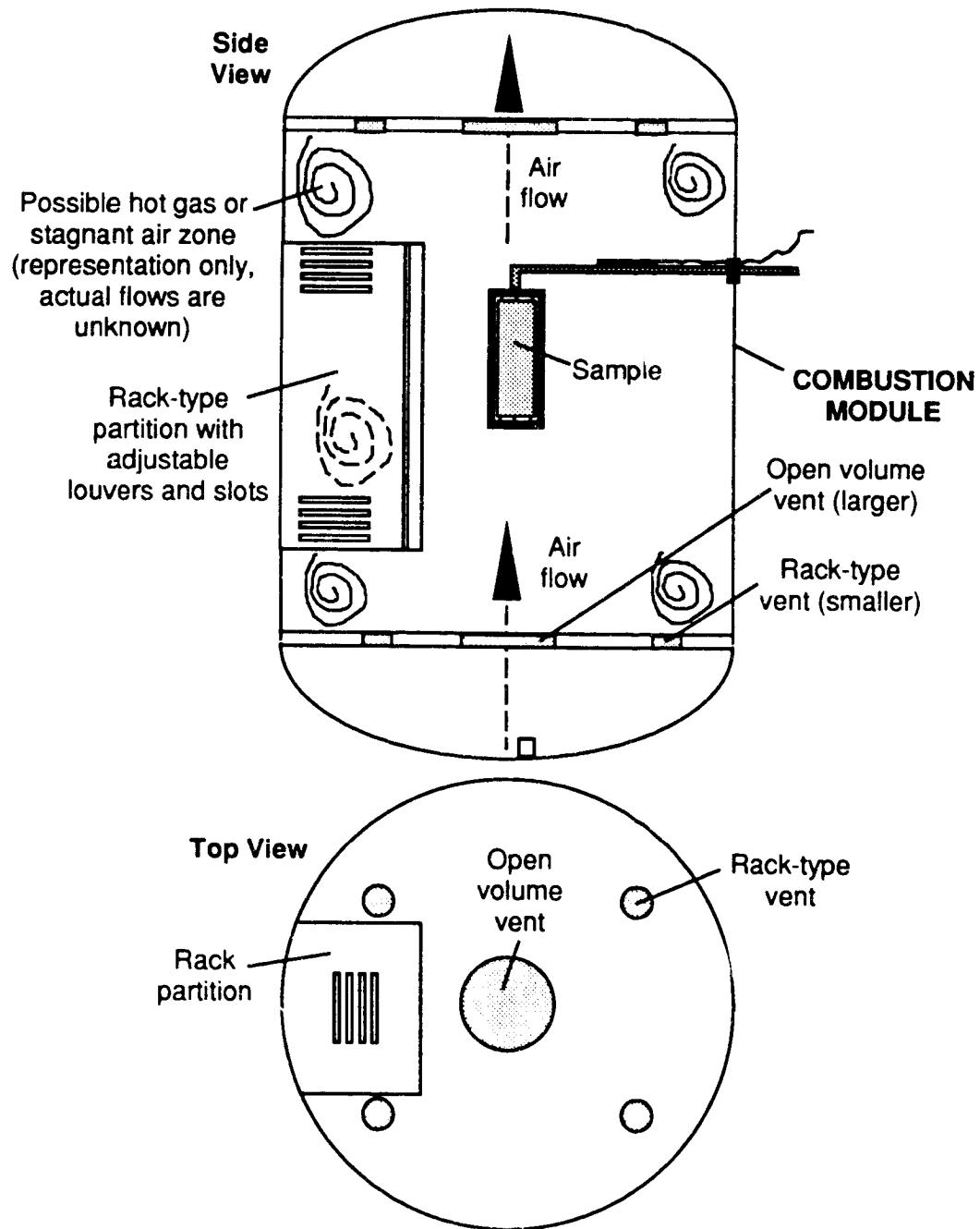


Figure 4.7. Air Flow Rates and Patterns.

The Particle Dynamics Analyzer and the video system will be the same as that used in other experiment areas. Some experimental runs will have the video cameras focused specifically on the flight of the suppressants to the burning sample.

4.3.11 Pressure

4.3.11.1 Chamber Pressure

The air pressure will be measured by a pressure transducer flush-mounted in the chamber interior wall. Chamber pressure will change from an initial pressure as a function of temperature. Another pressure transducer will be located within the flow simulation partition box which will be installed for selected experiment runs.

4.3.11.2 Suppression Discharge Pressure

The discharge pressure of various suppressants will be measured by pressure transducers at each point of discharge. The transducers will be located inside the suppressant source to preclude disturbance of chamber air flow, and will be situated in a way which will not change the flow of the suppressant.

4.3.12 Time

4.3.12.1 Fire Detector Response Time

The fire detector response times will be measured by timing the alarm activation signal with the computer's clock. This, and all other data will be time-tagged and recorded in solid state memory, hard disk, compact disk, or on tape.

4.3.12.2 Suppression Time

The time to suppression of various suppressants for various fire types will be measured by the computer's clock by recording the time of activation of suppressants and the time of suppression of the fire (temperature below the combustion or smoldering threshold), and computing the difference. This is the time elapsed between suppressant release and extinguishment of the fire.

4.3.13 Other Parameters to be Measured and Controlled (Sensitivity Studies)

4.3.13.1 Atmospheric Pressure

Atmospheric pressure within the combustion chamber will be held constant at \pm TBD Torr with a maximum variation of \pm TBD Torr over TBD seconds prior to igniting a sample, by use of a closed-loop controller. The atmospheric pressure within the combustion chamber will be measured TBD times per second.

A TBD off-the-shelf pressure transducer using 28 vdc will be selected. TBD pressure transducers will be used to ensure correct quantification of the pressure throughout the combustion chamber. An average value of the TBD pressure transducers will be obtained and this feedback will be used to automatically open or close the valve between the atmospheric gases and the combustion chamber. The pressure will be displayed. When the pressure has stabilized, a crew member will initiate the ignition sequence.

4.3.13.2 Fuel Orientation

The fuel and target will be oriented relative to the ignition source at TBD angle and distance from the source with TBD tolerances. The sample holders will support both single sample (Figure 4.8) and redundant sample fuel configurations (Figure 4.9 and 4.10). Redundant and parallel cable runs in a spacecraft will be simulated as shown in Figures 4.9 and 4.10. Numerous examples of this cabling approach are found on all spacecraft. Fire damage to one cable could cause damage to adjacent cables, thus, we are investigating the effect of fire on a variety of parallel cables, as well as other materials.

The sample holder and target holders will not be a source of heat release error. The holder will have TBD configuration and be constructed of TBD material. The fuel and target will be oriented mechanically or electronically by a crew member using simple tools (e.g., pre-set sample holder detents) to ensure the correct orientation.

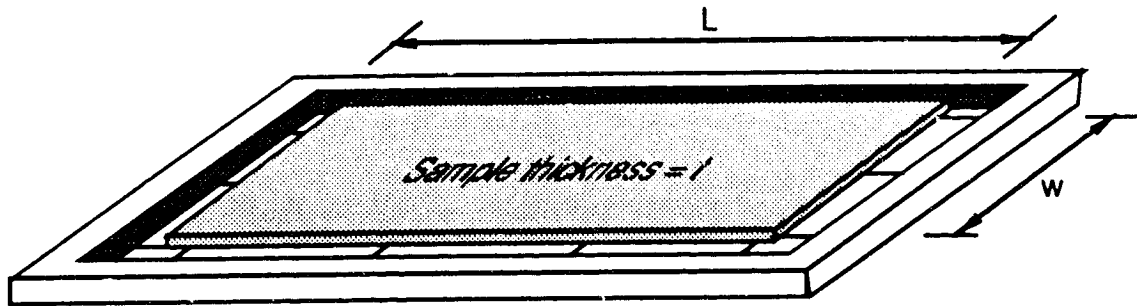


Figure 4.8. Sheet Sample in Sample Holder.

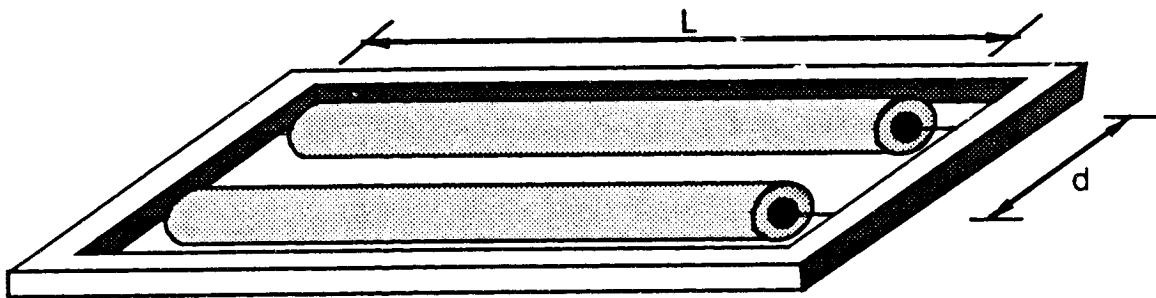


Figure 4.9. Redundant Cable Samples in Holder.

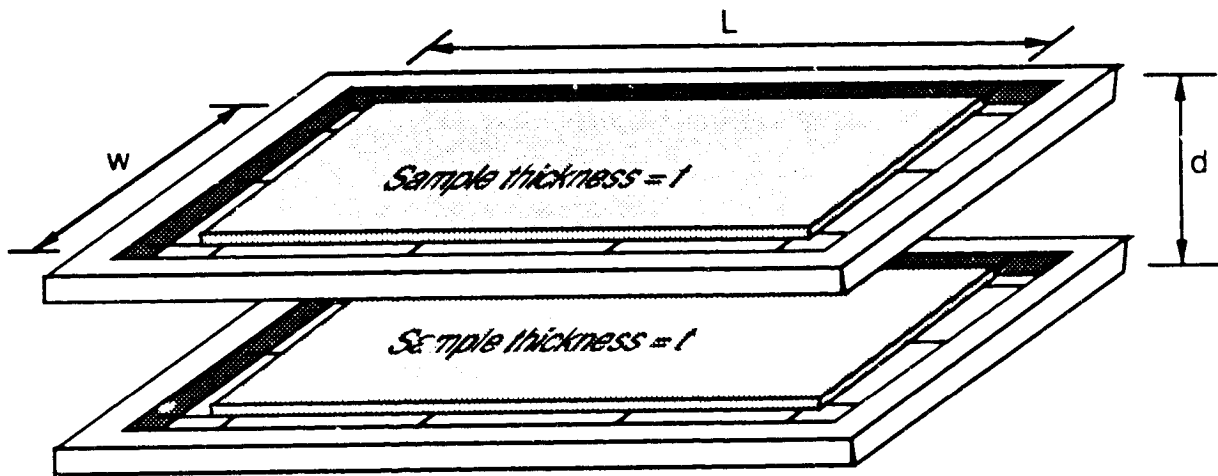


Figure 4.10. Redundant Sheet Samples in Holder.

4.3.13.3 Fuel Geometry

The fuel will have TBD geometries relative to the source of ignition, and relative to each other in the case of redundant fuel configurations (Figure 4.11).

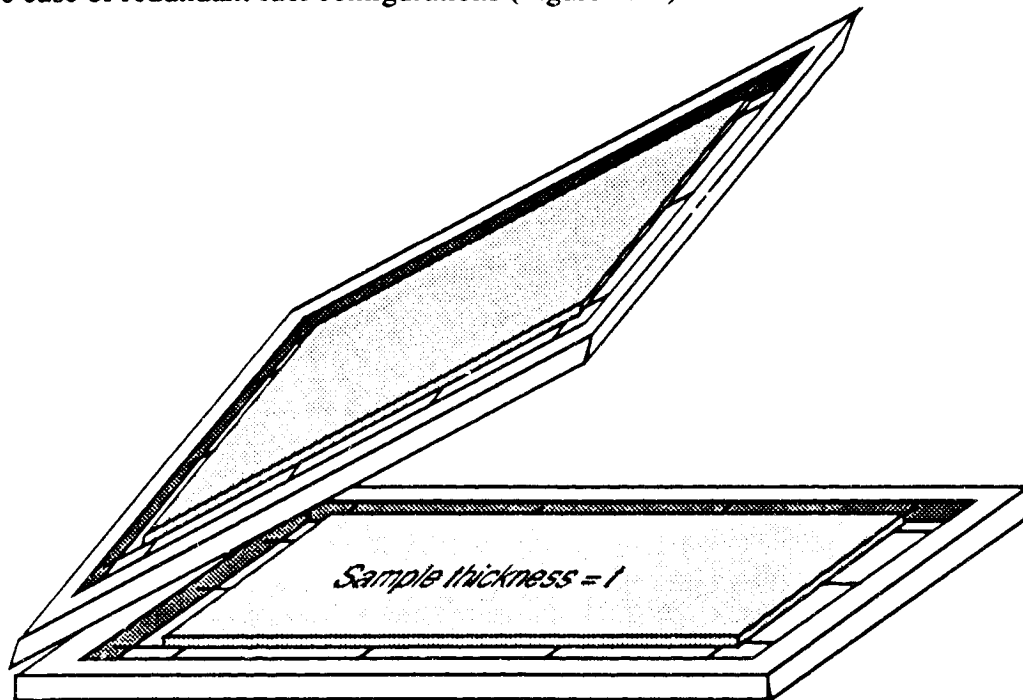


Figure 4.11. Redundant Sheets with Non-parallel Geometry

The holder will match the geometry requirements and will not introduce errors into the determination of the heat released.

4.3.13.4 Ambient Temperature

The ambient temperature of the sample will be maintained at \pm TBD K for TBD seconds prior to initiating the ignition sequence.

The temperature of the sample will be controlled by a closed-loop means using a non-intrusive diagnostic instrument (as a goal) such as the Thermal Imager. Feedback from the temperature sensor will be used to control sample heaters. The sample heaters will not introduce errors into the heat release determination. If non-intrusive measurements are not feasible, the use of extremely fine-wire thermocouples will be considered. The ambient temperature will be sampled TBD times per second.

The gases used in the experiments shall be maintained in their containers at a temperature of TBD \pm TBD K. The temperature of the gases prior to initiation of an experimental run shall be TBD \pm TBD K.

4.3.13.5 Relative Humidity

The relative humidity within the combustion chamber will be controlled to TBD percent using desiccant crystals and sampled TBD times per second. A hygrometer will be used to monitor the relative humidity

4.4 Experiment System and Subsystem Description

4.4.1 Introduction

The following section presents the Experiment System and subsystem description, configuration, and selected block diagrams. An extensive set of documentation will be produced at the outset of the development phase to provide guidance for the detailed design effort. The documentation consists of that appearing in Table 4.3.

Table 4.3. Future Detailed Design Documentation

- Design Criteria
- Requirements and Constraints
- Functional Block Diagrams and Circuits
- Functional Accuracies and System Capabilities
- Structure Design Criteria
- Inertial Properties
- Design Criteria for Temperature Control
- Flight Electronic Equipment Design
- Equipment List and Mass Allocation
- Environmental Design Requirements
- Electrical Grounding and Interfacing
- Data System Intercommunication Requirements
- Measurements and Data Formats

4.4.2 System Description

The Experiment System is divided into three modules: the Combustion Module, the Fluids Module, and the Command and Power Module (Figure 4.12). These modular divisions are driven by function. Tables 4.4 and 4.5 indicate the mass and peak power breakdown for each of the modules. The total mass is currently estimated at 496 kg (1092 lbm). The total peak power is estimated at 518 W. Both of these numbers are subject to revision as the design matures.

The host spacecraft is currently undefined, but the shuttle is preferred because of a greater likelihood of early experiment flight. If Spacelab, Spacehab, or space station are selected as the host spacecraft, the Experiment System would have rack-oriented configurations similar to that shown in Figure 4.12. The following discussion assumes Experiment System hardware interfaces with the shuttle Middeck Accommodations Rack (MAR) and middeck locker Avionics Bay 1 wire trays (Figure 4.13). It is important to note that the MAR is currently in concept development at JSC and its final configuration has not been established.

The MAR is located on the port (left) wall of the orbiter middeck, forward of the crew ingress/egress hatch and aft of the galley. It has an overall internal height of 1.95 m (76.82 in), a width of 0.53 m (21.062 in), and a maximum depth of 0.47 m (18.625 in). These MAR width and depth constraints are incompatible with the Combustion Module diameter of 0.64 m (25 in), but this diameter, as well as the length, will be the subject of much greater analysis in the development phase. For example, a one-tenth scale model of a space station laboratory module would have dimensions of approximately 1.22 m (4 ft) in length by 0.43 m (1.4 ft) in diameter which are roughly the current dimensions of the Combustion Module, and fit within the MAR envelope. The MAR can accommodate approximately 154.5 kg (340 lbm) of payload mass which is well within our estimate of the Combustion Module mass.

Table 4.4. Experiment System Mass Estimate.

Equipment	Mass (lbm)	Mass (kg)	Equipment	Mass (lbm)	Mass (kg)
Combustion			Command & Power Module		
Chamber (double-walled)	150	68	Computer	20	9
Door	10	5	Magnetic tape recorder	20	9
Mobile probe assembly	5	2	Power supply	10	5
Sample holders	3	1	Circuit breakers	5	2
Sting	1	0	switches	5	2
Ventilation simulation partition	10	5	batteries	20	9
Simulation vents	5	2	Fuses	2	1
Windows (4 VC, 3L, 3Ph, view)	20	9	Contact igniter	1	0
Thermal insulation	5	2	Radiator igniter	1	0
Seals (4+3+3+1)X3	2	1	Fans	5	2
Racks	20	9	Coatings	2	1
Bracketry	20	9	Heaters	2	1
Total Combustion Module	251	114	Insulation	5	2
Fluids Module			Cabling and connectors	20	9
Gas bottles-makeup (10)	200	91	Residual Gas Analyzer	6	3
Gas bottles-waste (2)	40	18	Thermal Imager	23	10
Gas lines	10	5	Particle Dynamics Analyzer	66	30
Gas valves	20	9	Radiometers	5	2
Suppressant bottles (6)	120	55	Fire Detectors	5	2
Suppressant lines	10	5	Thermocouples	3	1
Suppressant valves	10	5	Pressure transducers	2	1
Probe lines	5	2	Flowmeters	5	2
Probe valves	2	1	Hydrometer	5	2
Pumps	30	14	Accelerometer	1	0
Pressure regulator	10	5	Video cameras (4)	10	5
Filters	20	9	Video recorders	20	9
Storage Bags	5	2	Racks	20	9
Racks	20	9	Bracketry	20	9
Bracketry	20	9	Total Cmd & Pwr Module	309	140
Clean-up equipment & solvents	10	5			
Total Fluids Module	532	242			
			Grand Total	1092	496

Table 4.5. Experiment System Peak Power Estimate.

Equipment	Peak Pwr (W)	Equipment	Peak Pwr (W)
Combustion		Command & Power Module	
Mobile probe assembly	1	Computer	20
Windows (VC, 3L, 3 pH, view)	5	Magnetic tape recorder	20
Total Combustion Module	6	Power supply	10
		Contact Igniter	100
Fluids Module		Radiator Igniter	100
Gas valves	2	Fans	5
Suppressant valves	2	Heaters	20
Probe valves	1	Residual Gas Analyzer	20
Pumps	30	Thermal Imager	30
Total Fluids Module	35	Particle Dynamics Analyzer	100
		Fire Detectors	5
		Thermocouples	1
		Pressure transducers	2
		Flowmeters	2
		Hygrometer	2
		Accelerometer	1
		Video cameras (2 B&W, 1C)	34
		Video recorders	20
		Total Command & Power Module	477

Since the MAR and middeck locker areas are separated by the galley, two configurations are under consideration. The first configuration calls for physical transport by a crew member of gas bottles from the middeck locker experiment storage rack to the MAR for installation, as required. The crew members would connect the bottle to the fluid lines and proceed with the experiment run. Empty bottles would be disconnected and exchanged for full bottles, or for bottles with different gases. The second configuration would have a fluid line from the middeck locker experiment storage rack to the Combustion Module in the MAR. The line would run against the port wall beneath the galley. This mode would preclude the necessity for fluid bottle change-out by a crew member, but may not be acceptable because of safety reasons. A final configuration selection has not yet been made.

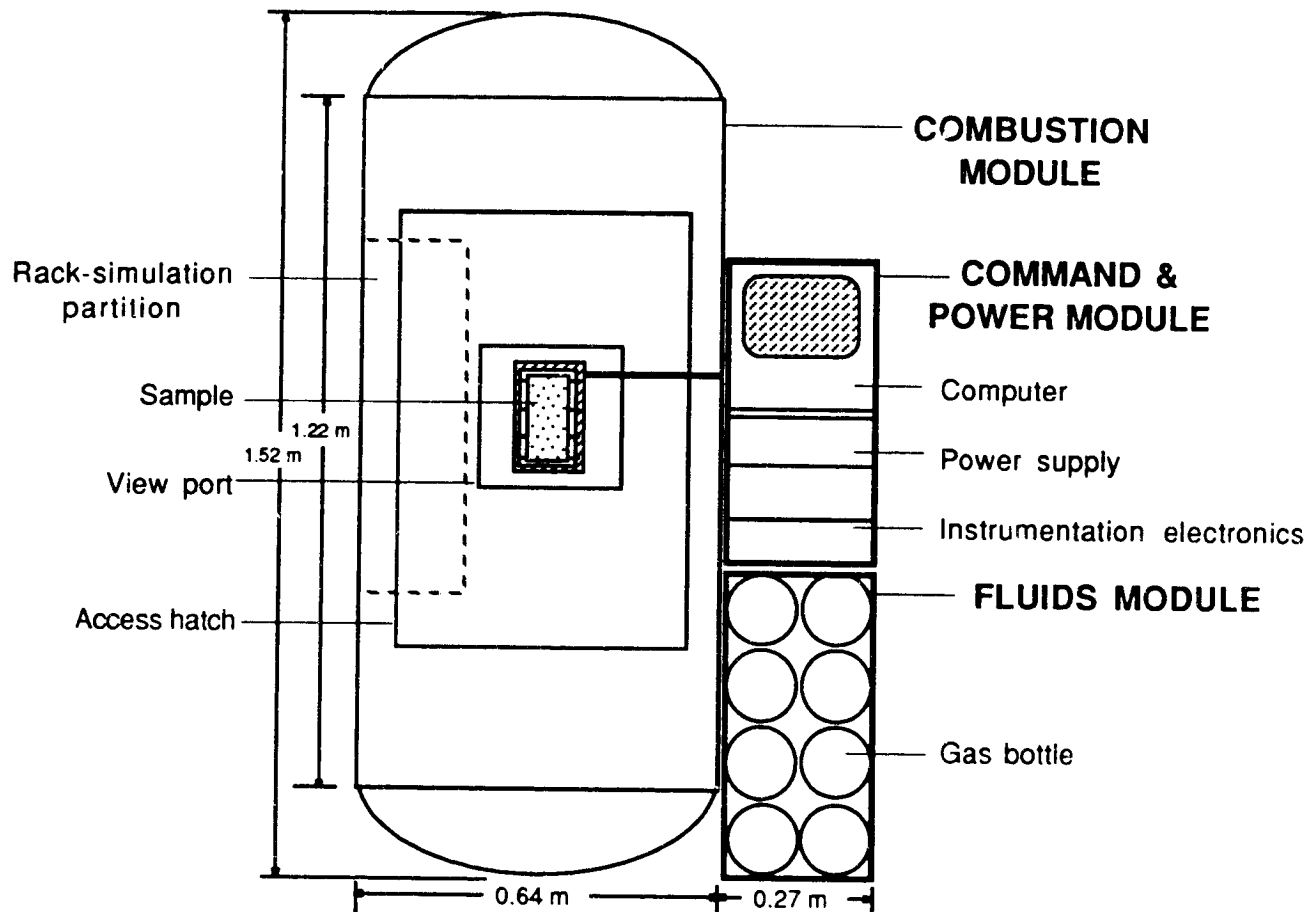
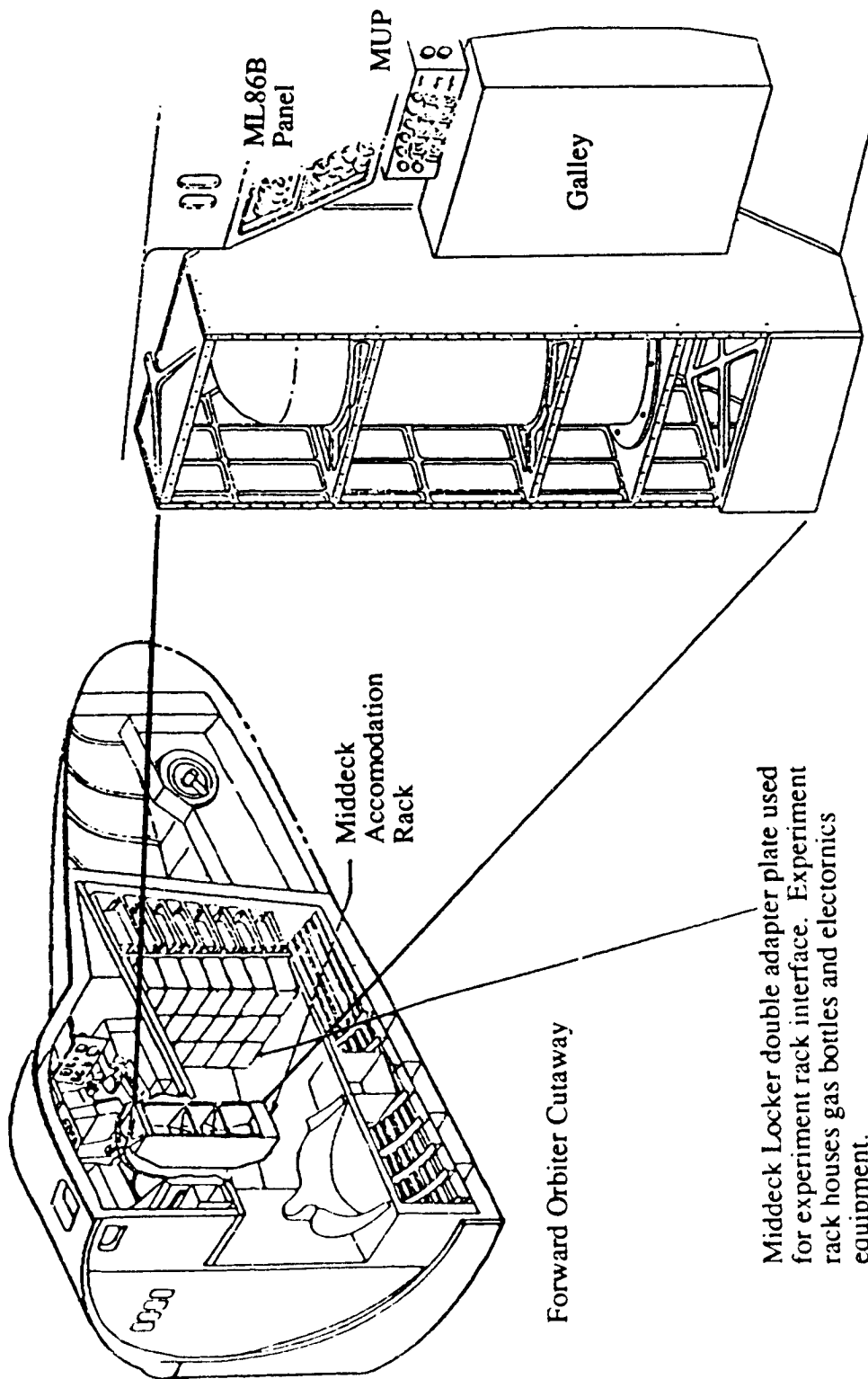


Figure 4.12. System Configuration with Spacelab or Space Station as Host Spacecraft.

Additionally, if the Combustion Module volume occupies most of the MAR volume, the computer and other electronics or instrumentation will not be mountable within the MAR for launch and landing, and will have to be stowed in the middeck locker experiment storage rack, or possibly within the Combustion Module. A crew member would have to transport this equipment from the middeck locker experiment storage rack to the area of the Combustion Module for experiment runs, and later, re-stow the equipment. The goal is to minimize the amount of equipment transport, as well as connecting and disconnecting fluid lines.



Middeck Accommodations Rack with representative Combustion Module installed.

Forward Orbiter Cutaway

Middeck Locker double adapter plate used for experiment rack interface. Experiment rack houses gas bottles and electronics equipment.

Figure 4.13. Shuttle Middeck Installation of Experiment System.

The following discussion assumes a shuttle middeck locker mechanical interface (shuttle Avionics Bay 1 wire trays) with the hardware, but would have similar rack-oriented configurations for Spacelab, Spacehab, or space station. No more than 31.8 kg (70 pounds) of payload and adapter plate will be permitted to interface with each of the middeck locker mounting areas, thus, the mass of the experimental hardware will be appropriately distributed to meet that shuttle requirement. Redundancy of the Experiment System equipment will be selective in nature. Functional redundancy will be emphasized, as opposed to block redundancy. Each safety-related function of the Experiment System will be two-fault tolerant. The following sections describe the three modules and seven subsystems.

4.4.2.1 Combustion Module

The structural components of the Combustion Module include the combustion chamber, the sample support sting and mobile probe assembly, and the brackets which interface the chamber to the middeck interfaces. The combustion chamber (0.64 m outside diameter by 1.52 m length) consists of a main cylindrical section (1.22 m in length) closed at both ends by elliptical domes. For the purposes of providing two levels of containment, the chamber and door will have a double-wall construction consisting of an inner wall that is completely surrounded by, and attached to the outer one by isogrid ribbing which will standoff by approximately 0.012 m. Thermal insulation will be provided between the walls. There will be a removable chamber access door in the front of the chamber which will be opened and closed relatively easily to permit set-up of the sample holders and other equipment before experiment runs, and clean-up after experiment runs. The door will use an easy-opening set of latches and will have three staggered layers of seals, corresponding to the inner and outer chamber walls. Both layers of the walls and door of the chamber will have several windows and other penetrations for the many pieces of equipment which will have to enter or view the chamber interior. These will be of varying nature, such as wires to small sensors, lasers, gas transport tubes, video cameras, and probes for the gas analyzer. Each window and instrument connection will be triple-sealed for leak prevention.

The sample, which is mounted in a sample holder, will be held in place by a support sting extending from the inner wall of the chamber to the chamber middle regions, where the sample holder will be attached via a fitting which serves as an adapter to the various types of sample holders (Figure 4.6). The sting itself will be afforded support by its attachment to the mobile probe bracketry assembly. This assembly consists of two attachments bolted to the inner

chamber wall which support a central worm gear. The mobile probe will be attached to the gear. Through exterior control, both manual and motor driven, the worm gear will rotate, and, as a result, move the probe vertically up or down, thus, allowing the probe to stay slightly forward of the flame front.

The interior of the chamber will be coated with a non-oxidizing material, or the chamber material selected will oxidize only at the surface level. This is required to ensure structural integrity as well as accurate oxygen concentration depletion measurements.

The Combustion Module (and other hardware) and its interfaces with the host spacecraft must withstand launch and landing (both nominal and emergency) loads. A minimum of three interface brackets will connect the chamber to the host spacecraft.

4.4.2.2 Fluids Module

The structural components of the Fluids Module consist of the racks necessary to contain the gas bottles and provide the interface of the Fluids Module with the host spacecraft (Figure 4.12). A number of gas bottles will be necessary in the experiment, some to continuously provide fresh gas to the chamber, some to hold suppressants, and others to store used/filtered gases. Each must be secured rigidly in position to preclude breaking loose during launch and landing, as well as to guard against possible leakage. The gas bottles are bulky, heavy, and potentially hazardous, and also run the risk of releasing gases which are important to the experiment and possibly harmful, so they must be well-secured. For this purpose, the Fluids Module will be equipped with a rack system which will in turn be bolted to the middeck locker (or other host spacecraft) mechanical interface plates. The racks will be custom-built for the exact positioning of required bottles so that all fitting integrity will be maintained. The connection of the racks to the interface plates will be made with high-strength bolts. The Fluids Module will also have a front panel which can be opened to further ensure the immobility of the gas bottles, as well as access to the bottle valves, pumps, and other hardware. The Fluids Module will provide filtering of all gases exiting the Combustion Module. The approach to disposal of the gases has not been established, and is a function of the host spacecraft. In the shuttle middeck, there are two approaches under consideration: extreme Fluids Module filtering and scrubbing of the gases and release into the cabin; and filtering and scrubbing of the gases and then carefully pumping them back into empty gas bottles. Both approaches have a number of safety implications which

must be addressed in the development phase. On Spacelab, the gases would be filtered and scrubbed before release into a vacuum line which vents to space.

4.4.2.3 Command and Power Module

The Command and Power Module will include a number of structural components, among them: permanent equipment racks and removable storage racks (Figure 4.12). The integrity of the structure in this area is essential because many of the instruments that are included in the Command and Power Module are somewhat fragile and must be stowed properly for launch and landing, and are also important to the operation of the experiment. As in the case of the Fluids Module, most of the interfaces to the adapter plates which interface the experiment system to the Avionics Bay 1 wire trays will come only from the Experiment System support racks, and not involve the instruments themselves. The rest of the equipment will be placed in a rigid rack system, which will be collectively bolted in position.

The racks will be designed specifically for the instrumentation and other equipment they are to hold, to ensure a secure fit. They will also be removable to facilitate access to the equipment.

4.4.2.4 Subsystem Summary

The Experiment System is composed of 7 subsystems (see system functional block diagram in Figure 4.14): Structures, Thermal Control, Fluids Control, Electrical Power, Command and Data, Software, and Instrumentation. Each of these is described in detail in later sections. This section will serve as an introduction to the interaction of the subsystems. The scenario-driven philosophy of the Experiment System is to take as much simultaneous data as possible so that data correlation is maximized and experimental runs are minimized. Thus, most experimental runs will have all of the instrumentation elements operating concurrently. The remaining subsystem equipment of the Experiment System services the Instrumentation Subsystem and/or provides an interface with the host spacecraft.

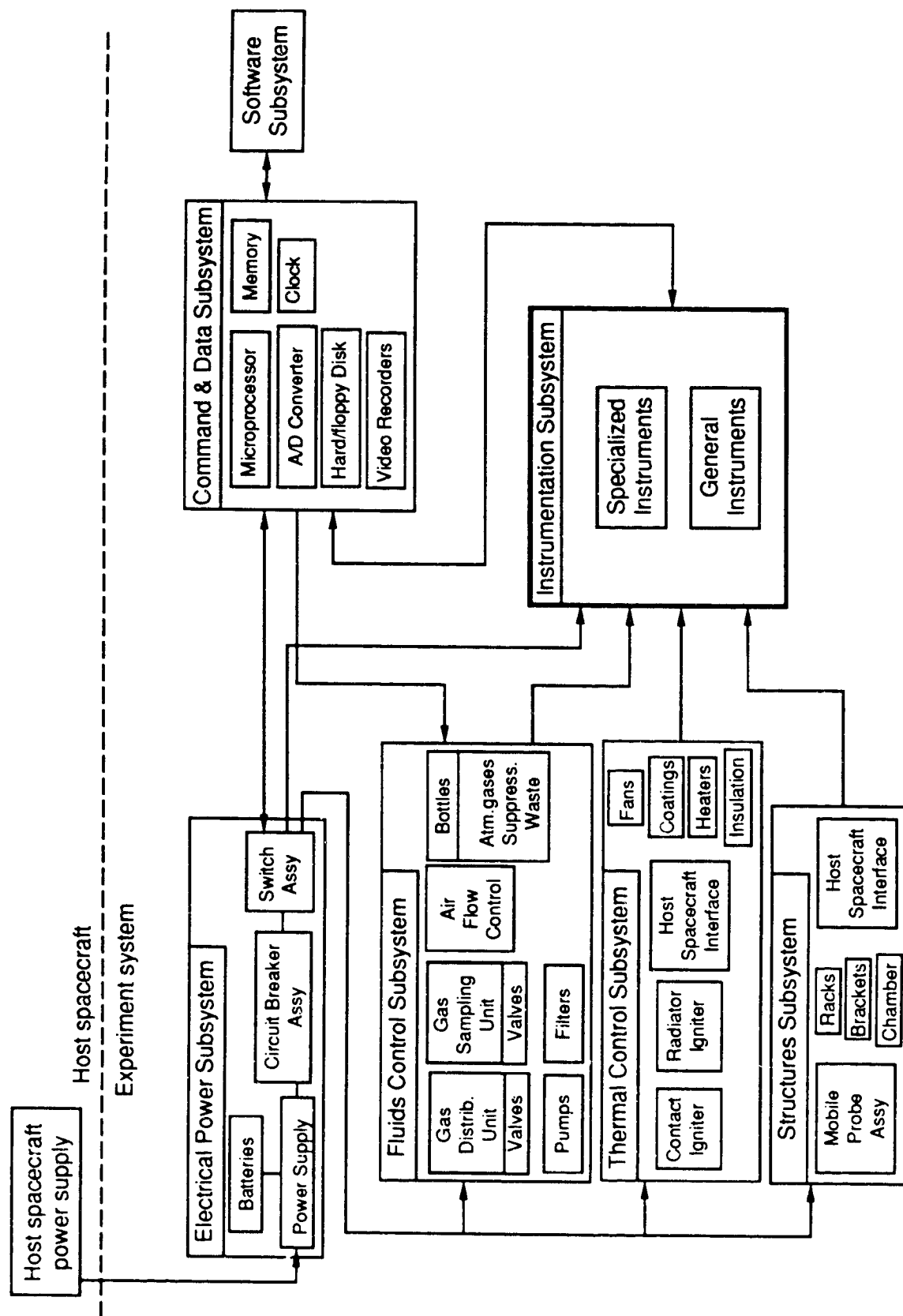


Figure 4.14. System Functional Block Diagram.

4.4.2.4.1 Instrumentation Subsystem

Under control of the Command and Data Subsystem, the Instrumentation Subsystem performs a data-acquisition function through two primary subsets of instrumentation: Specialized Instruments and General Instruments (see subsystem functional block diagram in Figure 4.15). The Specialized Instruments are typically complex in nature and consist of equipment which addresses the requirements of a specific experiment to be run. The General Instruments are typically those which serve to address the requirements of a number of different experiment runs and are somewhat less complex in nature. The Specialized Instruments are the: Residual Gas Analyzer, Thermal Imager, Particle Dynamics Analyzer (lasers), Radiometers, and Fire Detectors. Generally, each of these requires specialized software, resident in the central computer, to operate and provide data interpretation. Each is composed of a number of electronic or optical hardware elements which are discussed in detail later in this chapter. The General Instruments are the: Thermocouples, Pressure Transducers, Flow Meters, Hygrometer, Accelerometer, and Video Cameras. With the exception of the video cameras, whose data is stored in the video recorders, the remaining General Instruments' signals are fed directly into the central computer. That is, they do not require any additional electronic signal processing, other than that provided by the central computer itself, prior to being input to the computer for manipulation and data storage.

4.4.2.4.2 Electrical Power Subsystem

Electrical power is taken from the host spacecraft, or from the Experiment System batteries, by the Electrical Power Subsystem, and is transformed into the required voltage levels where it is distributed by appropriately sized cabling to the remaining electronic equipment. A switch assembly, actuated by the Command and Data Subsystem, will provide the turn-on and turn-off of most equipment. Major electronic equipment elements will have their own power switches, but all will be subject to shut-down through actuation of a common switch by the central computer as a safety precaution.

The Electrical Power Subsystem will convert the host spacecraft voltage (28 Vdc and 115 Vac is anticipated) and current supplied, to the required experiment levels. It consists of the power conditioning circuitry, chassis, cabling, power switching, fuses, and circuit breakers. Requirements will be defined to ensure that all host spacecraft interface requirements are met on: packaging, thermal, chassis-circuitry isolation, electrical bonding, magnetic fields, grounding of

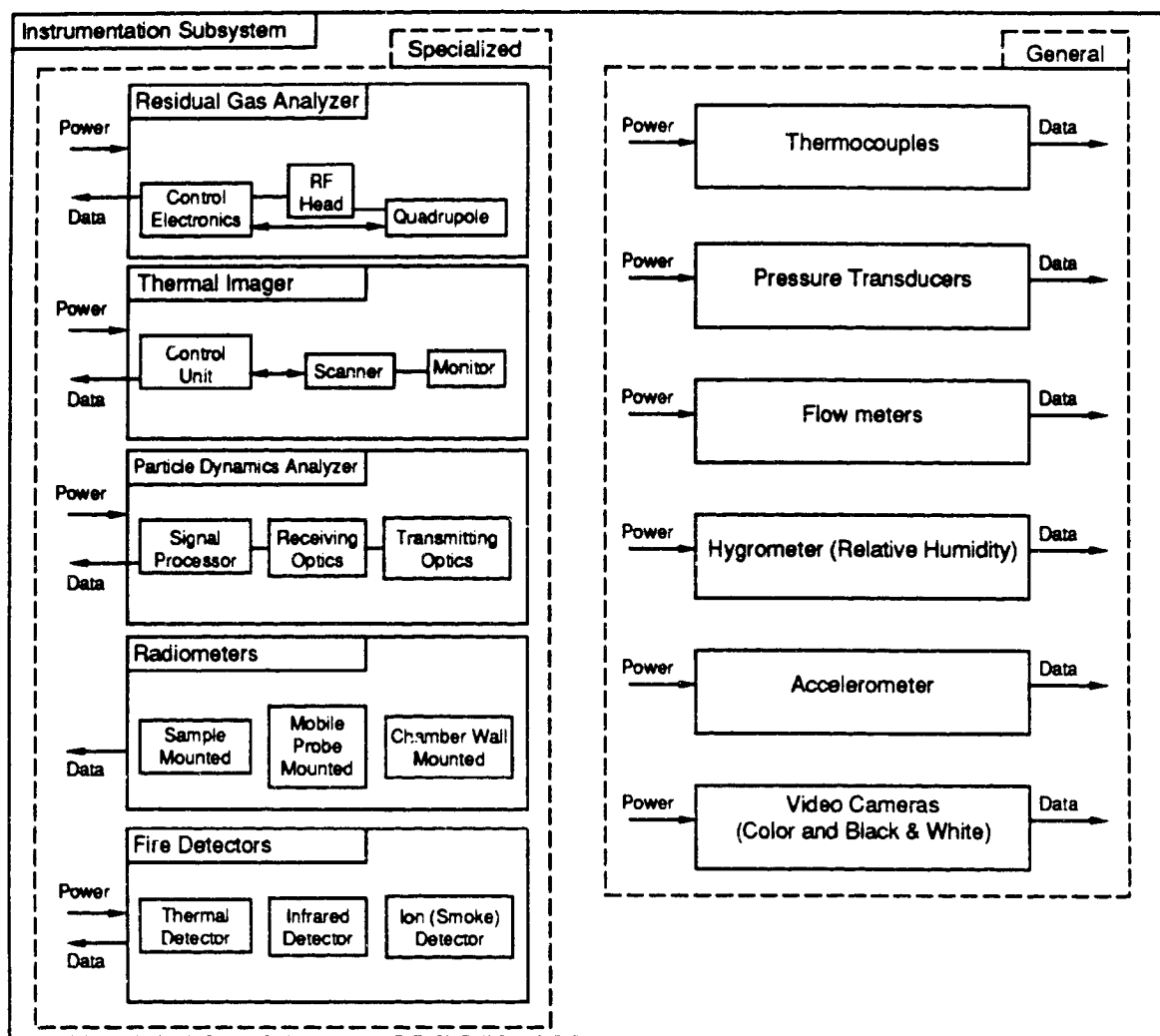


Figure 4.15. Instrumentation Subsystem Functional Block Diagram.

shields, and grounding of reference trees. Power usage and conversion losses will be minimized through design and selection of low power consumption components.

4.4.2.4.3 Fluids Control Subsystem

Various tanks containing the combustion-supporting gases and extinguishing agents along with the associated fluid lines and manual/automatic valving comprise the Fluids Control Subsystem. Flex lines of varying lengths will be considered to accommodate the tanks at various

locations imposed by shuttle, Spacelab or host spacecraft space requirements. The tanks will meet all pressure vessel safety requirements and will be designed to support multiple experiment runs. Tank mass trades will be performed to establish the best tank volumes versus pressures required for the experimental runs.

The Fluids Control Subsystem provides the selected gases from storage bottles to the Combustion Module at the appropriate flow rate and pressure by means of electrically actuated valves in the Gas Distribution Unit (a manifold system of valves and lines). The valves are designed to fail to the closed position in the event of power loss or other safety-related anomalous conditions. The Gas Sampling Unit consists of a set of miniature valves at each of the Residual Gas Analyzer probe tips, and the associated lines to the vacuum chamber which precedes the quadropole. Non-oil-diffusion pumps provide the required vacuum, and also pump scrubbed and filtered waste gas products into the waste gas storage bottles.

4.4.2.4.4 Thermal Control Subsystem

Temperature control of the Experiment System will be provided by components of the Thermal Control Subsystem. These components are the: cooling fans, heaters, thermostats, insulation, and various thermal coatings applied to temperature-sensitive equipment to increase absorbtivity or emissivity. Two igniter elements are also included: the contact igniter and the radiator igniter. The contact igniter consists of an electrical wire coil mounted on the sample holder to provide direct contact to ignite the sample. The radiator igniter provides a "space heater" effect which can be directed at remote sample targets without contact. Finally, the thermal interface with the host spacecraft is "bookkept" in this subsystem.

The Thermal Control Subsystem will emphasize passive measures such as paints, radiators, and thermal insulation to maintain the experiment within the required temperature limits. The temperature transducers will provide temperature data as a function of time at several locations on the interior and exterior of the Combustion Module. Cooling will be accomplished by radiation and conduction to the host spacecraft, as well as fan ventilation.

4.4.2.4.5 Structures Subsystem

The Structures Subsystem is comprised of the combustion chamber, structural support bracketry for the other subsystems, transport containers, and various mechanisms, such as the mobile probe assembly, sample holders, sample support structure, sample geometry adjustment mechanism, equipment racks and other structural elements. The Structures Subsystem also provides the structural interface with the host spacecraft.

The Structural Subsystem will be defined to accommodate the modular approach. To minimize the mass, 6061-T6 aluminum will be used to the maximum extent possible. Areas requiring more stiffness or strength will use titanium or stainless steel. The ultimate load/stress factor of safety will be 1.4 for primary and secondary structures, and 4.0 for pressure vessels. The shuttle orbiter (if that is the host spacecraft) attach points and launch and landing loads environment will be derived from the middeck (or other) interface control document. Computer models representing all frequencies below the highest frequency used for the orbiter interface reaction loads will be developed and updated as the design matures. Stress analyses will be performed on the structural elements. The structure will be sized to withstand a modal survey test, as well as sine and random vibration testing (to occur during the development phase) to verify the analysis and the structural integrity.

4.4.2.4.5.1 Functional Requirements

4.4.2.4.5.1.1 Interfaces

The Structures Subsystem shall provide for structural interfaces to the host spacecraft.

4.4.2.4.5.1.2 Equipment Mounting

The Structures Subsystem shall provide all mounting brackets for other subsystems components, such as video cameras, radiometers, transducers, etc.

4.4.2.4.5.1.3 Strength

All structures shall remain intact when exposed to vibrations greater than those encountered in worst case launch and landing loads in the shuttle.

4.4.2.4.5.1.4 Vibration

All structures supporting sensory instruments or other fragile equipment shall be designed for minimal vibration.

4.4.2.4.5.1.5 Safety

All structures shall be designed to the requirements of NSTS 1700.7B.

4.4.2.4.5.1.6 Containment

The combustion chamber shall have two levels of containment.

4.4.2.4.5.1.7 Equipment Ports

The combustion chamber shall have all the openings, windows, and other ports necessary for the access of instruments to the chamber interior, and all shall have triple, airtight, corrosion-proof seals.

4.4.2.4.5.1.8 Internal Instrumentation Support

The combustion chamber shall provide for the mounting of the sample support sting and mobile probe assembly, the partition box, the variable vent simulation partitions, and all other interior equipment.

4.4.2.4.6 Command and Data Subsystem

The Command and Data Subsystem (see subsystem functional block diagram in Figure 4.16) consists of a central computer (probably IBM PC-based compatible), keyboard, monitor, hard and floppy disk drives for storing data and software, video recorders for the video cameras and the Thermal Imager, and a multiplexer for sequencing the data input from various instrumentation into the computer analog-to-digital converter. The Command and Data Subsystem

provides control of the electrical switching of power to the equipment, and programmable sequencing of the probe sampling valves and other equipment. The Software Subsystem resides in the computer. Additionally, several special purpose circuit boards which operate and process certain instrumentation data are housed in the computer. All of these elements are connected by a data, address, and control bus. The microprocessor and random access memory devices chosen will be resistant to cosmic ray induced single event upsets. Mass, power, reliability, and cost trades will be performed to determine whether the non-video data will be stored on erasable programmable read only memory chips, hard disk, compact disk, or magnetic tape.

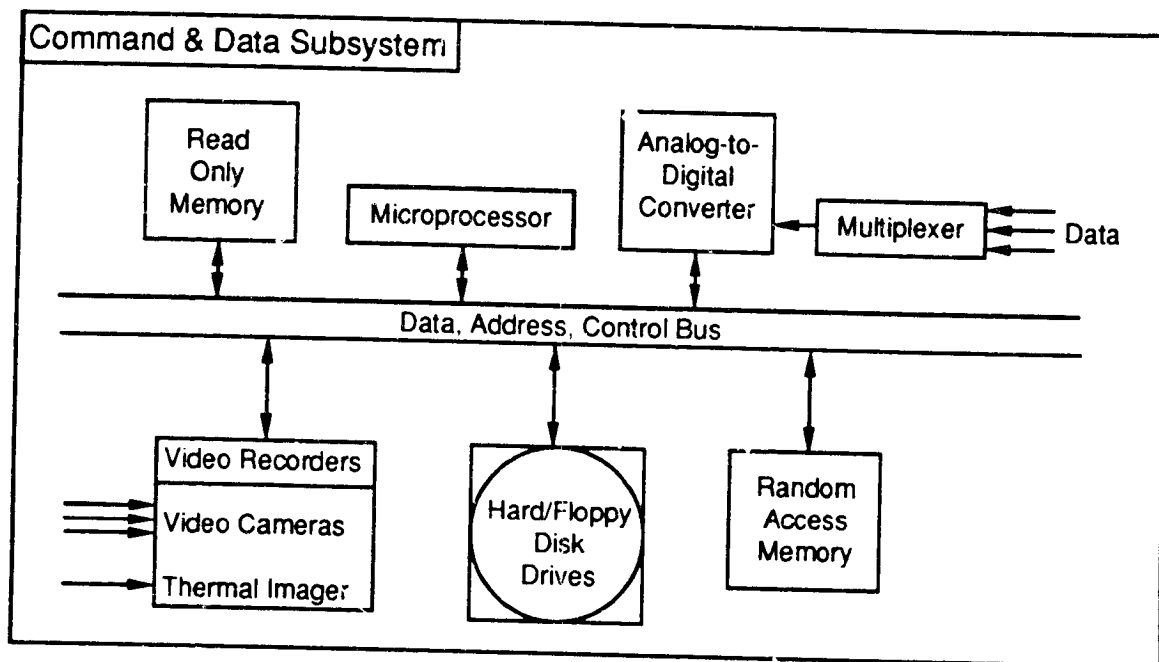


Figure 4.16. Command & Data Subsystem Functional Block Diagram.

4.4.2.4.7 Software Subsystem

Software required to operate the Experiment System as well as process data from each of the instrumentation elements, and caution and warning alarms for safety, is contained in the Software Subsystem. The software resides in the Command and Data Subsystem memory in the form of random access and read only memory, as well as on the hard and floppy disks. The software is programmable and modular in nature.

The software developed to control the microprocessor will be designed in a modular format to ensure ease of modification. The number of lines of code and the resultant checkout is not expected to be significant because much of it will be provided by the instrumentation vendors, and will require only selected modification and integration. The system software will be developed on an IBM PC-based compatible computer. The actual code will be developed after the software requirements specifications and the software design document. We will, then, generate some representative code to test the concepts developed, prior to proceeding with full software development. The approach to generating the requirements specification and design specification follows.

4.4.2.4.7.1 Software Requirements Specification Development

A software requirements specification will be written. This will define interfaces with the hardware (computer, the IBM PC-based development system, and other support equipment), software, and people. Constraints imposed on the design of the software because of its relationship to other hardware, software, or human interfaces will be described. All relevant hardware interfaces will be characterized, such as: computer characteristics, memory size, work size, access and instruction times, interrupt capabilities, and special hardware capabilities. Special hardware designed to test the software or required as part of the prototype implementation will be described. We will produce interface diagrams and data flow diagrams. Requirements for descriptions of each function will be made in terms of the inputs, processing, outputs, and design requirements.

4.4.2.4.7.1.1 Interfaces

A description of all software resources and/or functional software required to complete development of the software will be made. Software interfaces to be described are: the operating system characteristics, I/O capabilities, drivers, and special features; applications software; data base software; general system utilities and support; compilers, editors, special tools; and acquired software. User characteristics and training will be established; human engineering of the interface will be discussed; and special features, such as graphics. Software packaging considerations will be described such as transportation media; documentation shipped with software when released; special features required to satisfy varied interfaces such as different I/O drivers for different hardware configurations. The relationship of the software to other system elements will be graphically represented using functional block diagrams. The overall relationship of the

data flowing throughout the system will be presented at a fairly high level. The data will point out the input data and its sources external to the software being designed, the data required for each of the major functions listed in the software plan and the expected output data from the software to be designed.

4.4.2.4.7.1.2 Functions

Functional requirements of the software will be specified in quantitative terms with tolerances. Included will be a description of the information and its source(s). A description of each of the processing requirements for the function will be made, including its purpose and approach. The destination(s) and type(s) of output information associated with a function as a result of the processing will be defined. This includes a description of the information, its destination(s), and in quantitative terms its units of measure, accuracy/precision requirements and frequency of output information. Software design requirements will be written which will include: the specification of our programming language, the use of a programming standard to ensure module compatibility, program organization, program design resulting from consideration or modifications to the software during operation, special features to facilitate testing, and expandability to facilitate modification and additions.

4.4.2.4.7.1.3 Data Base

All software data base requirements will be described. Data base hierarchical structure will be described. Parameters such as total simultaneous message handling, total number of simultaneous elements controlled, total number of simultaneous displays and operator station requests, number and types of inputs processes will be described. The system capacities are directly related to computer storage capacities, interfacing subsystem timing rates, and interfacing equipment capacities. All global data items will be described, including: the file structure and format; content and quantity of each data item; relationship of software functions to data, and data limits or constraints. The data base access characteristics for all global data items will be described along with the frequency and method of update of the data environment.

4.4.2.4.7.1.4 Quality Assurance

Requirements for formal validation of software performance and functionality will be specified. The functional/performance requirements to be tested will be defined, along with the limits of each test. Validation requirements will include inspection of the software, review of analytical data, automated demonstration tests and review of the test results. The resources required during validation will be outlined. Requirements that cannot be verified until system integration testing will be identified.

4.4.2.4.7.2 Design Requirements Specification Development

A system software design requirements specification will be written to serve as the guide for implementation and test, as a critical review tool, and as an essential maintenance document. This document will establish the relationship between functional details and the software structure. It will address data flow and structure, procedural details for each module of a software system, database characteristics, and certain test and packaging provisions.

4.4.2.4.7.2.1 Design Description

The design description will be top level definition of the software structure and data flow/structure determined during preliminary design. The relationship between major software functions and the software structure will be addressed. Each function will be described with reference to both data flow or structure and software structure. A detailed description of data flow and the transforms applied during data flow will be made. Flow of control will also be described. With structured design methodology, the afferent, transform, transaction and efferent flow paths will be identified. The data structure logical and hierarchical organization of data will be discussed and the physical data configuration, such as tabular and linked list. Data flow graphs and a schematic graphical representation of data structure will be presented. The complete software structure will be described. Using one or more structure diagrams, each major software function described will be presented in terms of the modules that will accomplish the function, with the primary goal of showing the relationship among the modules and the hierarchy of control and processing.

4.4.2.4.7.2.2 Modules

An explicit description of the inputs, processing, and outputs will be presented. The primary goal is clarity and completeness. The design description will evolve in two stages: 1) during preliminary design where a top-level description (e.g., a flowchart, box diagram or design language) will be developed, and 2) during detailed design where a complete description of procedure will be developed. The detailed description will contain: 1) a definition of all important local identifiers and all global data; 2) a processing description that can be translated directly to code; and 3) design notes regarding procedural details. A detailed description of the external interfaces to the module will be presented. These will include: 1) a subprogram argument list in which each data/control item will be defined (including the argument identifier, data type, input/output indicator, and data bounds); 2) all file I/O including READs and WRITEs to standard I/O devices, parts and secondary storage devices, and 3) all modules called by the subject module. Comments containing all supplementary information will be included, such as restrictions, limitations, performance characteristics, and error-handling. A compiler-generated data dictionary will be included.

4.4.2.4.7.2.3 File Structure and Global Data

All files that exist prior to execution of the software or are retained after termination are considered external and will be described in terms of title, length in words or bytes, and access method. Global data will be described.

4.4.2.4.7.2.4 Requirements Cross Reference

A requirements cross reference matrix will be developed and used to relate satisfaction of a requirement with one or more software modules (traceability) and will be completed during preliminary design.

4.4.2.4.7.2.5 Test Provisions

Guidelines for unit testing, overall strategy for software integration, and special capabilities required for testing will be described.

4.4.3 Instrumentation Subsystem Detailed Description and Requirements

A number of general and specialized instrumentation devices will be needed to successfully gather the required science data. The specialized instrumentation consists of those such as the Residual Gas Analyzer to obtain gas species concentrations, the radiometer to obtain heat flux information, the laser system to obtain smoke particle sizes and velocities, and others. The general instrumentation consists of various thermocouples, the video camera system, the chamber and line pressure transducers, flowmeters, and a number of other data-taking instruments. Each will be discussed in detail in the following sections and will be followed by its specific functional requirements.

4.4.3.1 Residual Gas Analyzer

4.4.3.1.1 Introduction

This section will discuss the use of a quadrupole residual gas analyzer to monitor the concentrations of certain preset gases during the course of various experiments. It will deal with the operation of the quadrupole mass spectrometer; the use of a computer and specialized software to interpret and store data; the miscellaneous other equipment required; the modifications needed to be made to a standard gas analyzer to make it useful and most efficient in this application; and the relevant specifications, among them size, power, and accuracy, that apply to the instrument.

The function of a residual gas analyzer is to measure the concentrations of the various gases present in a gas sample. In this experiment, it will continually monitor certain gases which are important by-products of combustion, and which will be pre-programmed into the analyzer. These gases are: CO_2 , O_2 , NO , C_2H_2 , CO , N_2 , CH_4 , C_2H_6 , H_2O , and H_2 .

When the gas analyzer is in use, samples of the atmosphere in the combustion chamber will be taken through one of a number of probes, and pumped into a vacuum chamber before being analyzed by the quadrupole. The computer will find from the quadrupole's raw data the concentrations of the programmed atomic masses and, after resolving ambiguities due to gases of approximately equal mass, store the information. Gas will be cleared from the quadrupole and vacuum chamber which precedes the quadrupole, and the cycle will repeat with gas from the next sampling probe.

4.4.3.1.2 Quadrupole and RF Unit

The quadrupole mass spectrometer is the part of the equipment that does the actual measuring of gas concentrations. After entering the quadrupole from the vacuum chamber, a gas sample is subjected to an electromagnetic signal at a specified frequency, supplied by a radio frequency (RF) generator and RF controller. Each desired gas corresponds to a certain frequency. The first frequency excites only the gas type of smallest mass, and, by measuring the response to that signal, the quadrupole measures the amount present of that particular gas. Then, the signal is changed to the next frequency, and the next-heaviest gas is measured. After a full cycle, the gases are cleared from the quadrupole, the next sample enters, and the cycle repeats.

The quadrupole used in this experiment will be an adaptation of the type used in the VG Instruments Micromass PC Residual Gas Analyzer. There are two types of detection methods offered, the Faraday Cup and the Electron Multiplier. The Multiplier is the desired type, because of its superior sensitivity, but it may be too fragile for space flight. If it is determined that this is so, either a method of protecting the quadrupole will be developed, or the Faraday Cup, which is more rugged but slightly less sensitive, will be used.

Ranges of detectable mass vary with quadrupole used. Since the gases desired for this experiment only go as high as 44 amu in mass, a quadrupole with a standard 1-100 amu mass range seems sufficient, but larger ranges are available if deemed necessary. Even with the less sensitive Faraday Cup, the quadrupole is accurate to approximately 1 percent. Gas species of almost equal mass cannot be differentiated by the quadrupole, but are counted together. This confusion can be solved in the computer's analysis of the quadrupole data, and is discussed in the next section.

4.4.3.1.3 Residual Gas Analyzer Computer and Software Functions

The main functions of the central computer in the Command and Power Subsystem will be controlling the equipment (quadrupole, pump, valves, probes, and so on), interpreting data from the quadrupole, clarifying ambiguities in that data, and storing information.

To obtain sample gases from multiple probes in rapid succession, the computer will coordinate the opening and closing of valves on the various probes to let only the desired gas sample enter the equipment, and to ensure that gas from the previous sampling is no longer present. To make the process as quick and efficient as possible, once the quadrupole takes in gas to be analyzed, the currently-operating probe will be closed off, and the next one opened after the current gas has been expelled. In this way, when the quadrupole has finished with one sample, the correct next sample will be ready immediately, and the delay will be minimized.

When the computer receives data from the analyzer, it will organize them into a listing of the gas and the percentage of the sample that gas takes up. The data will be in the order of ascending atomic mass, since that is the order the quadrupole uses. For clearly-defined readings, meaning any gas which is the only desired one with a certain rounded-off mass, the data can be immediately stored in the computer's memory. For all but two of the monitored gases in this experiment, the amu's are clearly defined and do not overlap.

Both, N_2 (nitrogen gas) and CO (carbon monoxide), have molecular masses of about 28 atomic mass units (amu), and as a result cannot be differentiated by the gas analyzer, since it has only 1 amu accuracy. This problem can be solved with a formula that also takes into account the percentage in the sample of nitrogen atoms, as opposed to N_2 molecules. Since nitrogen gas molecules split into single nitrogen atoms at a known and regular rate, and that splitting is the only source of nitrogen atoms, one knows that the amount of N_2 is a certain multiple of the amount of N atoms. Thus, the concentration of nitrogen gas can be calculated, and subtracted from the total concentration given for 28 amu to give the carbon monoxide concentration. Software that performs this calculation is available, and will be employed. When this resolution is completed, the CO and N_2 concentrations can also be stored.

The computer will file each reading into memory with the following information: experiment, probe used, time sample taken, gas species, and concentration. The data must be organized according to probe used so that, in post-experiment analysis, the changes over time of specific gas concentrations can be understood for each location separately.

4.4.3.1.4 Other Equipment

The accessory equipment necessary include a vacuum chamber, a pump, a gas-storage container, valves, probes, wiring and gas transport tubes.

A number of probe tubes will be used to transport gas samples from the combustion chamber to the analyzer. The exact configuration has not been determined, but the plan is for a number of stationary probes placed around the periphery of the chamber, one or two mobile probes which would be close to the sample itself and, through computer or crew member control, follow the flame front of the burning sample, and possibly two more stationary probes, one on either end of the sample holder. With this combination of probe placement, the gas analysis would provide more varied and useful information. Since they will be far away from the fire, the stationary probes will take gas samples that include the original chamber atmosphere as well as the smoke from combustion. Incorporating data from a number of probes in different locations taking samples, the result will be a thorough picture of the changes that take place throughout the chamber environment during the experiment. The mobile, flame-following probe will take samples that are almost exclusively the immediate products of combustion, and will show the constituents of the smoke, and the changes over time that they undergo, more precisely.

All of the probes will lead into the same gas analyzer system, so only one can be in use at any one time. To allow for this and still retrieve enough samples from each location to have a coherent set of data, the computer control described above, as well as a specially-designed probe cycle, will be employed. The cycle, or repeating order in which the probes will be used, will have to include every probe, and also must be designed in such a way that there are no desired areas which have excessively long delays between samplings. For example, there will have to be more than one or two samplings per overall cycle from very close to the flame, because of that area's importance and variability. However, for reasons of room and the desire to minimize disturbance of the chamber environment there will be at most two, and probably only one, probe in that area. To solve this, one cycle will include multiple openings of that central probe. In addition, the cycle will be designed so that there will be samples from as many different regions as possible in a unit of time. Consecutive probes in the cycle will be far from each other physically, so that the data will be as close as possible to a complete picture of the chamber in any time interval. Lastly, the use of fewer probes will result in shorter cycles, and less holes in a set of data from a single location. However, with more probes, the volume monitored will be greater, and the large-scale picture more complete, but somewhat less precise. The final decision

regarding the number and location of probes, as well as the cycle order, will have to consider these factors, and strike a compromise between quickness and fine accuracy on one side and the larger view on the other. The decision may also be aided by testing of the equipment which will help determine the speed at which the apparatus can work, the total time and approximate rates of change of the experiment, and the frequency at which probes must be employed to garner sufficiently accurate data.

This rapid opening and closing of probes will be accomplished through the use of miniature, quick-opening valves, possibly located on the tip of each probe. Location of the valves on the probe tips guarantees "fresh" sample gas. An alternative approach under consideration involves locating the valves external to the combustion chamber so they are more accessible, but this results in having to clear the probe of "static" sample gas occupying the probe tube prior to sampling the fresh gas. This can be accomplished but it will result in a delay, which we are trying to minimize, in transporting the gas to the quadrupole. The valves will be controlled by the computer, but will also be manually operable. The main considerations regarding the valves is that they be fast, very reliable and effective, and as small as possible, since they will be inside the combustion chamber, where the disturbance to the air flow must be minimized. Several of the probe tips can be flush mounted with the interior combustion chamber wall because gas concentration measurements are required at those locations. This will help to alleviate disturbances to the naturally generated atmospheric flow patterns.

The Residual Gas Analyzer works only at pressures of less than 1.33×10^{-3} Torr and for extended uses, such as this, works best at a pressure of 10^{-5} to 10^{-6} Torr. This low pressure will be achieved with a pump drawing the gases into a chamber from which the quadrupole will take samples to analyze. The low-pressure chamber will have a very small inlet from the probe and a larger outlet which will lead to the pump, in order to maintain the necessary pressure. The pump will be relatively powerful, since it will have to keep the gases in the vacuum chamber at a low pressure throughout the experiment, and will have to keep them moving quickly so that it will not take long to clear the area of the just-used sample gas before allowing the next one into the analyzer.

After the gas leaves the vacuum chamber, it will be filtered, pressurized, and stored. This waste-gas filtering and storage system will also be employed for used gases directly from the combustion chamber. These gases will be pumped out of the top of the chamber and flow through a gas transport tube which will connect to the analyzer-system tube after that line exits

the main pump discussed above. The gases, now combined, will go through a multi-stage filter to make them safe for storage, then be pressurized, using another pump, and finally enter the waste-gas storage container. This container will be large, as it will eventually hold all the gases that have been used in the experiment. The size will be reduced as far as the amount of pressurization can be safely increased. A pressure transducer will monitor the pressure.

Many gas transport tubes will obviously be necessary in this apparatus. They should be as thin, flexible, and reliable as possible. Wiring will also be needed to make the connections to the power supply and computer. They will be positioned in such a way so as to create the least disturbance in and around the combustion chamber, and to take a minimal amount of space.

4.4.3.1.5 Functional Requirements

4.4.3.1.5.1 Residual Gas Analyzer

4.4.3.1.5.1.1 Quadrupole

4.4.3.1.5.1.1.1 Mass

The mass shall be TBD kg. (The VG Micromass PC quadrupole is about 0.65 kg.)

4.4.3.1.5.1.1.2 Dimensions

The quadrupole is a cylinder with radius of approximately 35 mm and length of about 225 mm.

4.4.3.1.5.1.1.3 Power

The power shall be TBD V dc at TBD amps.

4.4.3.1.5.1.1.4 Pressure

The vacuum chamber pressure shall be less than 1.33×10^{-3} Torr, preferably about 10^{-6} Torr.

4.4.3.1.5.1.1.5 Accuracy

The accuracy shall be approximately 1 percent.

4.4.3.1.5.1.1.6 Mass Range

The mass range shall be 1-100 amu.

4.4.3.1.5.1.2 RF Generator

4.4.3.1.5.1.2.1 Mass

The mass shall be 1.9 kg.

4.4.3.1.5.1.2.2 Dimensions

The dimensions shall be approximately 235 mm X 210 mm X 172 mm.

4.4.3.1.5.1.2.3 Power

The power shall be TBD V dc at TBD amps.

4.4.3.1.5.2 Computer Circuit Boards

4.4.3.1.5.2.1 Mass

The mass shall be TBD kg.

4.4.3.1.5.2.2 Volume

The volume shall be TBD m³.

4.4.3.1.5.2.3 Power

The power shall be TBD V dc at TBD amps.

4.4.3.1.5.2.4 Memory

The memory shall be TBD megabytes.

4.4.3.1.5.3 Probes

4.4.3.1.5.3.1 Mobile Probe

4.4.3.1.5.3.1.1 Dimensions

The probe shall be TBD mm in diameter and TBD mm in length.

4.4.3.1.5.3.1.2 Mobility

The probe shall be vertically mobile.

4.4.3.1.5.3.2 Stationary Probes

4.4.3.1.5.3.2.1 Mounting

The probes shall be mounted flush with the combustion chamber side wall.

4.4.3.1.5.4 Pump

4.4.3.1.5.4.1 Mass

The pump shall have a mass of TBD kg.

4.4.3.1.5.4.2 Volume

The volume shall be TBD m³

3.4.4.3.1.5.4.3 Power

The power shall be TBD V dc at TBD amps.

4.4.3.1.5.4.4 Vacuum Capability

The vacuum capability of the pump shall be TBD Torr. The pump shall not incorporate oil diffusion technology.

4.4.3.1.5.5 Valves

4.4.3.1.5.5.1 Computer Control

The valves shall be opened and closed by computer control.

4.4.3.1.5.5.2 Actuation Speed

The valves shall actuate in TBD seconds and shall fail safe to the closed condition in the event of power loss.

4.4.3.1.5.5.3 Size

The valves shall have a diameter of TBD mm, with a goal of not exceeding the probe diameter.

4.4.3.2 Radiometer

4.4.3.2.1 Introduction

4.4.3.2.1.1 Radiant Heat Flux (of Volume of Smoke)

The purpose of the experiment is to monitor the heat flux from the smoke and air in the chamber while combustion is taking place. This will be achieved with a number of radiometers positioned in such a way that they will cover a large volume of air from as much of the chamber as possible, but avoid measuring heat coming directly off the flame itself.

There will be a total of five to eight radiometers used in three different configurations. One will be mounted on the mobile arm used in other experiments to hold a probe for the residual gas analyzer and a thermocouple. This arm will move to follow the flame front on the burning sample, and will remain a short distance from the edge of the sample. The radiometer will be placed on the top side of the arm, a short distance from its tip. This is to ensure that the flame

is always out of the field of view of the radiometer. If it is deemed necessary, a small shield could be placed at the end of the mobile arm to achieve this goal. This radiometer will measure the heat flux from the smoke closest to the flame.

Two radiometers will be mounted on the ends of the sample holder to measure the air which is upstream and downstream from the flame. They will be located on the top and bottom corners of the sample holder on the same side as the support sting and mobile arm, and will be aimed horizontally across the width of the sample. To eliminate the radiometers' measuring of flame radiation, small shields will probably be used. The use of flame shields will be minimized as far as possible so as not to disturb chamber air flow.

Lastly, an undetermined number of radiometers will be flush-mounted on the walls of the chamber to monitor air farther removed from the flame. One each will be placed above and below the sample on the support sting side of the chamber. One may be placed in the middle of the opposite wall, but would be equipped with a partially-blocked aperture, since the flame would be near the center of its field of view. There may be one or two placed in corners of the chamber, which are adapted for significant flame interference. Finally, one radiometer may be oriented normal to the sample surface. This will require a variable view restrictor on the radiometer to keep the flame out of the field of view.

4.4.3.2.1.2 External Heat Flux (On the Unburned Sample and Target)

In this experiment, we will measure the heat flux radiated by the flame that impinges on the sample and the target. Two different external heat flux experiments will be performed. In one, the sample will be ignited with an electric wire coil contacting its edge, while in the other a remote source of heat will provide the ignition. In both cases, a number of radiometers will be used to give the heat flux measurements.

4.4.3.2.1.2.1 Contact Ignition

Three strategies of radiometer placement are under consideration for this part of the experiment. One calls for a large (2.54 cm diameter) radiometer to be mounted in the wall directly in front of the sample, with a field of view perpendicular to the plane of the sample. This radiometer would require an aperture shutter to keep the flame out of view, but would otherwise be able to monitor the complete sample.

The other two methods involve smaller (as small as 0.125" diameter) radiometers to be imbedded in, and flush-mounted with, the sample surface. The first configuration calls for a vertical column of an undetermined number (4 to 6) of radiometers evenly spaced along the middle of the sample. The other method positions the radiometers in two parallel vertical columns, one a quarter of the sample width and one three quarters of the width from one side of the sample. The final plan will probably include the wall-mounted radiometer and one of the two imbedded radiometer methods. The discriminating factors in the choice between the two configurations are completeness of data, which improves with number of radiometers, and the attempt to minimize disturbance of natural combustion, which is aided by fewer radiometers close to the sample surface.

4.4.3.2.1.2.2 Remote Ignition

Remote ignition will be accomplished by a heating coil or other source of radiation (such as that from a burning sample) being placed in front of the sample and aimed toward the sample's center. As opposed to the other experiments in which combustion will begin at the bottom of the sample, in this case, the flame will probably start near the center and spread outward.

The possible radiometer configurations are practically the same in this part of the experiment as in the contact ignition portion. The same two embedded methods are under consideration. The one difference in the final decision regarding these is that, since in this case combustion will begin in the center of the sample, the single centrally located column may be less effective, as it will not register the circular spreading of the flame. Also, the same type of remote radiometer set-up is possible, but in this case the shielding mechanism will have to be more sophisticated, as the flame will begin in the center of the radiometer's field of view. Again, in this portion of the experiment, the final set-up will probably consist of the large radiometer and one of the two configurations of small ones.

4.4.3.2.2 Radiometer

The radiometers under consideration for use are the Schmidt-Boelter type, made by the Medtherm Corporation, with modifications in some cases. Radiometers are small transducers which generate an electronic signal (voltage) proportional to the heat flux they absorb. When heat enters at the sensor surface it is transferred to an integral heat sink which is at a lower temperature than the sensor surface. Small thermocouples measure temperature at two points along

the path between the surface and heat sink. Since the difference in temperature at these two points is proportional to the heat transferred, and, as a result, the heat absorbed, the self-generated emf (electro-motive force) between the thermocouple output leads is directly proportional to the heat flux absorbed [4.12]. The radiometer's millivolt signal is amplified and then goes to the main computer A-D (analog-to-digital) board.

A primary consideration in many of the configurations proposed is the need to avert the influence of the flame view in radiometer readings. There are a number of ways to accomplish this. One is the placement of the radiometer in ways that use existing chamber components to block out the appropriate part of the radiometer's field of view. This strategy will be used with the radiometer on the mobile arm in the external heat flux experiment. In that instance, the radiometer will be placed some distance back on the arm in such a way that the arm itself will constantly block out flame radiation. This approach may also be used with other radiometers. A solution in some of the other situations is a special small metal plate designed and placed with the intent of shielding the radiometer from flame view. Also, view restrictor attachments, standard accessories to Medtherm radiometers which limit the angle of view to a predetermined amount, may be used in some cases. However, they are slightly less desirable, as they block out not only the flame, but also a useful portion of the field of view. Lastly, an aperture shutter will be considered for use in the cases that require a relatively precisely variable field of view. This shutter must be able to close at the rate that the flame takes up the field of view so that the radiometer will at all times have as much of the desired area in view, but none of the flame. Because a number of parts, including a number of shutters and the mobile arm, will have to react to flame movement, it is likely that they will be connected electrically and controlled together, possibly through a manual system operated by a crew member.

4.4.3.2.3 Radiometer Functional Requirements [4.12]

4.4.3.2.3.1 Output Signal

The output signal shall be approximately 10 millivolts at full range.

4.4.3.2.3.2 Maximum Body Temperature

The radiometer body temperature shall not exceed 673 K.

4.4.3.2.3.3 Accuracy

The accuracy shall be ± 3 percent.

4.4.3.2.3.4 Response Time

The response time shall be TBD msec.

4.4.3.2.3.5 Diameter

Radiometers of diameter 2.54 cm, and TBD cm will be used.

4.4.3.3 Particle Dynamics Analyzer [4.13]

4.4.3.3.1 Introduction

This section presents the instrumentation approach to non-intrusively obtain data on smoke particle and suppressant droplet sizes and velocities. The Dantec Electronics, Inc. Particle Dynamics Analyzer, to be modified for our application, which uses a helium-neon laser is under consideration to provide one-, two-, or three-dimensional data. The Particle Dynamics Analyzer uses the phase/Doppler principle for simultaneous, non-intrusive real time measurements of particle size, one to three velocity components, and concentration. Measurements will be made of particles that range from micrometers to millimeters in size, particles that are moving up to supersonic speeds (this experiment will not have speeds of that magnitude), stationary, or moving backwards in recirculating turbulent flows.

The Particle Dynamics Analyzer consists of three main components: optics, signal processor, and computer. The lasers and receiving optics will be externally mounted on combustion chamber brackets with selectable fields of view through windows to various smoke regions. Use of fiber optic probes will facilitate selection of the desired target areas, including the flame itself. The signal processor will be located in the Experiment System Command and Power Module.

and the operating software will be resident in the Experiment System computer. The following sections discuss the components as well as operation of the equipment.

4.4.3.3.2 Optics

Standard one, two, or three component laser Doppler assembly modules, typically mounted on a rigid mounting bench system, are used as transmitting elements in the Particle Dynamics Analyzer. By use of a Bragg cell module, reversing flows are measured. All the receiving optics are contained in a single unit to obtain easy alignment. Three or four photomultipliers are used in one-, or two-dimensional systems, respectively.

4.4.3.3.3 Signal Processor

The Particle Dynamics Analyzer is based on correlation analysis of the detector output signals. All the settings are controlled from the computer. The equipment has a high data rate and the ability to handle a low signal-to-noise ratio ensures reliable and accurate results even under severe measurement conditions (e.g., combustion). A built in laser diode generates calibration signals that, via a fiber optic cable, are fed to the receiving optics to ensure that the equipment is automatically calibrated. The processor is able to handle one-, two-, or three-dimensional flows. Extra flow dimensions require only an extra module to be inserted in the processor. A frequency shifter is included for measurements in reversing flows. The computer is connected via a dedicated high speed direct memory access interface.

4.4.3.3.4 Computer/Software

The IBM PC-based compatible computer in the Command and Data Subsystem is a required part of the signal analysis system. The signal processor is fully controlled and set from the computer. The menu-driven software for the Particle Dynamics Analyzer presents on-line histograms, distributions, and correlations of size and velocity. The vendor-supplied source code is modifiable for our specific application.

4.4.3.3.5 Operations

The phase/Doppler principle is an extension of the Doppler principle, which is used in laser Doppler velocimetry for determination of flow velocity. The Doppler principle is based on the fact that light scattered from moving particles will be of a different frequency than the light illuminating the particle, with the frequency shift or Doppler shift being proportional to the velocity. If a standard laser Doppler velocimeter is combined with a second photodetector, the phase difference between the photodetector signals is (under certain conditions) a direct measure of the particle size. A third photodetector is included to extend the dynamic range, and in two-dimensional flows a color separator and fourth photodetector are added to allow two velocity directions to be measured.

The particle size and velocity are found from measuring the relative phase and frequency of burst type Doppler signals. If the signal-to-noise ratio is less than approximately 10 dB, as may be the case in some of our measuring environments, the phase and the frequency cannot be accurately measured with the conventional counting techniques which have been widely applied in laser Doppler velocimetry. In the Particle Dynamics Analyzer signal processor, the relative phase and frequency estimations are based on covariance processing techniques, similar to those used in radar signal processing. The reduction in the required signal-to-noise ratio is 10 dB compared to counter based instruments.

To measure the relative phase, two photodetector signals of identical frequency but different phases are fed to a cross correlator. In a second cross correlator, the same two signals are compared with one of them 90 degrees out of phase. The integration part of the cross correlator is gated by a burst detector, which also is based on correlation techniques and in performance, and therefore, matches the high performance of the phase detector. The two cross correlations are proportional to the sine and cosine of the original phase difference between the photodetector signals, and performing an inverse tangent operation on the ratio, thus, gives the relative phase difference.

To measure the frequency, the signal from one photodetector is split into two signals, one of which is delayed by a known amount. This corresponds to adding a phase shift of the delay time times the frequency. The relative phase is then measured as above. Finally, the measured phase is divided by the delay time to give the signal frequency.

For two-, or three-dimensional flow measurements additional frequency measuring channels are added to the electronics.

4.4.3.3.6 Requirements

4.4.3.3.6.1 Measurement Range and Accuracy

The particle size measurement range shall be 1-10,000 micrometers, with a dynamic range of 1 to 40. The size accuracy shall be no less than 4 percent. The maximum measureable velocity shall be no greater than 500 m/s with an accuracy of no less than 1 percent. The maximum concentration shall be no more than $10^6/\text{cm}^3$ with an accuracy of no less than 30 percent.

4.4.3.3.6.2 Optics

The laser shall be of the helium-neon type and shall have a maximum laser power of 5 W. The configuration shall be near forward scatter, near backward scatter or side scatter. The measuring distances shall be compatible with the combustion chamber dimensions.

4.4.3.3.6.3 Electronics

The maximum frequency range shall be from -6 to +30 MHz with a maximum bandwidth of 36 Mhz. The bandwidth shall have selectable ranges. The minimum signal-to-noise ratio shall be 0 dB. The maximum average data rate shall be greater than 100,000 particles per second with a maximum dead time of 800 nanoseconds. The size and velocity shall be determined with 8 bit resolution with a time of arrival of no greater than 1 microsecond and a transit time of no greater than 0.1 microsecond.

4.4.3.3.6.4 Computer/Software

The Experiment System computer shall be an IBM PC-based compatible with a minimum of 640 Kb of random access memory, 512 Kb of extended memory, at least an EGA color monitor, DOS version 3.2 or higher, and compatible with an IBM or compatible printer.

The software shall possess an experiment set-up automatic mode with user definable measurement sequences and on-line help. On-line data acquisition and presentation with data logging to disk shall be provided. The software shall permit the following data processing and presentation capabilities: mean values, size and velocity histograms, concentration distribution, absolute concentration, volumetric and mass flow, Rosin-Rammler distribution, turbulence intensities, Reynolds shear stress, color graphics presentation, file management facilities, and hard copy output drivers.

4.4.3.3.6.5 Mass

The mass of the Particle Dynamics Analyzer shall be no more than TBD kg (approximately 9 kg for the receiving optics, and 20 kg for the signal processor).

4.4.3.3.6.6 Power

The power consumed by the Particle Dynamics Analyzer shall be no greater than TBD W (approximately 180 watts for the signal processor, and 60 watts for the lasers).

4.4.3.4 Thermal Imager

4.4.3.4.1 Introduction

An Inframetrics, Inc., infrared imaging radiometer to measure the surface temperature of the burning sample is under consideration. This instrument provides real-time infrared video images of a target region, in this case, the sample. The Thermal Imager may be mounted on the external combustion chamber wall, directly in front of the sample, for a head-on view of the sample, or at an angle to the sample and flame to view more of the flame itself.

4.4.3.4.2 Operation and Data Acquisition

In normal usage, the imager outputs a color or black-and-white picture in which intensity at a specific point on the screen corresponds to the amount of infrared radiation emanating from that location on the target. In this experiment, real-time physical imaging may be necessary for verifying that the system is functioning properly and for possible on-orbit analysis which could influence other experimental runs. The images will be transferred directly to videotape for future analysis. Videotape recording is an option regularly available from Inframetrics.

The videotaped images may be analyzed in a number of ways after the mission. The general nature of the pictures may be of sufficient accuracy and precision for the measurements needed. This decision will be made based on further study and ground-based experiment testing of the equipment. In all probability, however, more in-depth processing of the data will be necessary.

One approach may be to extract from the pictures, temperature measurements at individual points at many different specific times. This would be accomplished by taking data from periodic stopped-action images instead of moving pictures. The quality of data may also be improved by incorporating measurements from thermocouples embedded in the sample and a system of contact surface-temperature thermocouples. Using thermocouples may serve as a helpful calibration when combined with data from the Thermal Imager.

4.4.3.4.3 Functional Requirements

4.4.3.4.3.1 Mass

The mass shall be TBDm x TBDm x TBDm.

4.4.3.4.3.2 Power

The power shall be 20 W, 11-17 V dc.

4.4.3.4.3.3 Dimensions

The dimensions shall be TBD.

4.4.3.4.3.4 Temperature Range

The temperature range shall be TBD

4.4.3.4.3.5 Thermal Sensitivity

The minimum detectable temperature difference shall be 0.1 K at 303 K.

4.4.3.5 Pressure Transducers

4.4.3.5.1 Introduction

Measurements of pressure will be necessary in a number of areas and for a variety of purposes in this experiment. In all cases, pressure transducers will be used to make these determinations. Current planning calls for approximately TBD transducers in various locations in the experiment configuration.

One pressure transducer will be placed inside the combustion chamber to monitor ambient pressure prior to and during the combustion process. For general monitoring, pressure transducers will be located at the inlet and exit lines into the chamber. Another pressure transducer will be located between the combustion chamber wall and the partition which simulates racks and other equipment.

Each of the gas bottles used in the experiment (at least one for waste gas and an undetermined number for air constituent gases) will require a pressure transducer to ensure that all valves, lines, and bottles in the area are functioning properly. Each will be placed between a gas bottle and its corresponding valve. In the experiments which use the Residual Gas Analyzer, a pressure transducer will be mounted in the inner wall of the vacuum chamber to ensure knowledge of a continuous low pressure. The gas bottle and vacuum chamber transducers may not be as precise or closely monitored as the combustion chamber transducers, since they will not be used for essential science data, but simply for determining whether equipment is working correctly.

4.4.3.5.2 Operation and Data Retrieval

Pressure transducers operate on a simple basic principle: fluid that enters the transducer opening puts stress on a thin silicon diaphragm which then presses on a small piezo-resistor causing a change in the resistance and a corresponding change in the output signal proportional to the original pressure.

All of the pressure transducers will output signals to the computer, although differently, depending on the individual purpose of the transducer. Those inside the chamber will give data often and directly to computer storage for later analysis on the ground. Data from the other transducers will be monitored both by a crew member and the computer because it may show evidence of pending equipment failure. The computer will have the capability to sense indications of such a pending failure, and will provide an alarm and/or safely shut down the system if human intervention has not occurred.

4.4.3.5.3.1 Dimensions

The transducer shall be approximately 2 cm in length and 1 cm in diameter.

4.4.3.5.3.2 Power

The power shall be 5 V dc with a current of TBD amps.

4.4.3.5.3.3 Mass

The mass shall be approximately 15 g.

4.4.3.5.3.4 Accuracy

The accuracy shall be 1 percent of full scale readings.

4.4.3.6 Flowmeters

4.4.3.6.1 Introduction

Air flow is an important parameter to be measured and controlled in the combustion chamber environment. The air flow will not only need to be monitored with the purpose of accounting for and minimizing disturbance of combustion, but it will also be varied in a controlled manner during the experiment to study the effects of changes in air currents on combustion. To measure air flow at all times throughout the chamber, flowmeters will be used in a number of locations. Three-dimensional hot wire anemometers are under consideration to provide air current velocity information.

There will be a total of TBD flowmeters used. One each will be placed directly in front of the inlet and exit of the chamber to measure flow rates of the air entering and leaving the chamber. In addition, to complete measurement of the central flow of air, two flowmeters will extend from the mobile probe assembly to the middle of the chamber, one below and one above the sample. Four more flowmeters will be located around the periphery of the chamber, one extending from near the cylinder/dome interface. Lastly, several flowmeters will be attached to the special partition which will be used to create eddy currents. This flowmeter will extend perpendicularly outward from the front wall of the partition, and help monitor the effects of the change in air current.

4.4.3.6.2 Operation and Data Acquisition

Immersion probe style electronic mass flowmeters will be the type used to measure gas flow in this experiment. These instruments consist of a mass flow probe on which two resistance temperature detectors are installed. The first detector measures the initial temperature of the gas. The other is kept at a temperature 333 K above the gas temperature, as measured by the first detector. As gas passes by it, the heated sensor transfers heat to the gas at a rate which is proportional to the mass flow rate of the gas. The faster the sensor gives off heat, the more energy must be applied to it to keep it 333 K above the gas temperature. Thus, the output signal, which is the change in voltage required to maintain this constant temperature differential, is proportional to the air mass flow rate. [4.14]

All the flowmeters will input data to computer storage in the same manner as most other instruments in the experiment. Special emphasis will be given to the flowmeter on the removable partition when it is in operation, since it is in an area of relatively turbulent and quickly-changing conditions. Other than that, the flowmeters require no uncommon procedures in collecting data.

4.4.3.6.3 Functional Requirements

4.4.3.6.3.1 Mass

The mass shall be TBD kg.

4.4.3.6.3.2 Power

The power shall be 15-18 V dc, at TBD amps.

4.4.3.6.3.3 Dimensions

The dimensions shall be TBDm x TBDm x TBDm.

4.4.3.6.3.4 Accuracy

The accuracy shall be TBD.

4.4.3.6.3.5 Response Time

The response time shall be 50-200 msec.

4.4.3.7 Humidity Control

Relative humidity will be measured and/or controlled to varying degrees in certain areas of the experimental configuration. In general, only excess humidity is to be avoided, so none of the humidity-controlling apparatus will need to include humidifying elements, but only measurement and desiccation capabilities. The locations which are of concern are the combustion chamber inlet, the exit tubes leading to waste gas storage, and the tubes directly upstream of the Residual Gas Analyzer.

It is important that the gases entering the chamber are relatively dry, because they, more than at any other location, may affect the combustion process. The central part of the humidity-control system in the inlet area will be a small desiccant designed to dry the gases the expected necessary amount. After the gases pass through the desiccant, a small hygrometer will measure their humidity. To ensure that all gas entering the chamber is at the correct humidity, a special extra-desiccating loop of tube will be installed onto the inlet line. This loop will branch off the main gas tube starting immediately beyond the hygrometer. If the hygrometer measures the humidity as being above pre-set limits, a valve at the entrance to the loop will open, through computer control, to guide gases into the short piece of tube, which will have extra desiccant in it and add significantly to the drying of any gases that pass through it. The other end of the loop will rejoin the main tube directly before the chamber inlet. This should be sufficient to reduce

even unusually wet gases to acceptable humidity levels. This approach is taken as a precaution, since dry gases will be loaded into the storage bottles on the ground to preclude excess moisture.

Before entering the storage container, waste gas will be filtered of certain elements. One of these which must be limited before storage is water. A desiccant will be used for this purpose, and a hygrometer will monitor the humidity in the area. Since the sensitivity is not high in this location, this configuration should provide enough protection. This set-up will probably be connected to a system of filters which will clean the waste gases.

The Residual Gas Analyzer may have some sensitivity to excess water, and so some humidity control may have to be applied to the gases entering it. If that is the case, a simple desiccant and hygrometer system similar to the others described will be used.

4.5 Fire Safety Experiment System Interfaces

4.5.1 Shuttle and/or Spacelab and/or Space Station Interfaces

During the development phase of the project, this section will be generated to provide a listing of all mechanical, electrical, and computer (if required) interfaces with the host spacecraft. The listing will identify both sides of the interface and will have an appropriate numbering system.

4.5.2 Experiment System and Subsystem Interfaces

During the development phase of the project, this section will be generated to provide a listing of all system (e.g., mechanical, electrical, and computer) interfaces as well as experiment internal subsystem interfaces.

4.6 Fire Safety Experiment System Support Equipment Functional Philosophy

During the development phase of the project, this section will be generated to discuss the requirements for equipment which must be used to provide ground-based testing of the experiment system, as well as other equipment. The following contents are relevant to the support equipment:

Characteristics and Constraints
Functional Block Diagrams and Circuits
Facilities
Test and Telemetry Data Processing
Structural Subsystem
Thermal Control Subsystem
Fluids Control Subsystem
Electrical Power Subsystem
Command and Data Subsystem
Software Subsystem
Remote Operation Data System

4.7 Fire Safety Experiment System Safety Requirements

During the development phase of the project, this section will be generated to discuss the safety requirements to be imposed on the experiment system to ensure its safe transport and operation on the host spacecraft, as well as during ground-based testing and during handling at the launch site.

The over-riding requirement of all activities involved in this experiment, including transport, storage, and experimental procedures, is that they be safe in all ways. Safety concerns involve the protection, most importantly, of people, as well as of equipment and data. All systems will be designed to two-fault tolerance, and to fail to a safe state. Examples of these precautions include a double wall for the combustion chamber, triple seals, possibly automatic release of extinguishants and stoppage of the oxygen supply upon experiment failure or power outage, and capability for manual control in the event of computer malfunction, among many others. All designs will, above all, ensure safety by using fail-safe methods at every step.

4.8 Fire Safety Experiment System Design Verification

During the development phase of the project, this section will be generated to discuss the requirements which will govern the establishment of the experiment system verification (test) program. It will state requirements which will result in the determination of how well the experiment system performs relative to its design requirements.

4.9 Mission Plan

4.9.1 Flight Sequence Implementation

4.9.1.1 Pre-Launch

All the necessary equipment will be stowed safely until orbit is reached. The chamber itself will be equipped with removable racks and packing material, and much of the equipment will be stored inside of it. Some of the bulkier and less fragile parts will be outside the chamber, either already bolted in operational position or in storage lockers attached to the experiment assembly.

In order to minimize in-orbit assembly, as many pieces of equipment as are possible and considered safe will be placed in their working positions. These include all small sensors, such as thermocouples and pressure transducers, which are to be mounted on the inside of the chamber wall, and possibly those pieces of equipment which belong on the outside wall, such as radiometers and laser diodes. The computer will be bolted in its permanent position, near the main experiment assembly. Any equipment placed anywhere but in tight storage, however, will have to be rigidly attached to the chamber or back wall, and be able to withstand launch and loads without significant movement or any detachment.

4.9.1.2 In-orbit

4.9.1.2.1 Experiment Set-up

Before the experiments can begin, the equipment must be unpacked and assembled. First, the chamber will be completely cleared of everything (equipment being stored, racks, etc.) except for those pieces of equipment already in position, which will be only small instruments around the periphery. The first step in assembly will be attaching everything else that belongs on the inside wall. These include any pressure transducers, thermocouples, radiometers, or flowmeters not yet in place, and the peripheral gas analysis probes. Next, the support sting/mobile probe assembly will be put in position. The equipment that is to be affixed directly to the outside of the chamber will then be installed. This includes lasers, video cameras, and the Thermal Imager camera, among others. After that, the outermost layer of equipment, which includes the Residual Gas Analyzer System, the waste gas filtering system, and all gas bottles, can be positioned. Lastly, all electrical and gas-tube connections will be made.

Before each phase of the experiment, the sample(s) to be used must be put in position. First, the embedded thermocouples will be placed in the matching pre-drilled holes in the sample material. Then, the sample must be attached to the sample holder. The holder will have an adaptable sample connection so that it will facilitate the various geometries to be used. The ignition coil, if used in the particular part of the experiment, will be attached, and the chamber shut. The air-flow system, consisting of the inlet and exit openings, the make-up gas bottles and valves, the chamber vents, the exit pump, and the waste-gas filtering and storage system, will then begin operation, and all instruments will be turned on to stabilize and take initial readings. Finally, ignition, whether it be by nichrome coil or remote heat radiation, will initiate the experiment run.

4.9.1.2.2 Performing the Experiments

Almost all activity over the course of the experiment itself will be computer-controlled, and require little or no human participation. The process will be monitored by a crew member by checking gas bottle pressure, chamber temperature and pressure, and the physical appearance of the burning sample. The crew member will also be required in some experiments to release suppressants near the end of the experiment. Lastly, the crew member will control the motion of the mobile probe.

A typical "data take" would require approximately 10 minutes, followed by approximately 20 minutes of Combustion Module cleaning and set-up time. This would include: bagging of the burned sample remains; wipe-down of the Combustion Module interior and windows; placing a new sample in the holder, positioning the holder, mobile probe, and observation sensors; re-sealing the Combustion Module; performing a leak check; establishing the correct air flow; initializing the computer and other electronics; and starting the ignition sequence. As many as 180 data-taking runs are anticipated which would require approximately 90 hours of on-orbit crew work time. Full-up Experiment System testing in a laboratory environment will refine these time estimates, as well as the number of runs actually required. The total work-hours needed must be reduced to a level achievable during a typical shuttle mission duration, if the shuttle is the host spacecraft.

4.9.1.2.3 Between Experiment Runs

After each stage of the experiment, a sequence of operations must occur before the next stage can begin. First, whatever is left of the used sample must be removed and stored in a marked, non-contaminating bag. The inside of the chamber, particularly on and around instruments, will be thoroughly cleaned with a completely safe, non-toxic solvent, and all cleaning wipes will be stored in marked bags. Then, the next sample will be brought into the chamber and arranged correctly. Any changes that must be made to the chamber, involving parts such as the partition and the upper and lower vents, will be made. Certain instruments, may need some re-positioning before the next experiment run. For example, the video cameras and Thermal Imager camera, depending on the overall length of the experiment, may need new videotape at some point. In addition, some instruments will be turned on, and some turned off, to satisfy the next experiment's requirements. Movement of equipment will be minimized between separate phases. If this is not possible, some equipment will be moved at this time. After re-positioning the equipment the next experiment run can begin.

4.9.1.2.4 Experiment Shut-down and Stowage

After all the experiments are completed, all equipment will be shut off and restowed in the original manner. All experimental data, meaning computer memory and videotapes from video cameras and the Thermal Imager, will be stored as safely as is possible, and further precautions against loss of data, such as producing back-up copies prior to return from orbit, are under consideration. An experiment shut-down and stowage checklist will guide all preparations of the equipment after completion of the experiment.

References

- 4.1 J. Harper, *Interim Report of the Conceptual Design for the Space Station Modular Combustion Facility*, Sverdrup Technology, Inc. for NASA Lewis Research Center (LeRC), January 1989.
- 4.2 *Spacecraft Fire-Safety Experiments for Space Station Technology Development Mission*, Wyle Laboratories Report No. 68300-1, Huntsville, Alabama, April 1988.
- 4.3 S.L. Olson, *The Effect of Microgravity on Flame Spread Over a Thin Fuel*, NTM 100195, NASA LeRC, December 1987.

- 4.4 *Microgravity Combustion Diagnostics Workshop*, NASA Conference Publication 10017, G.J. Santoro, et al. (eds.), Lewis Research Center (LeRC), Proceedings from workshop at LeRC held July 28-29, 1987.
- 4.5 *Fire Protection Handbook*, Chapter 21, pages 39-41, A.E. Cote, Editor-in-Chief, J.I. Linville, Managing Editor, National Fire Protection Association, Quincy, Massachusetts, Sixteenth Edition.
- 4.6 B. A. Ostman, I.G. Svensson, and J. Blomqvist, "Comparison of Three Test Methods for Measuring Rate of Heat Release," *Fire and Materials*, 9, Wiley Heyden Ltd., 1985.
- 4.7 F.R.S. Clark, "Assessment of Smoke Density with a Helium-Neon Laser," *Fire and Materials*, 9, Wiley Heyden Ltd., 1985.
- 4.8 Discussions with William Meyer of LeRC, May 2, 1989.
- 4.9 Robert G. W. Brown and R.S. Grant, "Photon Statistical Properties of Visible Laser Diodes," *Review of Scientific Instruments*, 58, June 1987.
- 4.10 P. Chung and E. Smith, "Emissivity of Smoke," *Journal of Fire and Flammability*, 13, 104, Technomic Publishing Co., Inc., 1982.
- 4.11 R. Chitty, "Fast Surface-temperature Measurement for Fire Tests," *Fire and Materials*, 8, 217, 1984.
- 4.12 Medtherm Corporation brochure on 64 Series Heat Flux Transducers.
- 4.13 *1986 Complete Flow and Level Measurement Handbook and Encyclopedia*, Omega Engineering, Inc., D-6-7.
- 4.14 Dantec Electronics, Inc. "Particle Dynamics Analyzer," technical data, Allendale, NJ, 1989.

5.0 PRELIMINARY DEVELOPMENT PHASE PLAN

5.1 Implementation Plan

Generally, the approach to accomplishing the development phase will be to expand upon the work concluded in the definition phase. The development phase will consist of two primary areas of focus: theoretical development and hardware development.

The theoretical development is necessitated by the fact that we anticipate a need for refinement of the existing science requirements, as well as the possibility of the definition of new science requirements. The existing database of science requirements possesses a number of models for a particular phenomenon which must be further refined for the analysis of the experimental data to be obtained. Furthermore, there are a number of "to-be-determined" areas which must be better defined so that the functional requirements can be finalized.

Our work in Chapter 3 has demonstrated that the development of accident scenarios is inhibited by the absence of theoretical models which are needed to complete an event sequence. For example, while models for the mass burning rate and the obscuration exist separately, we have been unable to locate any models which relate the fire itself with the degree of smoke obscuration in a compartment. Filling this gap between models may result in the formulation of new science requirements to be imposed on the Experiment System. However, it is not our intention to significantly expand the present scope, but, rather, to take advantage of the existing experimental hardware and gather the required information with minimal modification and effort.

Although the Experiment System concept has been significantly advanced during the definition phase, particularly in the Instrumentation Subsystem area, a number of hardware-related issues must be addressed early in the development phase, including, for example: functional requirements expansion at both the system and subsystem levels; selection of the host spacecraft (currently targeted for the shuttle middeck, as well as Spacelab or space station); incorporation into the design, at an early stage, of features which address the safety requirements of the shuttle; a review of the engineering and safety approach taken by other related shuttle middeck experiments (e.g., Solid Surface Combustion Experiment) for applicability to this experiment; and keeping abreast of the evolution of the LeRC Modular Combustion Facility for potential applications to this experiment, e.g., diagnostic instrumentation which we may adopt.

Figure 5.1 indicates a preliminary implementation plan for the development phase. The theoretical development includes model development as discussed above, as well as the post-flight analysis of data, and will, therefore, continue throughout the project. The design of the experimental methods will be iterated with the hardware design. The preparation of the flight samples will be accomplished near the end of hardware development.

Hardware development spans approximately 2.5 years and includes: functional requirements definition; hardware and software detailed design; and fabrication, assembly and test. We have allocated approximately 2 years for preparing the launcher-related documentation, such as payload integration plans, interface control documents and annexes, and safety and readiness reviews. Also included here are the related tasks of shipping the experiment to the launch site, participating in the integration with the host spacecraft, supporting launch and flight operations, and post-flight recovery of the hardware and science data.

5.2 Project Management

The project will be conducted under the direction of the Principal Investigator, Professor George E. Apostolakis, working closely with Arthur T. Perry, System Manager and President of American Space Technology, Inc., the Experiment System subcontractor. They will be assisted by faculty associates, graduate students, company engineering staff, and consultants, as appropriate.

Figure 5.2 indicates the preliminary organization responsibilities. Primary UCLA focus is on program management, science data requirements, PRA modeling, theoretical research and development, preparation of sample materials, data analysis. Secondary UCLA focus is on selected student support to AmSpace in the areas of requirements definition, hardware and software design, fabrication, assembly, testing, and flight operations support.

Primary AmSpace focus is on requirements definition, hardware and software design, fabrication, assembly, testing, and flight operations support. Secondary AmSpace focus is on science data requirements, PRA modeling, theoretical research and development, preparation of sample materials, and data analysis.

TASKS	YEAR 1		YEAR 2		YEAR 3		YEAR 4	
	Start	Review	NASA CDR	Ship	Launch	Final Report		
MAJOR MILESTONES	Start	Review	NASA CDR	Ship	Launch	Final Report		
AUTHORIZATION TO PROCEED								
THEORETICAL DEVELOPMENT								
• Heat Release Model								
• Smoke Release Model								
• Heat Transport Model								
• Damage Model								
• Detection/Suppression Model								
EXPERIMENTAL APPROACH								
GROUND-BASED EXPERIMENTATION								
FLIGHT SAMPLE PREPARATION								
HARDWARE DEVELOPMENT								
• Requirements Definition								
• H/W-S.W Design								
• Fabrication, Assembly, Test								
SHIP								
INSTS DOCUMENTATION/REVIEWS/								
INSTS INTEGRATION								
LAUNCH/FLIGHT OPERATIONS								
POST-FLIGHT DATA ANALYSIS								
MODEL MODIFICATIONS/VERIFICATION								
FINAL REPORT								

Fig. 5.1 Preliminary Project Schedule

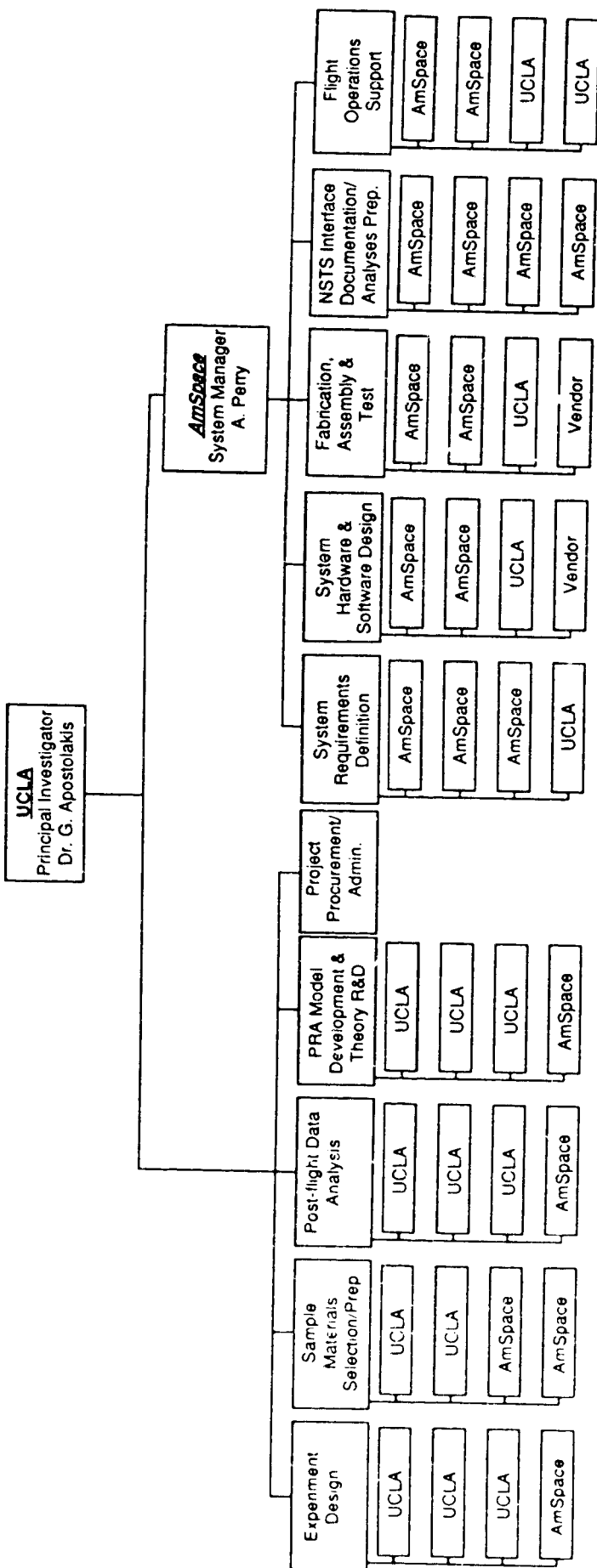


Figure 5.2. Development Phase Organizational Responsibilities.

AmSpace will use student support in many selected areas and will assist the Principal Investigator in the development of various challenging students projects. Students will use UCLA computers, machine shops and other laboratories, and will provide tangible products to AmSpace. System integration and testing will be performed in a UCLA laboratory under the direction of AmSpace using AmSpace engineers and UCLA students. UCLA faculty will manage lab usage and provide associated expertise. If necessary, some testing will be performed at an outside facility under the direction of AmSpace. Vendors provide: off-the-shelf equipment and raw materials; modifications to off-the-shelf equipment; and selective fabrication, assembly and test.

5.3 Cost Estimate

The development phase is estimated to cost \$3,800,000. Labor (engineering, fabrication, testing) is expected to absorb about 70% of the total cost, while the remaining will be expended for the purchase of hardware as follows: Combustion Module: 5%; Fluids Module: 5%; and, Command and Power Module: 20%.



Report Documentation Page

1. Report No.	2. Government Accession No.	3. Recipient's Catalog No.	
4. Title and Subtitle Risk-Based Fire Safety Experiment Definition for Manned Spacecraft		5. Report Date September, 1989	
		6. Performing Organization Code	
7. Author(s) G. E. Apostolakis, V. S. Ho, E. Marcus, A. T. Perry, S. L. Thompson		8. Performing Organization Report No. UCLA ENG 90-11	
		10. Work Unit No.	
9. Performing Organization Name and Address Mechanical, Aerospace and Nuclear Engineering Dept. University of California Los Angeles, CA 90024-1597		11. Contract or Grant No. NAS8-37750	
		13. Type of Report and Period Covered Final Report	
12. Sponsoring Agency Name and Address Office of Aeronautics and Space Technology National Aeronautics and Space Administration Washington, D.C. 20546-0001		14. Sponsoring Agency Code	
		15. Supplementary Notes 1. E. Marcus and A.T. Perry are with American Space Technology, 2800 20th Street, Santa Monica, CA 90405-2934 2. Contract Manager, F.E. Anthony, Jr., Marshall Space Flight Center National Aeronautics and Space Administration Huntsville, AL 35812	
16. Abstract Risk methodology is used in this work to define experiments to be conducted in space which will help to construct and test the models required for accident sequence identification. The development of accident scenarios is based on the realization that whether damage occurs depends on the time competition of two processes: the ignition and creation of an adverse environment, and the detection and suppression activities. If the fire grows and causes damage faster than it is detected and suppressed, then an accident has occurred. The proposed integrated experiments will provide information on individual models that apply to each of the above processes, as well as previously unidentified interactions and processes, if any. Initially, models that are used in terrestrial fire risk assessments are considered. These include heat and smoke release models, detection and suppression models, as well as damage models. In cases where the absence of gravity substantially invalidates a model, alternate models will be developed. Models that depend on buoyancy effects, such as the multizone compartment fire models, are included in these cases. The experiments will be performed in a variety of geometries simulating habitable areas, racks, and other spaces. These simulations will necessitate theoretical studies of scaling effects. Sensitivity studies will also be carried out including the effects of varying oxygen concentrations, pressures, fuel orientation and geometry, and air flow rates. The experimental apparatus described herein includes three major modules: the combustion, the fluids, and the command and power modules.			
17. Key Words (Suggested by Author(s)) Risk Assessment and management; Accident Scenarios; Fire ignition; Fire detection; Fire suppression; Spacecraft fire safety; Fire Experiments		18. Distribution Statement Unclassified - Unlimited	
19. Security Classif. (of this report) Unclassified	20. Security Classif. (of this page)	21. No. of pages 189	22. Price